Molecular evolution of fungicide resistance in *Blumeria graminis*

Thesis submitted to the University of East Anglia for the degree of Doctor of Philosophy.

Corinne Jane Arnold

John Innes Centre

September 2018

Abstract

Blumeria graminis, a powdery mildew pathogen which infects many wild grasses and cereals across the world, can cause significant losses in cereals. Applying fungicides is a main method for control, but resistance to quinone outside inhibitors and many triazole fungicides already occurs in *B. graminis*, and few other effective fungicides are available.

In this thesis, isolates were characterised from an outbreak of *B. graminis* f. sp. *tritici (Bgt)* on wheat where three major fungicides had lost effectiveness: cyflufenamid (Cyflamid), fenpropimorph (Corbel), and prothioconazole (Proline). All isolates from the study site were completely resistant to cyflufenamid at the recommended field rate. Additionally, isolates sampled following two sprays of fenpropimorph, had significantly lower sensitivity than field isolates.

RNA sequencing was used to identify the spindle assembly checkpoint protein MAD1 as a candidate target of cyflufenamid, implying that the mode of action of cyflufenamid may be to inhibit mitosis. A candidate mutation in MAD1 causing cyflufenamid resistance was also discovered. Sequencing the *Erg24* gene in isolates sensitive or resistant to fenpropimorph identified a mutation that may confer resistance in *Bgt*, which was subsequently confirmed by site-directed mutagenesis of yeast, and a different *Erg24* mutation was found in *B. graminis* f. sp. *hordei*, the barley mildew pathogen. Multiple copies of the *Cyp51* (*Erg11*) gene were identified in *Bgt* isolates. Some isolates with elevated resistance were heteroallelic, carrying both wild-type and mutant *Cyp51* genes. Triazole-resistant isolates had greater expression of *Cyp51* than more sensitive isolates, as did UK isolates compared to those from the USA.

In summary, this thesis updates knowledge of resistance to currently available fungicides and their modes of action against powdery mildew. This is important in helping to reveal how resistance to fungicides occurs. In turn, this knowledge can contribute to the discovery of new fungicides and to using new and existing chemicals more effectively.

Table of contents

List of figures

Chapter One

Chapter Two

Chapter Three

Chapter Four

Chapter Five

Chapter Six

Appendix II

List of tables

Chapter One

Chapter Two

Chapter Three

Chapter Four

Chapter Five

Appendix I

Appendix II

Acknowledgements

First of all, I would like to give a tremendous amount of thanks to my supervisory team, Prof. James Brown, Dr. Diane Saunders, and Dr. Laetitia Chartrain, for all of the help, support, and advice given throughout my Ph.D. I would also like to thank all those from the Brown group who helped me with various aspects of my Ph.D as well as making this a warm, fun, and friendly experience – Dr. Chris Judge, Rachel Burns, Cyrielle Ndougonna, Martha Clarke, Dr. Elizabeth Orton, Lorelei Bilham, and Sam Holden.

Additional thanks go to the Nicholson group – Prof. Paul Nicholson, Andy Steed, Dr. Rachel Goddard, Lola Gonzalez Penades, John Haidoulis, Ben Hales, Dr. Marianna Pasquariello, Miguel Santos, and Dr. Catherine Chinoy – for their extra bits of support and for the lovely coffee breaks, snacks, and pub lunches. I also thank Dr. Jitender Cheema, Dr. Guru Radhakrishnan, Dr. Antoine Persoons, and Nicola Cook for their technical advice, and the Horticultural Services and Field Trials team for help with growing plants and with fungicide spraying. I would like to extend my gratitude to those in North Carolina, particularly Prof. Christina Cowger and Emily Meyers, who welcomed me warmly into their lab and helped me experience the best bits of American culture.

I would like to thank my fellow students Thom Booth, Tom Eyles, Jessica Garnett, Catherine Gardener, and Billy Aldridge for our super fun board game nights and James Walker for being a lovely housemate and friend. A huge thumbs-up goes to my amazing family, Heather, Jamie, Ryan, Katie, the twinnies Olivia and Alice, Grandma Shirley, and particularly my mum and dad – even though they are crazy, they are full of love, fun, support, and endless encouragement. A final thanks goes to my two best friends, Stuart and Lauren. They have given me an enormous amount of help and happiness, and I am grateful for the amazing adventures we have had around the world.

1 General Introduction

1.1 The impact of wheat pathogens

Pathogens have colonised and infected plants for millions of years and over time many have evolved and adapted to infect particular hosts. The introduction and development of agriculture has accelerated pathogen evolution as many crops are grown as monocultures with fields of wheat, for example, often having very little genetic variation between varieties that are used. This means that there is a high chance of a pathogen spore coming into contact with a new host of the same genotype as that on which it was produced and the high density of plants makes it easier for pathogens to spread from plant to plant than it would in a field with diverse species or genotypes[1]. These pathogens include fungi, oomycetes, viruses, and bacteria which all affect the growth and fitness of crops in different ways. Examples of important wheat (*Triticum aestivum*) pathogens include three *Puccinia* species (*P. graminis*, *P. striiformis*, and *P. triticina*) which cause stem (black) rust, stripe (yellow) rust, and leaf (brown) rust of wheat[2], respectively, *Fusarium graminearum* and *Fusarium culmorum* which cause *Fusarium* head blight in cereals[2], *Blumeria graminis* which causes powdery mildew of cereals[2], and *Zymoseptoria tritici* which causes septoria tritici leaf blotch of wheat[2,3].

When *Z. tritici* disease levels are high and susceptible wheat varieties are used, yield losses can be up to 50 %, but this can be reduced to 5 – 10 % when resistant varieties are used and fungicides applied[4]. The downside to this is that resistant varieties and appropriate fungicides are not available in all wheat-growing areas, and where they are available, fungicide use can be expensive. In contrast to this, wheat stem rust in the UK has nearly been eradicated by breeding for resistance with the last major outbreak occurring in 1955, but with the emergence of the Ug99 race in Africa[5] and the yellow rust Warrior race in Europe[6], rust is becoming a major problem and increasingly poses a threat to wheat production in Europe[7]. *B. graminis* does not currently cause dramatic yield losses in the UK but is a persistent threat to cereals in temperate climates and must be controlled by using resistant or partially-resistant varieties[8] and fungicide applications[9]. When susceptible varieties are used, yield losses can reach 20 %[9]. *Fusarium* head blight is also currently not such a problem in the UK[10] but is a significant threat to cereals across North America[11], Canada[12], South America[13], other European countries[14,15], Asia[16], and Australia[17].

As a generalisation, 30 – 40 % losses in crop production are estimated worldwide per year due to pathogens affecting plant health[18]. This negatively impacts food availability and prices and threatens food security. In developing countries, it can also affect the self-sufficiency of farmers who may struggle to feed their families if they suffer high crop losses. Additionally, if farmers do

not make enough produce to sell then it may also impact their lifestyle if they cannot afford access to proper healthcare, education, and other amenities[18]. Although this is not as much of a problem in developed countries such as the UK, unpredicted outbreaks of disease are a problem and are the main source of variable costs in crop production causing reduced economic stability and risking farming businesses. As well as at the individual farmer level, crop production is valuable on a nationwide scale. Wheat harvests alone are worth approximately €2400 million to the UK economy per year (based on data from the 2013 harvest) and supply many other industries as well as food production, including biofuel production[4]. As such, it is important to be able to control diseases that heavily impact production in order to obtain high yields each year.

Farmers must ensure that the economic benefits of optimal farming practices, including sowing time, fertiliser applications, and cultivation methods, outweigh the costs. Crop diseases are near-impossible to avoid but these farming practices can promote disease amongst crops. For example, sowing crops at particular times of year can promote wheat disease, such as wheat powdery mildew which flourishes best through the summer while *Z. tritici* ascospores cause initial infection in winter wheat through the winter and spring[19]. It has in fact been shown that early sowing of winter wheat does increase *Z. tritici* disease levels[20]. Breeding for durable resistance in crops, using chemical control methods, and using crop rotation programmes are all crucial steps that need to be used together to effectively control disease while maintaining a profit.

Not only is it important to control these pathogens so the crops do not suffer, it is also important to control them as they may have harmful effects on human and animal health. For example, *Fusarium* head blight infections can produce mycotoxins that are harmful to humans and animals[2]. It is therefore important to use the most effective fungicides available and, in order to do this, the mode of action of the fungicides, and the mechanisms and evolution of fungicide resistance in target pathogens must be understood.

1.2 Wheat pathogen lifestyles

Pathogenic fungi are often classified into three groups according to their trophic habit: biotrophs, necrotrophs and hemibiotrophs. Biotrophic fungi are those that are completely dependent on the living host for survival[21]. For example, powdery mildew fungi are biotrophs and appear to have lost many of their secondary metabolism genes as they obtain many of the nutrients they need from their host plants[22]. Necrotrophic fungi are those which infect the host, kill it, and then obtain nutrients from the dead tissue. An example of this is *Parastagonospora nodorum* which causes *Septoria nodorum* blotch of wheat (SNB)[23]. However, it is not strictly

correct to classify organisms such as *P. nodorum* as necrotrophic as they have a short biotrophic phase when they initially infect the host. Finally, hemibiotrophs are those that initially infect living host tissue and establish a biotrophic relationship with the host[24]. These organisms begin to absorb nutrients, but also cause necrosis of the host tissue. In later stages of their life cycle, they continue to absorb nutrients from the dead host tissue, complete their life cycle and then pass on to a new host. *Z. tritici* is an example of a hemibiotrophic wheat pathogen which has a long latent biotrophic or endophytic period before causing necrosis[24]. As there is a fine line between biotrophic, hemibiotrophic and necrotrophic habits, it may be more suitable to say there are biotrophic and non-biotrophic pathogens.

1.3 Wheat powdery mildew (*Blumeria graminis*)

1.3.1 Asexual life cycle

In the asexual stage of the *B. graminis* life cycle, a conidium (asexual spore) lands on the leaf of its host and germinates if the humidity and temperature conditions are appropriate. Within minutes, the conidium releases an extracellular matrix that helps anchor it to the surface of the leaf[25]. A primary germ tube, a unique feature of *B. graminis*, then grows from the conidium and produces a small cuticular peg which gives an additional anchor and allows the conidium to absorb nutrients and water from the leaf[26,27]. This also plays a role in determining if the conidium has reached its target host and if it has, growth of the secondary (appressorial) germ tube is initiated[27]. The appressorial germ tube grows into a hypha on the host leaf and ultimately swells at the end to produce an appressorium. In *B. graminis*, this appressorium has a hooked, lobed shape[28]. Figure 1.3.1.1 shows a germinated conidium, demonstrating the presence of a primary germ tube and an appressorial germ tube giving rise to an appressorium.

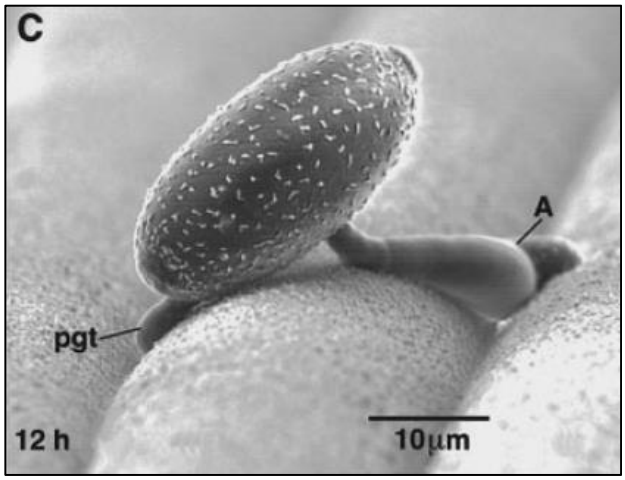

Figure 1.3.1.1: Taken from figure 9 in Carver et al. *(1999). Scanning electron microscope image of a germinated* B. graminis *conidium on a barley leaf, 12 hours after inoculation. pgt is the primary germ tube and A is the appressorium.*

The appressorium produces a penetration peg which attempts to penetrate the host cell wall[29]. As part of the pathogen-associated molecular pattern (PAMP)-triggered immunity defence mechanism, the host will often form a papilla made of cell wall components, such as callose, in an attempt to stop the pathogen from

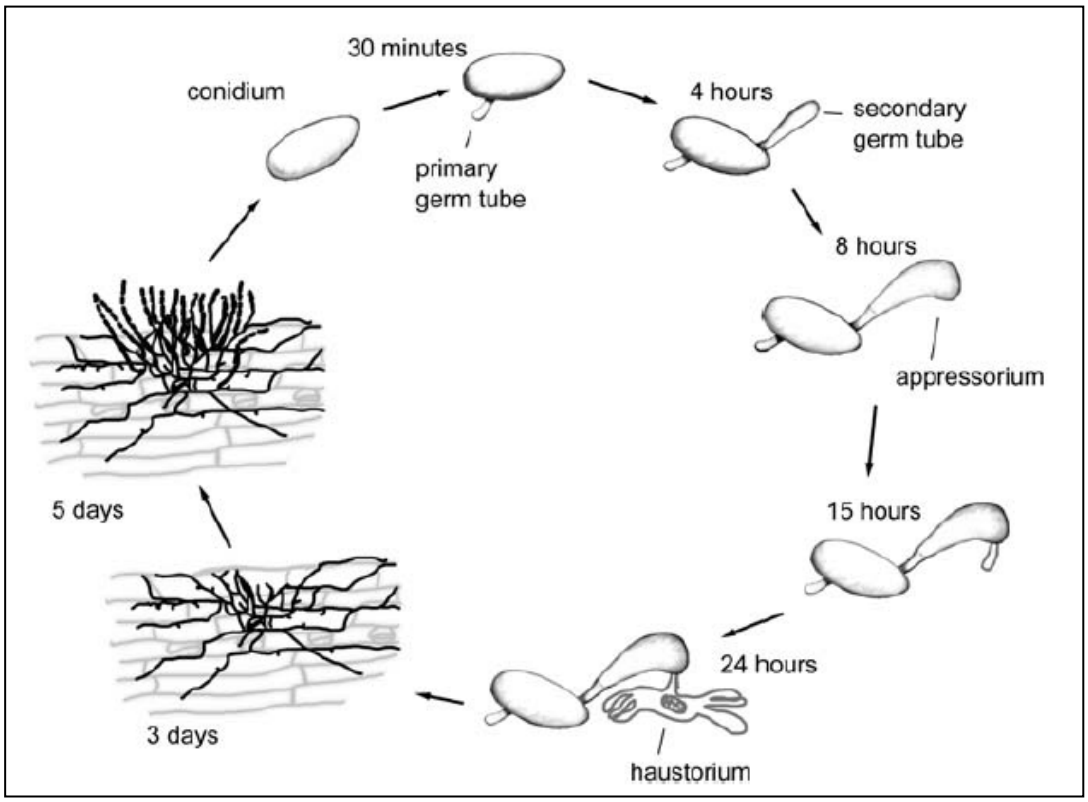

Figure 1.3.1.2: Asexual life cycle of B. graminis*. Taken from figure 1 in Both* et al*. (2005).*

penetrating through the cell wall[30]. If the penetration peg can break through this defence then it will grow into the host between the cell wall and the cell membrane, swell to cause invagination of the cell membrane, and form a haustorium[27]. The haustorium acts as a feeding organ for the pathogen as it absorbs nutrients from the host, and the interface between the haustorium and the host cell is where most of the plant-pathogen interactions occur[27]. Two days after the conidium has attached to the leaf, a secondary hypha grows from the appressorial germ tube and begins to form more haustoria[29]. After approximately four days, the fungus will begin to form conidiophores which are reproductive structures protruding from the hyphae[29]. At the base of the conidiophore is a foot cell from which chains of conidia are produced and can be dispersed[27]. Many of these conidia will land on fresh leaves and the asexual life cycle will begin again. A summary of the asexual life cycle is shown in figure 1.3.1.2[31].

As part of the asexual life cycle, another event can occur where the germinated conidium produces a conidiophore from the conidium wall itself rather than from the hyphae. This has been named microcyclic conidiogenesis and occurred at a low rate (0.5 – 4 % of germinating conidia) when 150 – 500 conidia were screened[32]. This is a faster way for the germinated conidium to produce spores and it has been shown that *B. graminis* conidia are capable of producing one to two conidiophores per conidium. The germinating conidia will produce germ tubes, appressoria and haustoria as they normally would and may even produce conidiophores

later when conidiophores have already been produced by the hyphae (see figure 1.3.1.3)[32]. This process does not replace any part of the normal asexual life cycle.

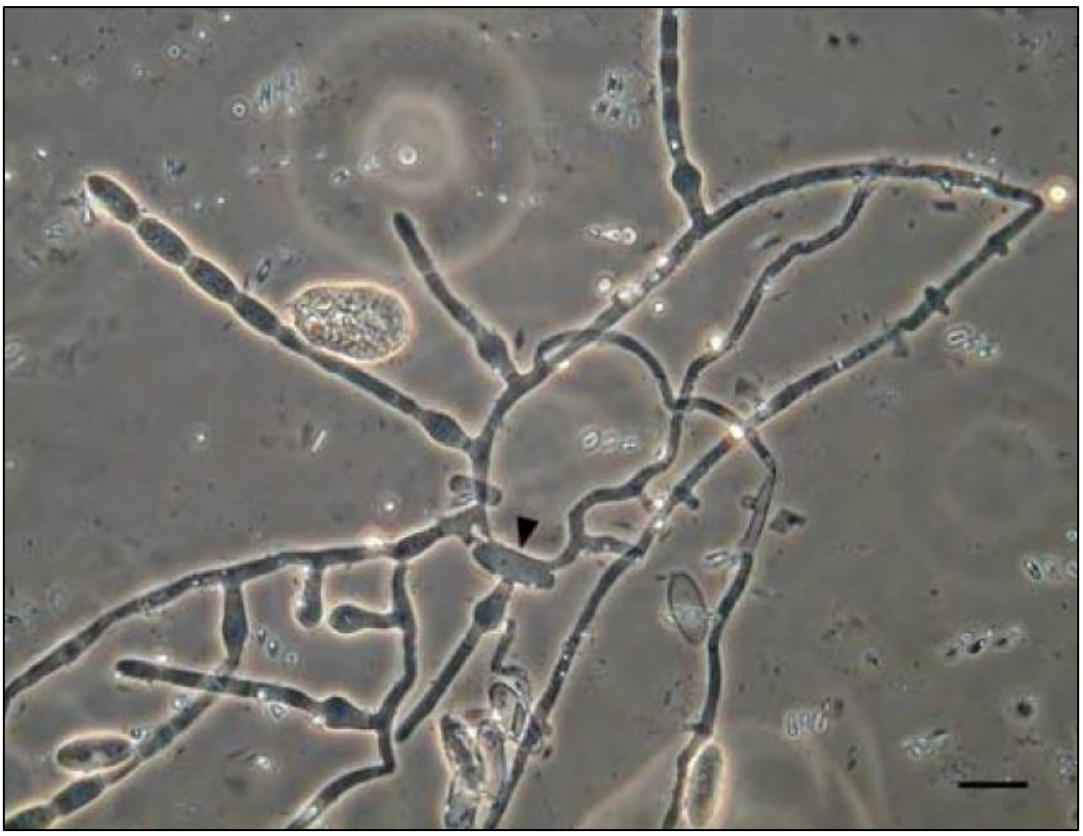

Figure 1.3.1.3: Light microscopy image showing microcyclic conidiogenesis from a B. graminis *conidium. Here the conidium is producing a conidiophore after several hyphae have formed and produced their own conidiophores. The black arrow indicates where the initial conidium is. Figure taken from Kiss* et al*. (2010).*

1.3.2 Sexual life cycle

B. graminis is an hermaphrodite and the mitochondrial DNA can be inherited from either of the parental isolates[33]. In one developing chasmothecium, one of the parental isolates will contribute cytoplasm, thus mitochondria, but the cytoplasm cannot come from both parents therefore all progeny from that chasmothecium will have the same mitochondrial inheritance. However, the inheritance of mitochondria between chasmothecia from the same parental isolates can differ[33].

When mycelia from *B. graminis* individuals with opposite mating types interact, the male antheridium and female ascogonium fuse in a process called plasmogamy[27]. In *B. graminis*, these sexual structures are less differentiated due to it being hermaphroditic, meaning that an isolate cannot be defined as male or female from the beginning of its life[33]. Individual parents only become male or female when the sexual stage is initiated. As a result of plasmogamy, a dikaryotic cell is produced and mycelia from both parental isolates grow to completely cover

this cell, forming a peridium. This structure darkens and develops into a chasmothecium where meiosis occurs, resulting in ascospore formation[27]. However, there is a delay between when the chasmothecium is formed and when ascospores are produced. It has been suggested that chasmothecia may be useful structures for allowing powdery mildew fungi to survive harsh conditions, such as very hot, dry summers (termed oversummering)[34]. During these times, the chasmothecia contain asci that are filled with undifferentiated protoplasm. It is only when they are subjected to moist conditions that they complete the production of ascospores within the asci[35-37].

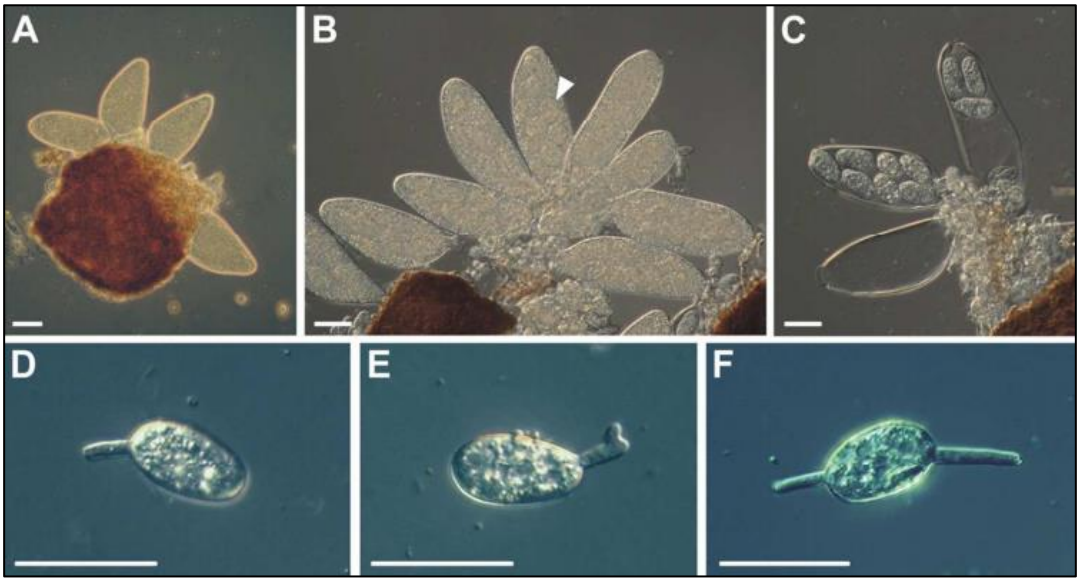

Figure 1.3.2.1: Development of ascospores in the B. graminis *sexual life cycle. Panels A to C show the development of immature chasmothecium containing undifferentiated protoplasm into a chasmothecium containing mature ascospores when submerged in water. The white arrow in panel B shows the beginning of ascospore formation in the protoplasm-filled chasmothecium. Panels D to F show germ tubes protruding from germinating ascospores. The white bar represents 20 µm. Images are taken from figure 3 in Jankovics* et al*. (2015).*

When the chasmothecia are mature and contain differentiated ascospores, they take in water from the moist environment which increases the turgor pressure within the chasmothecium and causes it to split. This releases ascospores which land on a leaf surface and germinate within ten days[36,37]. Germinating ascospores can produce between one and four germ tubes. Only one germ tube is needed at this stage to develop an appressorium leading to haustorium development as in the asexual life cycle. The growth of a colony can begin from any number of these germ tubes and within days, the hyphae begin to form conidiophores[35]. From this point, the colony continues to grow and reproduce as it does in the asexual life cycle.

Figure 1.3.2.1 shows ascospore formation and release from burst chasmothecia. Panel A shows that the asci from an immature chasmothecium contain only undifferentiated protoplasm and no ascospores, panel B shows the ascospores developing within the asci, and panel C shows the absence of protoplasm and the presence of mature ascospores after the chasmothecium has been exposed to moisture. Panels D to F show germ tubes protruding from germinating ascospores highlighting that germination of ascospores leading to establishment of a colony is a slightly different process to that from conidia[35].

1.3.3 Epidemiology and control

Powdery mildew fungi affect a whole range of plants all over the world from strawberries, grapes and cucumbers to cultivated oats, barley and wheat. Different powdery mildew species are adapted to certain host genera or families. Within the *B. graminis* species it has been observed that different *formae speciales* (ff. spp.) will only affect particular hosts and there is no cross-infection except in special circumstances[38]. In other words, *B. graminis forma specialis* (f. sp.) *hordei* (*Bgh*) will only infect barley and *B. graminis* f. sp. *tritici* (*Bgt*) will only infect wheat. The special circumstance is that *Bgt* may infect barley if the plant is already infected with *Bgh* or vice versa with wheat, by the process of induced accessibility[39]. In early research this was thought to be strict host specialisation[40,41] but in more recent years it has been found that these *formae speciales* are not strictly specialised but are well-adapted to certain hosts[42]. Additionally, isolates from wild grasses, such as ff. spp. *poae*, *bromi*, and *dactylidis*, are much less specialised than those from the cultivated cereals clade, such as ff. spp. *hordei, tritici*, *secalis* (on rye) and *avenae* (on cultivated but not wild oats)[43]. This cultivated cereals clade also includes f. sp. *agropyri* which is specific to *Agropyron*, *Elymus*, and closely-related genera of wild grasses[42].

As previously mentioned, powdery mildew fungi are obligate biotrophs therefore require the host organism to remain alive in order for the pathogen to survive and proliferate. The host will continue to grow and produce flowers and seeds, but it is possible for high yield losses to occur when susceptible varieties are grown if conditions are conducive to the disease[44]. High disease levels can also greatly affect the appearance of fresh produce making it less likely to be bought by consumers. In addition to this, lower yields can cause prices to rise through the relationship of supply and demand. As discussed earlier, this could have a negative impact on farmers if the pathogen is not controlled. However, the impact of powdery mildew fungi has been significantly decreased with the production of new fungicides, such as succinate dehydrogenase inhibitors (SDHIs) discussed in chapter 4, and successful selective breeding of varieties containing several genes giving durable disease resistance, especially in wheat and spring barley (*mlo11*[45]). The accumulation of minor genes *Lr27*, *Lr34*, *Lr46*, and *Lr67* in wheat, for example, confer a reduction in wheat powdery mildew infections and also in yellow and brown rusts[46]. Breeding for durable,

partial resistance, including the use of gene stacks such as this where available, are very effective in controlling the spread of disease whereas reliance on fungicides brings problems in the form of fungicide insensitivity.

As pathogens are constantly changing and evolving spontaneously, the continuous use of the same fungicides will eventually select for individual genotypes conferring fungicide resistance. When single-site inhibitors, such as SDHIs, triazoles or quinone-outside inhibitors (QoIs), are continuously used, quite often one or a small range of mutations conferring partial or full resistance to these fungicides become more common amongst the pathogen population[47,48], but there are several other mechanisms besides individual mutations that can develop in pathogens which also confer resistance (discussed in chapters 3 to 5). The emergence and selection for resistant individuals in pathogenic populations increases the demand for more new fungicides, especially as some resistance mechanisms can confer cross-resistance to other fungicides, as is seen particularly with the triazole fungicides (discussed in chapter 5).

To reduce the demand for new fungicides, breeding more wheat varieties with durable, partial resistance to powdery mildew fungi and other diseases is encouraged. By selectively breeding cultivars containing several moderately-effective resistance genes as opposed to cultivars with a single strongly-effective resistance gene, durable, partial resistance may be introduced, often providing strong disease control, e.g. in spring barleys such as Power[8]. With this, a less intense programme of fungicide spraying is needed to control these diseases as the pathogen should remain at a moderately low level thus reducing yield losses too.

1.4 Fungicides used to control wheat powdery mildew

Fungicides are categorised into several groups, including benzimidazoles, dicarboximide fungicides (DCFs), sterol demethylation inhibitors (DMIs), QoIs[49], sterol double-bond inhibitors (morpholines) and SDHIs. These groups are broadly based on the mode of action of these fungicides but chemicals within a group do not necessarily have closely-related chemical structures. Table 1.4.1 summarises the main fungicides currently available to control wheat powdery mildew[50,51].

Many fungicides have a single target site whereas some have a broader mode of action, such as copper salts and sulphur, e.g. Bordeaux mixture[52,53]. Resistance to fungicides that target a single site is common because it is possible for a single mutation in the fungal DNA to alter the binding affinity of the fungicide molecule to its target reducing the effectiveness of the fungicide. An example of this is with QoI fungicides (namely the strobilurins) which target the Q_o site of complex III in mitochondria (cytochrome bc_1 complex). A single G to C nucleotide change within

the cytochrome *b* gene resulting in a G143A mutation confers complete resistance to QoI fungicides in wheat powdery mildew[33,54].

With a fungicide that has a broad mode of action, more changes need to be made to confer resistance and it is unlikely that these cumulative changes will emerge in an individual at one time. This means that resistance may eventually emerge to these fungicides, but it requires more evolutionary steps to occur within a pathogen population. Although resistance occurs in many crop pathogens to several classes of fungicide, in this thesis I focus on four groups in particular: DMI, SDHI, morpholine, and amidoxine fungicides. The emergence of resistance to several products from these groups is discussed in more detail in the relevant chapters.

Two groups (DMIs and morpholines) studied in this thesis target key enzymes in the ergosterol biosynthesis pathway (figure 1.4.1[55]). DMIs target sterol C-14 α-demethylase (ERG11, also known as CYP51[49]) and morpholines target both $\Delta^8 \rightarrow \Delta^7$-isomerase (ERG2) and Δ^{14}-reductase (ERG24)[56]. Modes of action of products from these two groups and mechanisms of resistance that have emerged in target pathogens are discussed in chapters 3 (morpholines) and 5 (DMIs).

Table 1.4.1: A summary of the main fungicides available to control wheat powdery mildew based on field trials performed by the Agricultural and Horticultural Development Board. The activity rating is on a scale of 1 – 5 with 5 being the highest control of wheat powdery mildew. Chemical group, active ingredient, and activity rating are sourced from the AHDB[50]. The date that active ingredients were first introduced and their action are sourced from the Pesticide Properties DataBase[51].

Chemical group	Active ingredient	Activity rating	Action	Target site	First introduced
Amidoxine	cyflufenamid	4	Preventative & curative	Unknown	2002
Benzophenone	metrafenone	4	Protective & curative	Actin cytoskeleton regulation	2006
Morpholine	fenpropidin	3	Protective & curative	Sterol biosynthesis inhibitor	1986
Morpholine	fenpropimorph	2	Protective & curative	Sterol biosynthesis inhibitor	1983
Quinolene	quinoxyfen	2	Protective	Inhibits appressoria development	1996
Quinazolinone	proquinazid	4	Preventative & curative	Inhibits appressoria development	2005
SDHI & other	bixafen prothioconazole	3	Protective, curative & eradicative	Respiration inhibitor Sterol biosynthesis inhibitor	2006 2002
	bixafen fluopyram prothioconazole	3	Protective, curative & eradicative	Respiration inhibitor Sterol biosynthesis inhibitor	2006 2008 2002
	benzovindiflupyr prothioconazole	3	Protective, curative & eradicative	Respiration inhibitor Sterol biosynthesis inhibitor	2013 2002
Triazole	prothioconazole	3	Protective, curative & eradicative	Sterol biosynthesis inhibitor	2002
	tebuconazole	2	Protective, curative & eradicative	Sterol biosynthesis inhibitor	1986

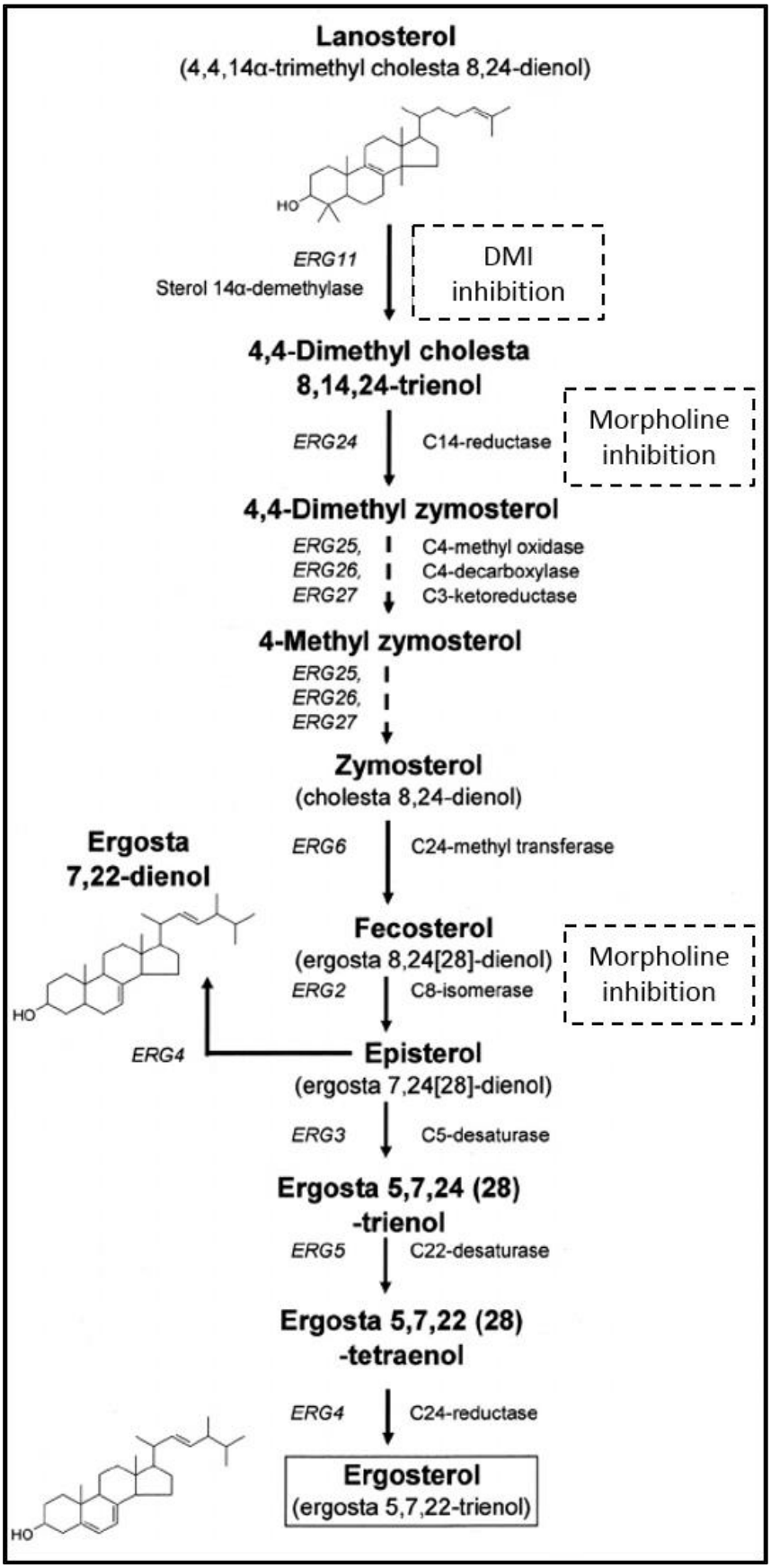

Figure 1.4.1: Schematic representation of the ergosterol biosynthesis pathway in Candida glabrata*. Sites of inhibition by DMI and morpholine fungicides are shown by dotted boxes. Figure modified from figure 1 in Hull* et al*. (2012).*

1.5 Molecular phylogeny and evolutionary divergence estimations of powdery mildew fungi

1.5.1 Phylogeny of powdery mildew fungi

Powdery mildew fungi have been shown to form a monophyletic clade using the characteristic of obligate biotrophy as a distinguishing feature of these organisms[57]. The main morphological characters used to separate the powdery mildew fungi into different genera are the number of asci that the fungi produce, the number of ascospores within each ascus, the development of conidia, the morphology of the appendages protruding from chasmothecia, endo- or ectoparasitism[58], and the decoration of the spore surface[59]. These characters can separate organisms down to the species level within this clade, but when looking at differences at a sub-species level, it is necessary to use molecular markers alongside morphological characteristics as molecular markers can highlight more subtle differences between organisms[e.g.43,60-62].

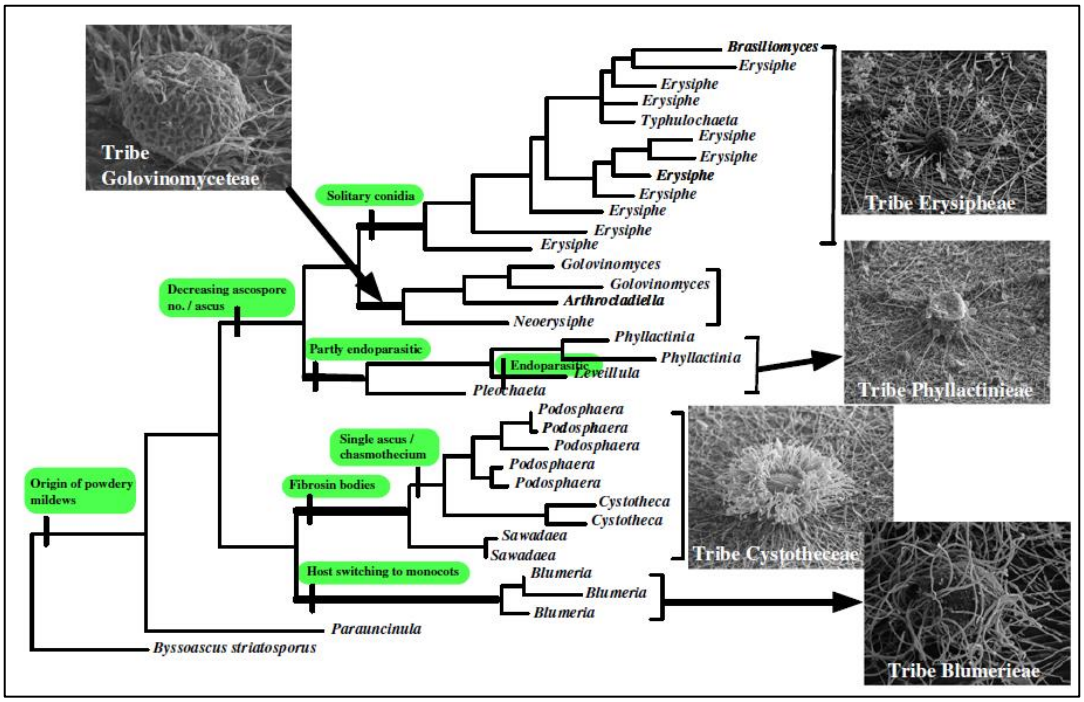

Figure 1.5.1.1: A summary of powdery mildew fungi phylogeny based on morphological features and molecular analysis of ITS sequences. Highlighted in green are evolutionary events which distinguish clades from each other. The SEM images show distinguishing features of chasmothecia and appendages of five tribes. Figure taken from Takamatsu (2013) review.

Figure 1.5.1.1 shows the current powdery mildew fungi phylogeny based on a summary of the morphological characters that identify the different genera in conjunction with molecular analysis of internal transcribed spacer (ITS) sequences[58]. From this, the genus *Blumeria* can be seen diverging from the other powdery mildew clades early in the tree due to its adaptation of

only infecting monocots. Additional characters that separate *B. graminis* from the rest of the *Erysiphales* tree include it being an ectoparasitic organism and the absence of fibrosin bodies in the conidia, which are a feature of its sister clade comprised of the *Podosphaera, Cystotheca* and *Sawadaea* genera. *B. graminis* also demonstrates euoidium-type conidiogenesis at the anamorph stage, producing several conidia per day in chains on each conidiophore[63]. At the teleomorph stage, *B. graminis* produces chasmothecia which have myceloid appendages attached to them[27] and there are several asci within each chasmothecium[27,58]. Finally, one of the most distinguishing features of *B. graminis* is that it resides only on monocots from the *Poaceae* family[43].

1.5.2 Estimating *B. graminis formae speciales* divergence times

Producing a cladogram based on morphological characters is useful at the species level but beyond that, it becomes difficult to distinguish between pathotypes of a species by looking at their physical features alone. The classification of *B. graminis* into eight *formae speciales* was originally based on its ability to infect specific hosts[40,41]. It was believed that these eight pathotypes could only infect their particular hosts, but it is now more commonly considered on the basis of molecular and pathology evidence that this is only a loose classification as it has been demonstrated on several occasions that these pathotypes are not strictly confined to certain hosts. For example, isolates from barley, oats and wheat have been shown to infect wild grasses from several genera but isolates from cultivated barley cannot infect wheat and vice versa showing specialisation within the *formae speciales* infecting crops[38]. Additionally, isolates from wild grasses can infect other wild grass hosts but not cultivated crops[64]. This points towards the idea that the divergence of the different *formae speciales* was accelerated by the cultivation of wheat, barley, oats and rye, particularly of the cultivated cereals clade of *formae speciales*[60]. Several attempts have been made to study the relationships between the eight *formae speciales* and to date the point in time at which they diverged from one another[43,60,61,65-67].

There is a great discrepancy between estimations of divergence time of the different *formae speciales* and none of the studies performed so far have included samples from all of the eight named *formae speciales* or from the diverse range of other *B. graminis* genotypes which infect many wild grassses[60,61,68] so a more thorough analysis needs to be done in order to determine the true phylogeny of *B. graminis*. As several studies suggest, using the ITS region does not supply adequate information to determine relationships at this sub-species level therefore more phylogenetically informative regions need to be used[60,68]. A closer look at these studies also reveals that the sampling of each of the *formae speciales* is not adequately representative and greater numbers of isolates from cultivated crops and wild grasses should be included in future studies along with a different species of powdery mildew to be used as an outgroup. If possible,

including isolates from a variety of geographical locations across the world would be useful for obtaining further information about the genetic diversity among the *formae speciales*.

The divergence time of the *formae speciales*, however, cannot be accurately estimated regardless of how many representative samples are included without first estimating a rate of mutation that is appropriate for powdery mildew fungi. So far it can be seen from the huge discrepancy between estimations that there is no accurate method of calculating the date of divergence of these eight *formae speciales*. Until an accurate rate can be found, current estimations can only generate hypotheses about the evolution of *B. graminis* with relation to its hosts. As soon as the divergence time can be reliably calculated and compared to the host divergence times, there should be more solid evidence for the means of divergence, whether it be through co-speciation, host-jumping, host range expansion or a combination of all three.

As it stands, divergence time estimations have been calibrated using mutation rates calculated from the *RbcL* gene in the *Golovinomyces* Asteraceae host[43,69,70] and sequence variation between two rice subspecies[61,66,67]. Due to *B. graminis* having a much shorter life cycle than these plants do and that its reproductive structures are completely exposed to natural mutagens, such as UV, on the surface of the host leaves (which is almost unique to powdery mildew fungi among the eukaryotes), it is highly improbable that it will have the same mutation rate as the host plants. Therefore, using their mutation rates as calibration points seems inappropriate. Estimations using these calibrations place the divergence time of the *B. graminis formae speciales* approximately 4.6 – 12 million years ago[43,61,65,66] which is within the Miocene epoch[71]. A more recent study instead used the estimated divergence time of powdery mildews from other fungi[72,73], of the *B. graminis* monocot hosts from dicots[74], and of *B. graminis* f. sp. *poae* from other *formae speciales*[75] as calibration points for estimating the divergence times of the *formae speciales*. This gave a divergence time between *B. graminis* ff. spp. *tritici*, *secalis*, and *dactylidis* from other *formae speciales* of 170,000 – 280,000 years ago[62] which is within the Pleistocene epoch[76]. Although the divergence time estimation of the Ascomycetes was based on fossil records, the other calibration points were again based on mutation rates of plants which is inappropriate for dating powdery mildew fungi. This suggests that this divergence time estimation is still a large over-estimation and the hypothesis proposed by Wyand and Brown (2003) is more probable. In particular, it is difficult to explain why the sister group of ff. spp. *tritici*, *secalis* and *hordei*, which infect hosts in the tribe Triticeae, is f. sp. *avenae*, which infects cultivated oats (*Avena sativa*) in the tribe Poeae, unless these *formae speciales* emerged from a common ancestor and became specialised in early agriculture, as proposed by Wyand and Brown (2003).

This earlier study suggests that divergence of the *B. graminis formae speciales* is more likely to have occurred during the current Holocene epoch[77] approximately 14,000 years ago, coinciding with the beginning of agriculture, the domestication of cereals, and their cultivation as stands of single species[60]. If this hypothesis is true, then the mutation rate of *B. graminis* genes is likely to be much faster than of genes in the plants that have been used for calibration so far. A recent study estimated the date of divergence between *B. graminis* ff. spp. *tritici* and *secalis* using both the Wyand and Brown (2003) estimation and the Wicker *et al*. (2013) estimation as calibration points separately. These two calibrations set the divergence between *Bgh* and *Bgt* as 10,000 – 14,000 years ago and 5.2 – 7.4 million years ago, respectively, and give estimations of *B. graminis* ff. spp. *tritici* and *secalis* divergence times as 638 – 1280 years ago and 168,245 – 240,169 years ago[67]. This is a 131- to 376-fold difference in rate of mutation which clearly shows the need for a better study of powdery mildew-specific rate of evolution. It seems much more likely for the Holocene epoch hypothesis to be true, particularly as the phylogeny of *B. graminis* isolates from cultivated cereals matches the phylogeny of cultivated hosts while the phylogenies of the wild *formae speciales* and their hosts are much less congruent[42,43].

1.6 Aims of this thesis

1.6.1 Fungicide resistance in *Blumeria graminis* f. sp. *tritici* isolates.

Blumeria graminis f. sp. *tritici* (*Bgt*) is a high-risk pathogen for developing resistance to fungicides, for example, it rapidly evolved resistance to QoI fungicides (e.g. azoxystrobin)[33] as well as DMIs (e.g. triadimenol)[78]. Four groups of fungicides (DMIs, morpholines, SDHIs and amidoxines) currently reported to be effective at controlling *Bgt*[79] were found to be ineffective when used in the John Innes Centre (JIC) glasshouses in 2014. Unfortunately, excessive use of the amidoxine cyflufenamid and of the combination formula Aviator[235] Xpro containing bixafen (SDHI) and prothioconazole (DMI; triazole) was unable to control *Bgt* in the glasshouses which suggested resistance to one or more of these fungicides had occurred. As SDHI resistance has emerged amongst other pathogens, such as *Z. tritici*[48], this seemed like the most likely candidate for resistance emergence therefore this was investigated first followed by resistance to cyflufenamid (chapter 4). Investigating SDHI resistance led to exploring the mechanisms of resistance to DMIs (chapter 5) as they were both sprayed in combination in the glasshouses and additional applications of the DMI prothioconazole were also unable to control *Bgt* in the glasshouses. It was noted that two applications of fenpropimorph (morpholine) also failed to control *Bgt* therefore the emergence of resistance to this fungicide was investigated and characterised (chapter 3).

1.6.1.1 Characterisation of increased resistance to the morpholine fungicide fenpropimorph

Based on the poor control of *Bgt* in the glasshouses and previous emergence of resistance, the effectiveness of fenpropimorph against current UK *Bgt* isolates compared to an older isolate was investigated. This fungicide is still used in agriculture and medicine therefore it is important to check its effectiveness and to track the emergence of resistance. Isolates with increased resistance to fenpropimorph were identified which were then used to identify mutations within the target protein ERG24 that were associated with resistance. This is the first known report of the identification of specific mutations in ERG24 linked to morpholine resistance in natural populations of a fungus.

1.6.1.2 Identifying resistance to cyflufenamid and its potential targets in Bgt

The effectiveness of the SDHI fungicide bixafen against *Bgt* isolates from the JIC glasshouses compared to isolates from the UK field population and an older isolate was investigated. As resistance to SDHIs had not occurred within the glasshouse *Bgt* population, the emergence of resistance to a newer fungicide, cyflufenamid, was also investigated. An RNA-seq approach was used to identify potential candidate targets of this fungicide as the mode of action is currently unknown. This is the first identification of a likely target site for cyflufenamid and the first report of the molecular genetic basis of resistance to amidoxines.

1.6.1.3 Characterisation of resistance mechanisms present in Bgt *isolates to DMI fungicides*

As the application of the DMI fungicide prothioconazole also failed to control the *Bgt* in the glasshouses and increased resistance to DMIs is widespread across many pathogens, including wheat powdery mildew, the mechanisms of resistance present in these *Bgt* isolates were explored. Mutations within the *Cyp51* gene as well as alterations in copy number, gene expression, and promoter region sequences were identified and characterised, with the presence of at least two copies of the *Cyp51* gene being identified in *Bgt* isolates for the first time. It was shown that heteroallelism, with two alleles of *Cyp51* being present within a single *Bgt* isolate, contributes to resistance to triazole fungicides.

1.6.2 Molecular evolution of *formae speciales*

As there is currently no appropriate mutation rate available for dating the divergence of the *B. graminis formae speciales*, the aim of this part of the thesis was to estimate a rate of evolution using the mutation accumulation method. The hypothesis is that the *formae speciales* had begun to diverge millions of years ago but this divergence was rapidly increased at the beginning of agriculture around 10,000 – 14,000 years ago in the Holocene Epoch. If this is the case, then *B.*

graminis most likely evolves at a much faster rate than has been suggested by previous divergence time estimations which were based on calibrations using plant mutation rates. A faster mutation rate would also explain how *B. graminis* acquires resistance to fungicides so rapidly. The mutation rate calculated using this method could then be applied to date the divergence of the *formae speciales*. This work is discussed in Appendix II.

2 General materials and methods

2.1 Sample collection

UK isolates were collected from farms and the natural environment in various locations around Norfolk. Small sections of leaf surrounding individual colonies were cut from trays of seedlings of the mildew-susceptible wheat cultivar Cerco for *Bgt* isolates and barley cultivar Golden Promise for *Bgh* isolates that had been placed outside to capture airborne spores. Individual colonies were also collected from wheat plants in the glasshouses at Norwich Research Park. All isolates were grown for one or two generations then reduced to single-spore colonies to ensure they were pure samples. Swiss isolates 96224 and 94202 were obtained from Prof. Beat Keller, University of Zurich. US isolates were obtained from Emily Meyers and Prof. Christina Cowger, USDA-ARS and North Carolina State University. Tables 2.1.1 to 2.1.7 contain information about isolates used in this thesis.

Table 2.1.1: Summary of Bgt *isolates collected in JIC's glasshouses in 2014/5 to investigate responses to cyflufenamid (Cyflamid).*

Isolate	Location of collection	Year of collection	Isolate	Location of collection	Year of collection
CAW14S6101	Glasshouse S61	2014	**CAW14S6313**	Glasshouse S63	2014
CAW14S6102			**CAW14S6314**		
CAW14S6103			**CAW14S6316**		
CAW14S6104			**CAW14S6317**		
CAW14S6301	Glasshouse S63		**CAW14S6318**		
CAW14S6302			**CAW15S6320**	Glasshouse S63	2015
CAW14S6303			**CAW15S6323**		
CAW14S6304			**CAW15S6324**		
CAW14S6305			**CAW15S6325**		
CAW14S6306			**CAW15S6327**		
CAW14S6307			**CAW15S6328**		
CAW14S6308			**CAW15S6330**		
CAW14S6309			**CAW15S6331**		
CAW14S6310			**CAW15S6332**		
CAW14S6311			**CAW15S6334**		
CAW14S6312					

Table 2.1.2: Summary of Bgt *isolates collected in JIC's glasshouses in 2015 to investigate responses to both cyflufenamid (Cyflamid) and fenpropimorph (Corbel).*

Isolate	Location of collection	Date of collection	Isolate	Location of collection	Date of collection
CAW15W101	West-1 glasshouse	2015	**CAW15S6337**	Glasshouse S63	2015
CAW15W102			**CAW15S6338**		
CAW15W103			**CAW15S6339**		
CAW15W104			**CAW15S6340**		
CAW15W105			**CAW15S6341**		
CAW15S6335	Glasshouse S63		**CAW15S6342**		
CAW15S6336			**CAW15S6343**		

Table 2.1.3: Summary of Bgt *isolates collected from JIC's glasshouses and polytunnels in 2016 by Rachel Burns.*

Isolate	Location of collection	Date of collection	Isolate	Location of collection	Date of collection
RBPT32	Ben Hales' Polytunnel (no fungicide applied)	2016	**RBPTM9**	Rachel Burns' Polytunnel for mildew trial (no fungicide applied)	2016
RBPT33			**RBPTM44**		
RBPT34			**RBPTM60**		
RBPT35			**RBS54_1**	Glasshouse S54	
RBPT36			**RBS54_3**		
RBPT39			**RBS54_8**		
RBPT40			**RBS54_9**		
RBPT22	James Simmonds' Polytunnel		**RBS54_11**		
RBPTM2	Rachel Burns' Polytunnel for mildew trial (no fungicide applied)		**RBS54_14**	Glasshouse S54	
RBPTM3			**RBS57_3**	Glasshouse S57	
RBPTM5			**RBS57-6**		
RBPTM8					

Table 2.1.4: Summary of UK Bgt *isolates from the air spora, wheat fields or isolated from wheat plants growing as weeds in gardens, referred to in this thesis as "UK field isolates". The number in brackets indicates how many isolates were collected from that location.*

Isolate	Location of collection	Date of collection
EOW15 (x2)	Wymondham	2015
JBW15 (x5)	Hockering	
CMW15 (x5)	Swaffham	
ADW15 (x3)	Kenninghall	
ASW15 (x5)	Ingworth	
AEW15 (x4)	Holt	
TKW15 (x5)	Lowestoft	

Table 2.1.5: Summary of US Bgt *field isolates collected by our collaborators Prof. Christina Cowger and Emily Meyers, USDA-ARS and North Carolina State University.*

Isolate (UK name used in this thesis)	US name	Location of collection
Harry	OKH-A-2-1	Hinton, Oklahoma
Hermione	OKS-B-1-4	Stillwater, Oklahoma
Ron	OKS(14)-A-2-3	Stillwater, Oklahoma
Ginny	OKS(14)-B-3-5	Stillwater, Oklahoma
Malfoy	NEL-6	Lincoln, Nebraska
Dumbledore	KSM-C-2-4	Manhattan, Kansas
Snape	KSM-C-3-4	Manhattan, Kansas
Moody	KSM-C-2-5	Manhattan, Kansas
McGonagall	GAT-A-3-4	Thomasville, Georgia
Hagrid	GAP-B-2-2	Pine Mountain, Georgia
Sirius	MOB(14)-B-1	Bronaugh, Missouri
Filch	MOB(14)-D-2	Bronaugh, Missouri

Table 2.1.6: Summary of European Bgt *isolates.*

Isolate	Location of collection	Date of collection	Isolate use
JIW11[33]	UK	1985	Older UK isolate
Fel09[33]	Germany	1998	Older EU isolate
96224[66]	Switzerland	1996	Older EU isolate (reference genome)
94202[66]	Switzerland	1994	Older EU isolate

Table 2.1.7: Summary of Bgh *isolates.*

Isolate	Location of collection	Date of collection
DH14[80] (reference genome)	England	1976
CC52[78]	Aberystwyth	1980
CC148[81,82] (clone of CC151)	Cambridge	1985
W4	Norfolk	2017

2.2 Isolate maintenance

All wheat powdery mildew samples were maintained on detached leaves of Cerco. Barley powdery mildew isolates were maintained on detached leaves of susceptible barley cv. Golden Promise. Infected leaves were laid on 5 g/L water-agar containing 100 mg/L benzimidazole and were kept at a constant 15 °C with a 16-hour day length of maximum intensity white light supplied by fluorescent tubes and supplementary near-UV light. Conidia from each sample were transferred to fresh detached wheat or barley leaves every 10 – 12 days.

2.3 DNA extractions

DNA was extracted from all isolates in tables 2.1.1 to 2.1.7. Three infected detached leaves per isolate were used for DNA extraction 12 – 14 days after inoculation. Leaves were wrapped in tin foil, frozen in liquid nitrogen and ground to a fine powder using a pestle, mortar and a small amount of sand. Liquid nitrogen was periodically added to ensure the sample stayed frozen while it was being ground. DNA was extracted from each isolate using the QIAGEN DNeasy Mini Plant Extraction Kit according to the manufacturer's protocol. DNA was quantified using a NanoDrop2000 spectrophotometer. It is important to note that NanoDrop readings of DNA from infected leaves were only a guideline to the amount of *B. graminis* DNA as there was a mix of DNA from the fungus and the leaf.

2.4 RNA extractions

To collect material for RNA extraction, epidermal peels were taken from approximately 40 infected detached leaves per isolate. This was done by generously painting 5 % cellulose acetate onto the surface of the infected leaves, leaving this to dry and peeling off the cellulose acetate. This removed the mycelium and upper epidermis of the leaf thereby removing most of the plant tissue. All peels for one isolate were wrapped in tin foil and stored at -80 °C. Epidermal peels were ground using a pestle, mortar, liquid nitrogen, and small amount of sand for added friction. RNA was extracted from ground samples using a QIAGEN RNeasy Plant Mini Kit according to the manufacturer's protocol using buffer RLT. Two minor modifications were made to the protocol: after adding ethanol to the lysate, this mixture was passed through the RNeasy mini spin column

two to three times instead of once to collect as much RNA as possible, and at the end of the protocol, the RNA was eluted in 35 µL RNase-free water which was passed through the column a second time to collect any remaining RNA. To measure the quality and quantity of RNA, the samples were analysed on an Agilent 2100 Bioanalyser.

2.5 RNA-seq

RNA for each isolate (~3 µg) was sent to GENEWIZ UK (Takeley, Essex) for library preparation and sequencing on the Illumina HiSeq platform (2 x 150 bp). Once the sequences were obtained, adapters and barcodes were trimmed using the FASTX toolkit version 0.0.13.2. This toolkit was also used to obtain quality plots for the sequences to assess nucleotide distribution and the quality of the data. The relevant reference genome (*Bgt* 96224 or *Bgh* DH14) was indexed using Burrows-Wheeler Alignment (BWA) version 0.7.7 and Bowtie version 2.2.1 software[83]. The 150 bp paired-end reads were aligned to the reference assembly using the TopHat package version 2.0.11 which employs the Bowtie program (version 2.2.1) to align reads to the assembly and identify transcript splice sites[84,85]. After alignment, SAMtools version 0.1.19 was used to convert the alignment from BAM (Binary Alignment/Map) into SAM (Sequence Alignment/Map) files by removing duplicate sequences so they are not reported multiple times, sorting the mapped reads by co-ordinate and indexing them so alignments in a particular region can be retrieved later. These BAM files were then used by SAMtools for single nucleotide polymorphism (SNP) calling. Files were then generated for each isolate that included the chromosome each SNP was located on, the nucleotide position, the reference genome nucleotide, the given isolate's nucleotide, and the frequency of the given nucleotide in the reads. SNPs were identified at both 10x and 20x coverage[83,86,87]. Further analysis performed is discussed in the relevant chapters. This alignment and SNP calling pipeline was developed by Dr. Diane Saunders' group and was adapted for this thesis by Dr. Antoine Persoons and Dr. Guru Radhakrishnan.

2.6 Fungicide agar tests

In order to compare the levels of sensitivity between isolates, their responses were initially tested by adding increasing doses of the relevant fungicide to molten water-agar and making up one Petri dish per fungicide dose per isolate. Once the agar had set, the central section was cut out, three susceptible detached leaves were placed over the gap in the middle, and the cut-out agar was placed over the ends of the leaves to sandwich them between agar. The fungicide is taken up by the leaf from the ends that are sandwiched between agar. This setup can be seen in figure 2.6.1.

The Petri dishes were inoculated by placing all doses for one isolate inside an inoculating tower and blowing spores into the top of the tower. The spores should then be distributed evenly across the three leaves which act as three replicates for each dose.

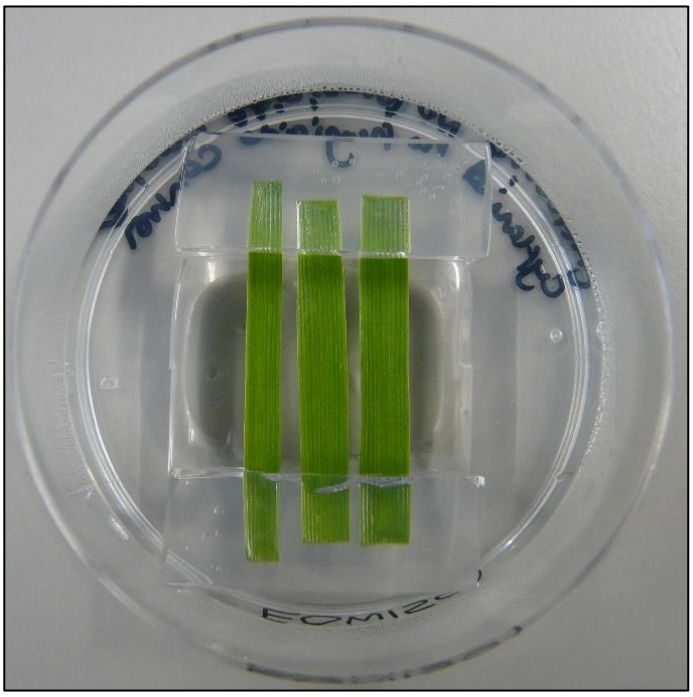

Figure 2.6.1: Fungicide agar test setup. Fungicide is aliquoted into the molten agar which is then poured into each Petri dish. Once set, the middle portion of agar is cut out, three detached leaves are placed across the gap and the cut-out agar is placed over the ends of the leaves. The fungicide is taken up from the agar through the ends of the leaves.

For all fungicides tested (Aviator^{235} Xpro, Proline, Cyflamid and Corbel), an initial broad 10-fold dilution series was used from 0.01 µg/mL to 100 µg/mL. This was to identify the best range of doses to be used for each fungicide. Doses used were then narrowed down to the appropriate range for the fungicide. This is discussed further in the relevant chapters. As there were three detached leaves per dose per isolate, the number of individual colonies on each leaf were counted and an average number of colonies per Petri dish (i.e. per dose per isolate) was calculated.

2.7 Fungicide spray tests

As adding fungicides into agar does not reflect the normal method of application of agrochemicals in field or glasshouse practice, spray tests were also performed. As this is how fungicides are normally used in the field, this gives a more realistic view of how isolates respond to the fungicides. The method used here is based on that from Brown and Evans (1992).

For all wheat powdery mildew fungicide spray tests, trays of Cerco seeds were sown and grown for 10 – 11 days in a glasshouse with additional lighting. For barley powdery mildew tests, trays

of Golden Promise were sown instead. Seedlings were sprayed with fungicides using a Berthoud 5 L Elyte 8 compression sprayer fitted with a flat fan nozzle producing a fine mist at 1.5 bar pressure. One tray of seedlings was sprayed with one dose of fungicide and as the trays were being sprayed, four additional trays of seedlings were placed around that tray to reduce edge-effects of spraying. Each fungicide dose was made up to 0.5 L and each seedling tray was sprayed four times to obtain the desired final dose. This meant that the coverage of the seedlings was more even than it would have been with a single spray. Once sprayed, each seedling tray was placed separately into plastic propagators with clear lids. Propagators were placed in a glasshouse overnight to allow the fungicide to dry.

The first leaf of seedlings was cut to 3 cm in length and three detached leaves per dose were placed in Petri dishes of water-agar containing 50 mg/L benzimidazole. All doses for one isolate were placed under an inoculating tower and conidia were blown into the top of the tower to inoculate the leaves evenly. This was repeated for all isolates included in each test. Petri dishes were incubated at 15 °C with a 16-hour day supplemented with near-UV light. Eight days after inoculation, the number of colonies present on each leaf were counted and an average of all three leaf scores was calculated. Specific dose ranges and methods for each fungicide are discussed in the relevant chapters. Two replicates were carried out for every fungicide spray assay.

2.8 Calculating median effective doses (ED_{50})

To calculate ED_{50}s, isolates were first grouped into categories (see relevant chapters for details on which isolates were put into which categories). Average colony counts were averaged across all isolates within each category for each dose and doses were $\log_{10}$-transformed. For the purposes of the calculations, the no-fungicide control dose of 0 mL/ha was entered as being one step below the actual minimum dose in the series. Mean colony counts for each of the categories were fitted to a logistic curve and the maximum colony count (C in equation 1 below), gradient of the curve at the point of inflection (B), ED_{50} (M) and ED_{50} standard errors were estimated. The Genstat v.18 package was used for statistical analysis.

$$1)\ Y_i = C\left\{1 + e^{-B(X_i - M)}\right\}^{-1}$$

where Y_i is the fitted value of colony number at dose X_i. The least significant difference between the ED_{50}s of the field resistant and GH resistant categories was calculated using equation 2.

$$2)\ LSD_P = z_{P/2}\left({SE_{FR}}^2 + {SE_{GHR}}^2\right)^{0.5}$$

where P is the test probability, $z_{P/2}$ is the standard normal deviate for a probability of $P/2$ to give a two-sided test, and SE is the standard error of the ED_{50}.

3 Identification of increased resistance in *Blumeria graminis* f. sp. *tritici* and *Blumeria graminis* f. sp. *hordei* isolates to fenpropimorph, and characterisation of mutations associated with this resistance

3.1 Introduction

Fenpropimorph is a morpholine fungicide first introduced into agriculture in 1983[51] and is applied as Corbel (BASF) in the UK. Corbel, and other fenpropimorph-containing products, have since continued to be used in agriculture and have remained at least partially effective at controlling cereal powdery mildew fungi and rusts[88].

Morpholines target the ergosterol biosynthesis pathway in many organisms causing membrane disruption and the inhibition of cell division[89]. Previous studies have shown that application of fenpropimorph and other morpholines to *Penicillium italicum*[90], *Saccharomyces cerevisiae*, *Botrytis cinerea*, and *Ustilago maydis* results in an accumulation of intermediate sterols, namely Δ^8-sterol (fecosterol in *S. cerevisiae*[91]) and $\Delta^{8.14}$-sterol (ignosterol in *S. cerevisiae* and *U. maydis*[91]), suggesting that these fungicides inhibit two key enzymes in the pathway: $\Delta^8 \rightarrow \Delta^7$-isomerase (encoded by the *Erg2* gene in *Blumeria graminis*) and Δ^{14} -reductase[56] (encoded by the *Erg24* gene in *B. graminis*). The locations of these enzymes within the ergosterol biosynthesis pathway are shown in chapter 1 figure 1.4.1.

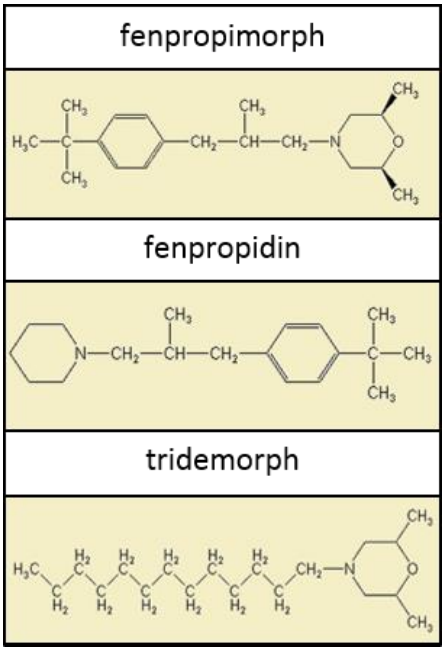

Figure 3.1.1: Molecular structure of three morpholine fungicides: fenpropimorph, fenpropidin, and tridemorph from the Pesticide Properties DataBase.

In *S. cerevisiae*, it was shown that $\Delta^8 \rightarrow \Delta^7$-isomerase was most strongly inhibited by fenpropimorph, followed by tridemorph (another morpholine) then fenpropidin (a piperidine fungicide similar to morpholines), whereas Δ^{14} –reductase was most strongly inhibited by fenpropimorph, followed almost as strongly by fenpropidin, then much more weakly by tridemorph[92]. The molecular structures of these three fungicides are shown in figure 3.1.1 for comparison. In contrast to this, it has been demonstrated that in *U. maydis* $\Delta^8 \rightarrow \Delta^7$-isomerase was most potently inhibited by tridemorph, followed by fenpropimorph then fenpropidin, and Δ^{14} –reductase was most inhibited by fenpropidin, and significantly less by fenpropimorph and

tridemorph[91]. Interestingly, the experiments with *S. cerevisiae* were performed *in vitro* with cell-free enzyme assays[92], whereas the *U. maydis* experiments were performed *in vivo*[91]. It is possible that the three fungicides may behave differently in *S. cerevisiae in vivo*. Isolation of sterol biosynthesis enzymes and tests of their activity in the presence of fenpropimorph, fenpropidin, and tridemorph have not been done with cereal powdery mildew fungi. Phenotypic assays showing the level of resistance to the three fungicides, however, have been reported.

A study on barley powdery mildew *Blumeria graminis* f. sp. *hordei* (*Bgh*) described the collection of many isolates from across eastern England, north-east England and eastern Scotland where these three fungicides had been used in agriculture[81]. Two groups of isolates were identified and categorised as resistant or sensitive to both fenpropimorph and fenpropidin as responses to these two fungicides were highly correlated. Additionally, there was a weak positive correlation between increased resistance to fenpropimorph and fenpropidin, and to tridemorph[81]. Although there was an increased resistance to fenpropimorph and fenpropidin in the resistant isolates, the ED_{50} values (the median effective dose; 0.022 mL/L and 0.045 mL/L, respectively) were still significantly lower than the recommended field application rates of these fungicides (0.06 mL/L and 0.063 mL/L, respectively) showing that complete resistance to these fungicides had not occurred, but the effectiveness was reduced from excellent to moderate control of *Bgh*. These results correlated with the results obtained from experiments with *S. cerevisiae* and *U. maydis* as both of these showed that fenpropimorph and fenpropidin interacted more strongly with Δ^{14} –reductase than tridemorph did[91,92]. This suggests that fenpropimorph and fenpropidin do target this enzyme in *Bgh* and perhaps that tridemorph preferentially targets $\Delta^{8} \rightarrow \Delta^{7}$-isomerase instead, but this hypothesis has not been tested biochemically in *Bgh*.

A further study highlighted the increased frequency of fenpropimorph-fenpropidin-resistant *Bgh* isolates since 1988[82]. This study reinforced the results from the 1991 paper demonstrating that isolates more resistant to fenpropimorph were also more resistant to fenpropidin showing that they exhibited cross-resistance[81,82]. Interestingly, the correlation between fenpropimorph-fenpropidin resistance and tridemorph resistance was reversed in one location in this study as it was shown that the application of tridemorph actively selected against isolates that were fenpropimorph-fenpropidin-resistant, with a stronger selection against isolates that had a higher ED_{50} value for fenpropidin than fenpropimorph. Selection against isolates with a higher ED_{50} value for fenpropimorph than fenpropidin was not significant. Fenpropimorph minimum inhibitory concentrations (MIC) of isolates from tridemorph-treated plots were lower than from the untreated plots, but it was not a significant difference. It was suggested that the negative correlation between selection for responses to tridemorph and the other compounds could be

due to the slightly different mode of action of tridemorph indicated by the previous studies already described here[82,91,92].

Additionally, it was shown in this study that there was some degree of cross-resistance between fenpropimorph and tridemorph in *Bgh* isolates, but it was not as strong as with fenpropimorph and fenpropidin[82]. It was suggested that this weak correlation could be due to tridemorph targeting $\Delta^8 \rightarrow \Delta^7$-isomerase which fenpropimorph has a weaker affinity for. This complemented the results from *U. maydis* which showed tridemorph was a more potent inhibitor of $\Delta^8 \rightarrow \Delta^7$-isomerase than fenpropimorph or fenpropidin[91], suggesting the same mode of action occurs in *Bgh*. Another study in *S. cerevisiae* highlighted that the introduction of a high-copy plasmid containing the *Erg2* gene (encoding $\Delta^8 \rightarrow \Delta^7$-isomerase) did not increase resistance to fenpropimorph[93]. This suggests that either *Erg2* was not overexpressed as expected, or that fenpropimorph has a weak or no affinity for $\Delta^8 \rightarrow \Delta^7$-isomerase[93]. This study also showed that *Erg24* is an essential gene. All of these studies together suggest that fenpropimorph mainly targets Δ^{14}–reductase (i.e. ERG24) in yeast and other fungi and has a weak affinity for $\Delta^8 \rightarrow \Delta^7$-isomerase (i.e. ERG2), and that resistance is more likely to come from mutations associated with the former enzyme than with the latter.

An additional study showed that *Erg24* mutants were lethal in a wild-type *S. cerevisiae* background, but were rescued when two suppressor mutant genes, *fen1* (flap endonuclease 1 involved in DNA damage repair; UniProtKB ID P26793) and *fen2* (pantothenate transporter; UniProtKB ID P25621), were present[94]. This study suggested that rather than the loss of ERG24 activity causing lethality to the cells, it was caused by the accumulation of the intermediate sterol ignosterol and *fen1/fen2* genes allowed the cell to adapt to this change in sterol composition[94]. A later study also showed that *Erg24* mutants were viable in a *fen1* mutant background, but also that they were able to grow in a wild-type background on rich medium supplemented with Ca^{2+} or Mg^{+2} [95]. This complements a previous study which suggested that the addition of Ca^{2+} was able to stabilise membrane integrity when ergosterol was substituted for intermediate sterols, such as ignosterol[96].

There are currently no reliable transformation methods available for powdery mildews *Bgh* and *B. graminis* f. sp. *tritici* (*Bgt*), therefore it is not possible to produce mutants and study the phenotypic effect on sensitivity to fenpropimorph. However, genetic crosses between a fenpropimorph-fenpropidin-resistant *Bgh* isolate and a sensitive *Bgh* isolate showed a 1:1 segregation between resistant and sensitive progeny which suggested a single gene (labelled *fen1* in this study) was involved with resistance[97]. Responses of the more-resistant progeny isolates to fenpropimorph and fenpropidin separately showed that there was greater resistance to fenpropidin suggesting that modifications to this gene may cause slightly different responses

to these fungicides[97]. These progeny isolates also displayed reduced sensitivity to tridemorph, but the reduction was not as large as with fenpropimorph and fenpropidin which complements previous studies[81,82,97].

A second cross between a resistant and sensitive isolate resulted in a 3:1 segregation in progeny that were resistant and sensitive to fenpropimorph and fenpropidin, and those resistant progeny seemed to have no increased resistance to tridemorph compared to the sensitive progeny[97]. This suggested that two unlinked genes may be involved in resistance and that at least one of them was not located at *fen1*[97]. This supports all of the other studies described here that two enzymes are targeted by morpholine fungicides.

Additional studies have been performed in *Aspergillus niger* and *U. maydis*, both showing that two unlinked genes seem to be involved in fenpropimorph resistance[98,99]. In *A. niger*, it was demonstrated using UV-induced mutants that fenpropimorph resistance was a recessive phenotype and was associated with two loci[98]. These mutants also exhibited resistance to fenpropidin[98] which complements all previous studies described here.

In *U. maydis*, two loci labelled *U/fpm-1* and *U/fpm-2* were identified as being associated with high resistance to fenpropimorph[99]. Additionally, in mutants showing low levels of resistance to fenpropimorph only one locus was identified, which was labelled *U/fpm-x*. A series of crosses between mutants with high resistance and with low resistance resulted in the *U/fpm-1* and *U/fpm-x* loci being identified as different alleles of the same gene. The *U/fpm-1A* (formerly *U/fpm-1*) allele conferred high resistance to fenpropimorph and the *U/fpm-1B* (formerly *U/fpm-x*) allele conferred low resistance. The crosses also showed that progeny with both *U/fpm-2* and *U/fpm-1A* mutations, and progeny with *U/fpm-2* and *U/fpm-1B* exhibited high resistance conferred by *U/fpm-2*, and neither the *U/fpm-1A* nor *U/fpm-1B* alleles had an additive effect[99].

As well as identifying the loci involved in resistance, this study showed that mutations at these loci also conferred increased levels of resistance to fenpropidin and tridemorph[99]. The *U/fpm-1A* allele and *U/fpm-2* locus were identified as having increased resistance to fenpropidin, but this increase was not as high as with fenpropimorph, and they also gave a low resistance to tridemorph. The *U/fpm-1B* allele gave a relatively low level of resistance to fenpropidin compared to the other allele and locus, but also the same low level of resistance to tridemorph. Further analyses of cross-resistance showed that *U/fpm-1A* allele and *U/fpm-2* locus mutants had unaltered sensitivity to inhibitors (e.g. triazoles) that act on enzymes of the ergosterol biosynthesis pathway preceding Δ^{14}–reductase, whereas mutants with the *U/fpm-1B* allele had increased sensitivity[99]. This is indicative of fenpropimorph and fenpropidin having strong inhibitory effects on Δ^{14}–reductase potentially encoded by a gene at the *U/fpm-2* locus and

having very low inhibitory effects on the product of the *U/fpm-1B* allele, which could potentially be $\Delta^8 \rightarrow \Delta^7$-isomerase or another enzyme earlier in the ergosterol biosynthesis pathway.

Although most studies show that fenpropimorph and related morpholine-like fungicides target the $\Delta^8 \rightarrow \Delta^7$-isomerase and Δ^{14}–reductase enzymes in the ergosterol biosynthesis pathway, there is evidence to suggest that fenpropimorph also has a general inhibitory effect on sterol composition and transport across the plasma membrane in *S. cerevisiae*[100,101]. Marcireau *et al*. (1996) suggested that fenpropimorph may affect other metabolic pathways and regulation, such as the regulation of ergosterol synthesis in the presence of excess nitrogen, lack of nitrogen catabolism repression, and control of amino acid synthesis. They suggested that the usual target enzymes ($\Delta^8 \rightarrow \Delta^7$-isomerase and Δ^{14}–reductase) were not involved in resistance in mutants analysed containing a disrupted *FEN2* gene as the membrane sterol composition did not show increased sterols associated with those enzymes being defective[100]. A further study on *FEN2* showed that it is a membrane-bound transporter enzyme involved in the symport of H^+ and pantothenate[101]. Exposing *fen2-1* mutants to fenpropimorph resulted in a 76.1 % reduction of pantothenate in these cells compared to the wild type. In addition to this, there was a 76.8 % reduction in D-glucose, 85.5 % reduction in L-lysine, and a 92.9 % reduction in biotin compared to wild-type cells. These results were indicative of transportation across the membrane in general being inhibited by fenpropimorph, and, as the authors suggested, it could have been due to fenpropimorph interacting with the hydrophobic components of the membrane, such as fatty acids[101].

This hypothesis was reinforced by a study that exposed *A. niger* to sub-lethal doses of fenpropimorph and performed transcriptome analysis[102]. The application of fenpropimorph was associated with increased expression of 41 genes involved in membrane reconstruction, lipid signalling, cell wall remodelling, and oxidative stress responses[102]. This showed a more general inhibitory influence on normal cell growth by fenpropimorph in addition to the specific inhibition of the two ergosterol biosynthesis enzymes, although it is possible that these alterations were a response to changes in the membrane sterol composition caused by applying fenpropimorph.

As it is likely that the $\Delta^8 \rightarrow \Delta^7$-isomerase and Δ^{14}-reductase enzymes are involved in resistance to fenpropimorph, it seemed appropriate to study these two genes in wheat powdery mildew (*Bgt*) isolates collected from the JIC glasshouses after application of fenpropimorph failed to control the disease. In this chapter, I compare the levels of resistance to fenpropimorph in *Bgt* isolates obtained from the glasshouses in 2014/5 and in the UK *Bgt* field population in 2015 to those of an older UK isolate (JIW11, collected in 1985) and US field isolates that have not been exposed to this fungicide. I then examine the *Erg24* gene encoding Δ^{14}–reductase (ERG24) and the *Erg2* gene encoding $\Delta^8 \rightarrow \Delta^7$-isomerase (ERG2) for any mutations that may be associated with

increased resistance. I hypothesise that mutations in one or both of these genes will be associated with increased fenpropimorph resistance in the UK *Bgt* population. I also compare the levels of resistance to fenpropimorph of four *Bgh* isolates and I hypothesise that increased resistance to fenpropimorph, if present, will also be associated with mutations in these genes. I then characterise the relevance of these mutations using protein structure predictions and molecular docking techniques.

3.2 Methods

3.2.1 Determining the level of sensitivity among *Bgt* and *Bgh* isolates to fenpropimorph

Fungicide spray tests were performed as described in chapter 2 (section 2.5). Both *Bgt* and *Bgh* isolates were tested, therefore both Cerco and Golden Promise seedlings were used. A 1.9-fold dose range up to the recommended field rate consisting of eight doses (11, 21, 40, 77, 146, 277, 526, and 1000 mL/ha) was applied and an additional no-fungicide control was used where only water was sprayed onto the tray of seedlings. The control isolate used in the *Bgt* tests was JIW11 as it is an older isolate collected shortly after fenpropimorph was first used in agriculture[103] therefore represents the baseline sensitivity to this fungicide amongst *Bgt* isolates. *Bgh* isolate CC148 was used as a control in the barley powdery mildew test as it is a clone-mate of CC151 (no longer available in living culture) which has previously been shown to have high resistance

Table 3.2.1.1: Table summarising the Bgt *and* Bgh *isolates used in the fungicide spray tests.*

Type of isolate	Name of isolate	Type of isolate	Name of isolate
2014 glasshouse isolates (Bgt)	CAW14S6303	**2015 glasshouse isolates with two sprays of Corbel (*Bgt*)**	CAW15S6335
	CAW14S6307		CAW15S6336
	CAW14S6317		CAW15S6337
	CAW14S6318		CAW15S6338
2015 glasshouse isolates with no Corbel spray (*Bgt*)	CAW15W101		CAW15S6339
	CAW15W102		CAW15S6340
	CAW15W103		CAW15S6341
	CAW15W104		CAW15S6342
	CAW15W105		CAW15S6343
2015 glasshouse isolates with one Corbel spray (*Bgt*)	CAW15S6320	**Swiss isolates (*Bgt*)**	96224
	CAW15S6330		94202
	CAW15S6332	**US field isolates (*Bgt*)**	Hagrid
UK field isolates (*Bgt*)	AEW1504		Ron
	CMW1502		Harry
	EOW1501	***Bgh* isolates**	DH14
	JBW1504		CC52
	TKW1503		CC148
Older UK isolate (*Bgt*)	JIW11		W4

to fenpropimorph[82]. Isolates used in both wheat and barley spray tests are stated in table 3.2.1.1.

For every isolate, individual colonies were counted on each leaf and an average colony count was calculated across all three leaves per dose. These average colony counts represent the amount of growth of that isolate at a given dose. The dose with the maximum growth was identified and the average colony count from each dose was then calculated as a percentage of that maximum for that isolate. Percentage of maximum growth was then plotted against fungicide dose.

3.2.2 Sequencing of the *Erg2* and *Erg24* genes targeted by fenpropimorph

As mentioned, fenpropimorph targets the ERG24 protein and potentially ERG2 therefore I designed primers (shown in table 3.2.2.1) for PCR amplification and sequencing of the *Erg24* gene in *Bgt* (assembly scaffold 39, accession KE375101.1) and *Bgh* (assembly scaffold sca005483, accession HF943546.1), and the *Erg2* gene in *Bgt* (assembly scaffold 49, accession KE375133.1) in order to identify any possible mutations that may have arisen in isolates that showed reduced sensitivity to this fungicide. The locations of these primers relative to the coding sequences of the genes are shown in figure 3.2.2.1.

Table 3.2.2.1: Primer sequences designed to amplify the Erg24 *gene in* Bgt *and* Bgh*, and the* Erg2 *gene in* Bgt*. F in the primer names indicates a forward primer and R indicates a reverse primer.*

Primer name	Primer sequence (5' to 3')	Target organism and gene
ERG24-F1	TGCAGCTCAGAGTGAAGTGA	*Bgt Erg24*
ERG24-F2	GCCCAAGCCATAATCCAATCT	
ERG24-R3	TGTTGTGGCCACCGTACTAT	
ERG24-F4	GGCCACCGTACTACCAAATG	*Bgh Erg24*
ERG24-R4	ACGAAAGCTCTGCGACTCTG	
ERG24-F5	CGAACTTAACCCACGTGCTC	
ERG2-F1	CCTTAGCGTCCAGGAGTCTT	*Bgt Erg2*
ERG2-R1	GCCCAGATGATGTTTGCTGG	

In *Bgt* isolates, primer pair ERG24-F1 and ERG24-R3 were used to amplify the *Erg24* gene, and primers ERG24-F1, ERG24-F2, and ERG24-R3 were used to sequence through the entire gene. In *Bgh* isolates, primers ERG24-F4 and ERG24-R4 were used to amplify and sequence the gene. Primer ERG24-F5 was used to sequence the middle section in order to capture the whole gene. Primers ERG2-F1 and ERG2-R1 were used to amplify and sequence the *Erg2* gene in *Bgt* isolates. *Erg2* was not sequenced in *Bgh* isolates.

Table 3.2.2.2: PCR amplification conditions for the Erg24 *and* Erg2 *genes.*

Temperature	**Time**	**Step**	
98 °C	30 s	Initial denaturation	
98 °C	10 s	Denaturation	33 cycles
66 °C (*Bgt Erg24*) 64 °C (*Bgh Erg24*) 68 °C (*Bgt Erg2*)	20 s	Annealing	
72 °C	50 s	Elongation	
72 °C	2 min	Final extension	
4 °C	-	Hold	

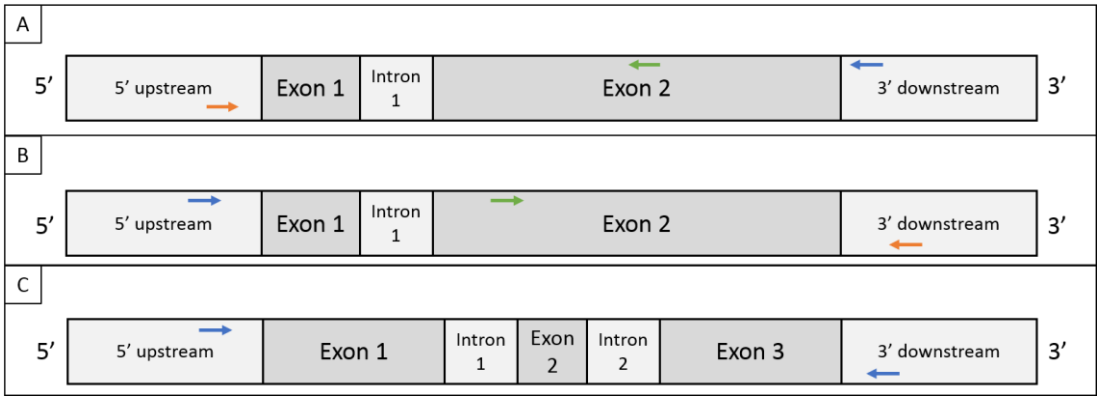

Figure 3.2.2.1: Diagrammatic representation of the Erg24 *and* Erg2 *genes. Panel A shows the* Bgt Erg24 *gene (situated on the minus strand). The arrows show primer positions relative to the coding sequence with blue showing F1, green showing F2, and orange showing R3. Panel B shows the* Bgh Erg24 *gene. The blue arrow shows F4, green shows F5, and orange shows R4. Panel C shows the* Bgt Erg2 *gene with the blue arrows showing the positions of ERG2-F1 and -R1.*

PCR amplification of the *Bgt* and *Bgh Erg24* genes, and *Bgt Erg2* gene was performed in 25 µL reactions containing 3 % DMSO, 1x Q5® reaction buffer, 0.5 µM of each primer, 200 µM dNTPs, 0.5 U Q5® High-Fidelity DNA polymerase (New England BioLabs Inc., UK), 30 ng template DNA, and made up to 25 µL with nuclease-free water. The reactions were performed with their respective annealing temperatures according to the programme in table 3.2.2.2 above.

All PCR products were purified using a QIAGEN QIAquick PCR Purification Kit according to the manufacturer's instructions. DNA was quantified using a NanoDrop2000 spectrophotometer, diluted appropriately, and sequenced using Sanger sequencing by Eurofins Genomics. Sequences were trimmed and aligned using Vector NTI ContigExpress.

3.2.3 Modelling the ERG24 protein and molecular docking of fenpropimorph

The ERG24 protein sequence from the *Bgt* reference isolate 96224 (GenBank accession: EPQ63705) was submitted to Phyre2[104] to be modelled based on homologous sequences and

models from other organisms, and then automatically submitted to 3DLigandSite[105] for binding site prediction. This sequence was also submitted to the TMHMM server v. 2.0[106] to predict which portions of the protein are likely to be transmembrane helices. The ERG24 protein sequence from the *Bgh* reference isolate DH14 was also submitted to Phyre2 and 3DLigandSite. In addition to this, I aligned protein sequences homologous to ERG24 in *Bgt* and *Bgh* from *Marssonina brunnea* (Marssonina leaf spot of poplar), *Monilinia fructicola* (brown rot of stone fruit), *Botrytis cinerea* (grey mould), *Schizosaccharomyces pombe*, *Saccharomyces cerevisiae*, *Homo sapiens*, *Mus musculus*, and *Danio rerio* (zebrafish), and compared this alignment with the TMHMM output.

For molecular docking, a homology model of ERG24 was generated using the I-TASSER server[107] based on the crystal structure of MaSR1 from *Methylomicrobium alcaliphilum*[108]. This is the only structure currently available in the Protein Data Bank that bears significantly similar sequence to ERG24, with 37 % identity over 411 aligned residues out of a total of 489. Starting with the coordinates of the partially observed NADPH in the template, the NADPH cofactor was then modelled into the predicted protein structure using the COOT molecular graphics programme[109]. The nicotinamide-ribose moiety was placed to one side of the predicted binding site which minimised steric clashes of the binding substrate with the protein model. Fenpropimorph was then manually docked into the predicted binding site of the protein model. Structural figures showing the NADPH cofactor and fenpropimorph molecule docked into ERG24 were generated using CCP4mg[110]. Molecular docking using I-TASSER, COOT, and CCP4mg was performed by modelling specialist Dr Dave Lawson at the John Innes Centre.

3.3 Results

3.3.1 *Bgt* and *Bgh* responses to fenpropimorph

Bgt isolates collected from the JIC glasshouses in 2014 and 2015 as well as UK, US, and Swiss field isolates, and older UK isolate JIW11 were exposed to increasing doses of fenpropimorph to test the levels of resistance. As shown in figure 3.3.1.1, JIW11, 94202, and the US isolates were sensitive to fenpropimorph and had an MIC of 40 mL/ha. In contrast to this, 96224, the 2014 glasshouse isolates, the 2015 glasshouse isolates with no spray and after one spray, and the UK field isolates had reduced sensitivity to fenpropimorph. From these, 96224 and two out of five UK field isolates had an MIC of 277 mL/ha which is 9.6-fold higher than the sensitive isolates, and the remaining isolates had an MIC of 526 mL/ha which is 13-fold higher than the sensitive isolates. Four out of nine 2015 glasshouse isolates collected after a second spray also had an MIC of 526 mL/ha. The remaining five 2015 glasshouse isolates collected after a second spray showed a further 1.9-fold increase in resistance and had an MIC of 1000 mL/ha.

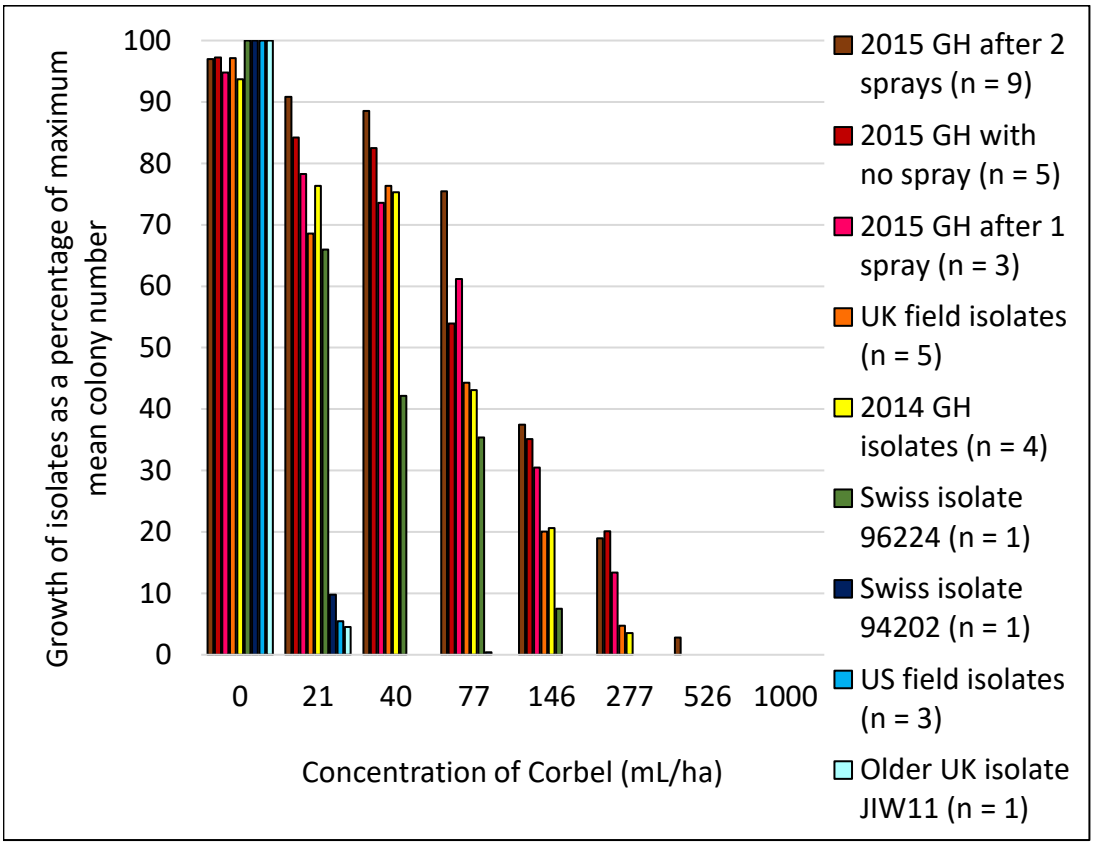

Figure 3.3.1.1: Responses of four Bgt *isolates from the glasshouses in 2014, five 2015 glasshouse (GH) isolates with no spray, three 2015 glasshouse isolates with one spray, nine 2015 glasshouse isolates with two sprays, five UK field isolates from 2015, three US field isolates, two Swiss isolates, and two older European isolates as controls to increasing doses of fenpropimorph (Corbel). N values for each grouping are shown in parentheses.*

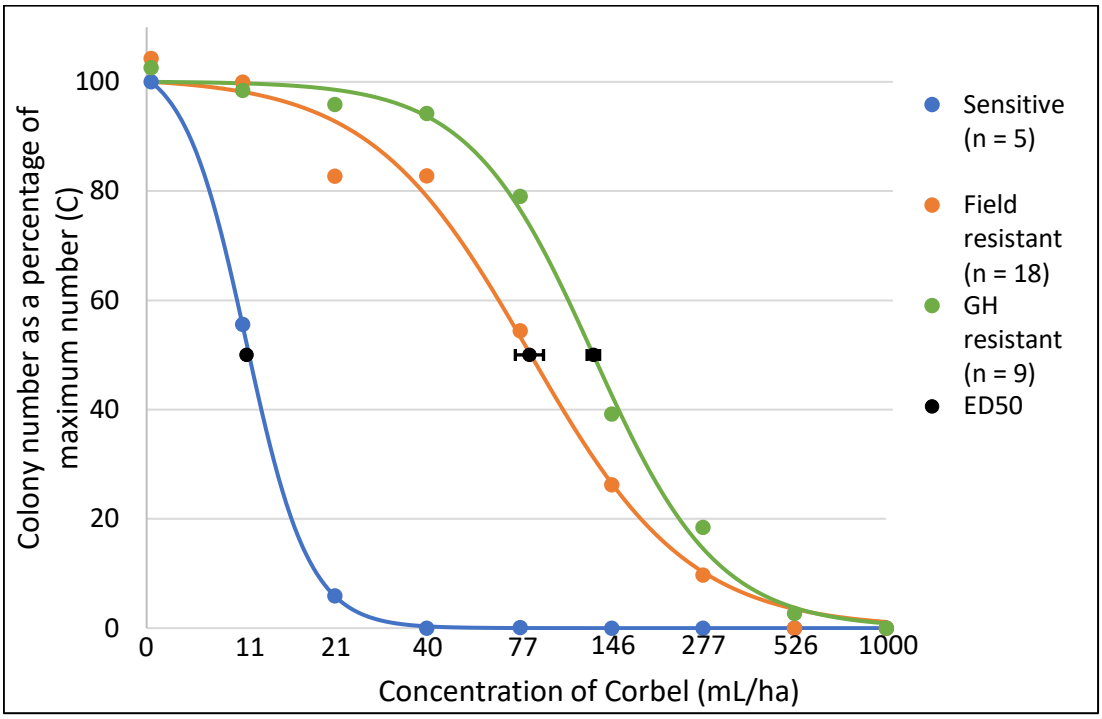

Figure 3.3.1.2: Fitted dose-response logistic curves for five "sensitive", eighteen "field resistant" and nine "glasshouse (GH) resistant" Bgt *isolates to fenpropimorph (Corbel) concentration. ED_{50} values and error bars are shown in black. N values for each grouping are shown in parentheses.*

ED_{50} values for these isolates were calculated as described in chapter 2 section 2.8 by grouping JIW11, 94202 and the US isolates into the "sensitive" category, the 2015 glasshouse isolates after two sprays into the "glasshouse (GH) resistant" category, and all other isolates into the "field resistant" category. This final category included all UK field isolates included in the spray test, Swiss isolate 96224, and 2014/15 glasshouse isolates collected before a second spray was applied. Logistic dose-response curves fitted to colony number data for these three categories and their ED_{50} values are shown in figure 3.3.1.2. See Appendix I for ED_{50} ± standard error ranges as standard errors were calculated from $\log_{10}$(dose) so are on a logarithmic scale. The ED_{50} for sensitive isolates was $11.3 \pm 10^{(7 \times 10\text{-}4)}$ mL/ha, for field resistant isolates was $82.1 \pm 10^{(0.043)}$ mL/ha, and for glasshouse resistant isolates was $128.5 \pm 10^{(0.019)}$ mL/ha. The resistance factor for the UK *Bgt* field population was 7.3 and was 11.4 for isolates sampled following the second spray of Corbel in the JIC glasshouses. This means there was a 7.3-fold increase in resistance in the field population compared to the sensitive isolates. Likewise, there was an 11.4-fold increase in resistance in isolates collected after a second spray was applied compared to sensitive isolates.

Bgh isolates were tested with the same dose range as *Bgt* isolates. DH14 and CC52 were very sensitive to fenpropimorph and only grew on the control leaves with no fungicide, whereas CC148 and W4 were less sensitive as CC148 had an MIC of 77 mL/ha and W4 had an MIC of

40 mL/ha. Even though CC148 and W4 were less sensitive than DH14 and CC52, their responses were similar to those of the sensitive *Bgt* isolates (figure 3.3.1.3).

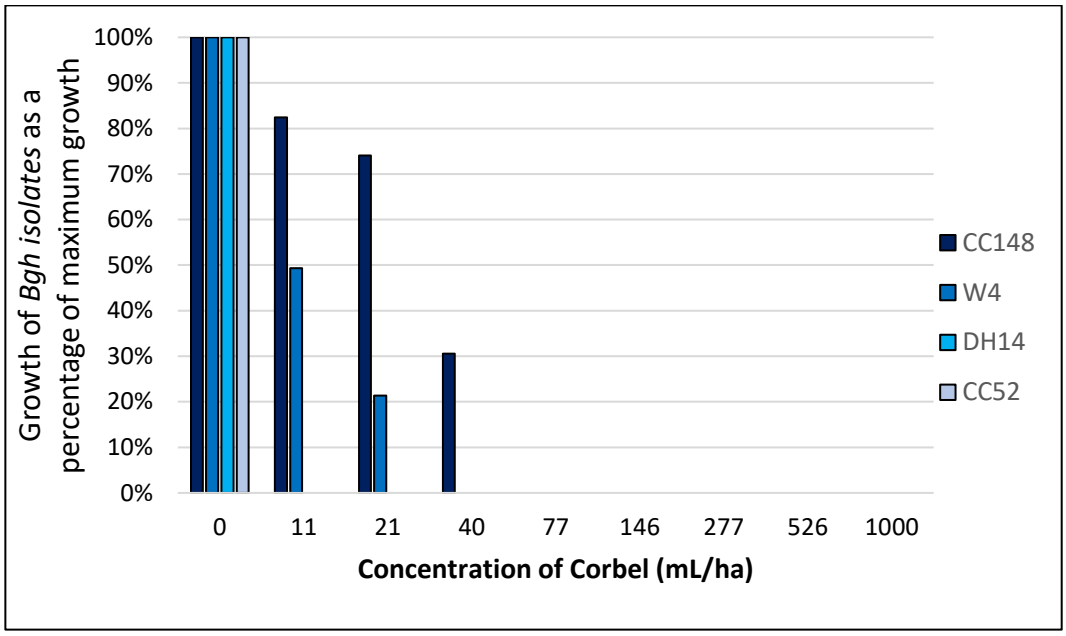

Figure 3.3.1.3: Responses of four Bgh *isolates to increasing doses of fenpropimorph (Corbel).*

3.3.2 Sequencing of the *Erg24* gene in *Bgt* and *Bgh*

In *Bgt* isolate 96224 and *Bgh* isolate DH14*, Erg24* is 1595 bp long and is made up of two exons and one 55 bp intron. The structure of these genes is shown in figure 3.3.2.1 panels A and B. The *Erg24* gene was sequenced in the following *Bgt* isolates: 96224, four 2014 glasshouse isolates, seven 2015 glasshouse isolates (two with no spray, three after one spray, and two after two sprays), JIW11, 94202, and three US isolates. The *Erg24* gene in all four *Bgh* isolates was sequenced. All *Bgt* isolates were aligned to the reference 96224 sequence and all *Bgh* isolates were aligned to the reference DH14 sequence. Both of these *Erg24* reference sequences were re-sequenced by me to check that the sequence was correct and all four of these were included in the alignment.

When comparing the *Bgt Erg24* sequences with the *Bgh* sequences, a total of 111 single nucleotide polymorphisms (SNPs) were identified. Five of these SNPs were in the intron, 68 were synonymous and 38 were non-synonymous. All of these SNPs were between *Bgt* and *Bgh* isolates as a whole; there was no variation amongst the *Bgt* or *Bgh* isolates therefore these mutations were not studied further as there was no association with increased resistance in *Bgt* or *Bgh*.

In all *Bgt* isolates that had either of the two levels of resistance to fenpropimorph, there was a G to C SNP at nucleotide 938 resulting in a V295L mutation. This mutation was not present in

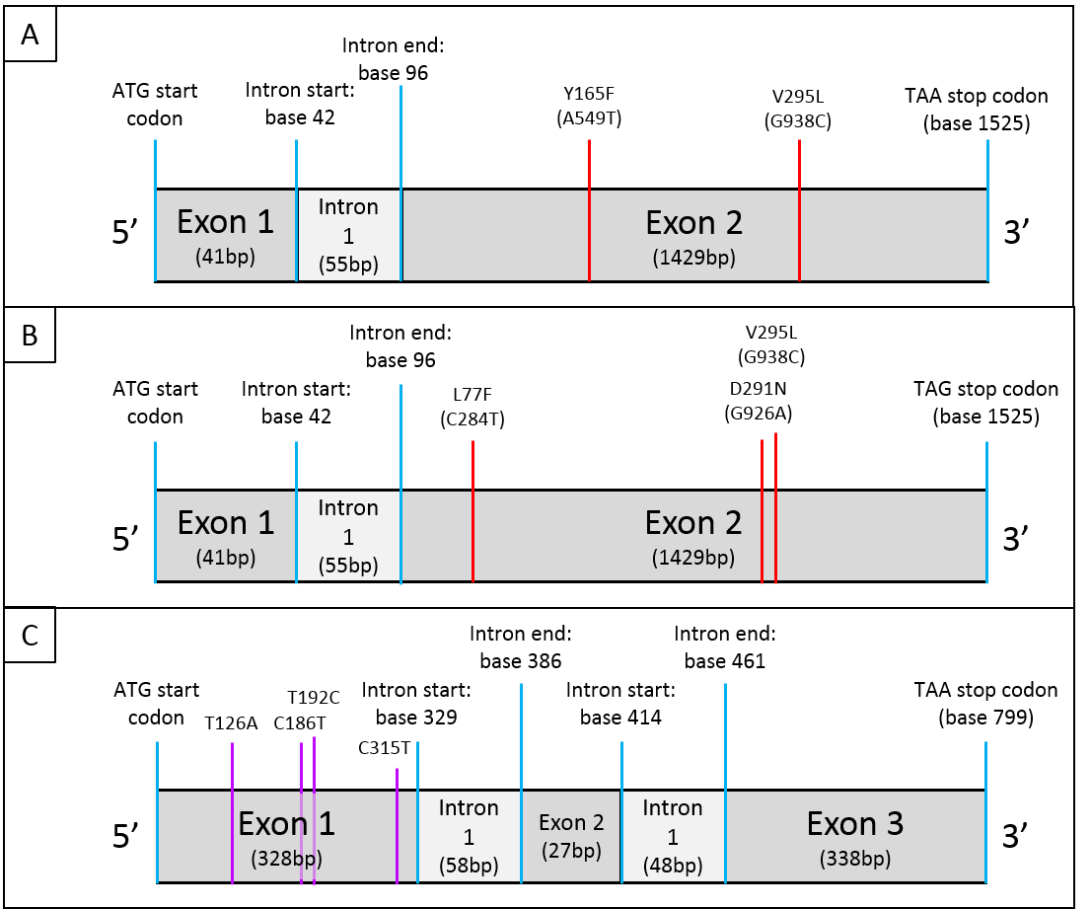

Figure 3.3.2.1: Diagrammatic representation of the Bgt *and* Bgh Erg24 *genes (panels A and B, respectively), and the* Bgt Erg2 *gene (panel C). Red lines indicate the positions of non-synonymous mutations identified within the genes with the amino acid substitution indicated above and the nucleotide substitution in brackets. Purple lines indicate the positions of synonymous mutations with the nucleotide substitution labelled above. Blue lines indicate key nucleotide positions within the gene, including start and stop codons, and the locations of introns.*

any of the sensitive isolates. Interestingly, this mutation was also present in *Bgh* isolate W4 which showed increased resistance to fenpropimorph. *Bgh* isolate W4 had an additional C to T SNP at nucleotide 284 resulting in an L77F mutation.

In *Bgh* isolate CC148 G at base 926 was substituted for A which resulted in a D291N mutation and was associated with increased resistance to fenpropimorph (see figure 3.3.1.2). In two of the *Bgt* isolates tested, 96224 and CAW15S6320 (a 2015 glasshouse isolate after one spray), there was an A to T nucleotide substitution at position 549 resulting in a Y165F mutation. However, as can be seen in figure 3.3.1.1, this mutation was not associated with responses to fenpropimorph.

3.3.3 Sequencing of the *Erg2* gene in *Bgt*

In *Bgt* isolate 96224, *Erg2* is 799 bp long containing three exons and two introns that are 58 bp and 48 bp in length. The structure of this gene is shown in panel C of figure 3.3.2.1. Isolates sequenced included two 2014 glasshouse isolates, four 2015 glasshouse isolates (two with no spray, one with one spray, and one with two sprays), JIW11, and three US isolates. No non-synonymous mutations were identified but four synonymous SNPs were. Two of these SNPs were in all sequenced isolates compared to the reference 96224, one was identified in all isolates except US isolate Hagrid which was the same as the reference, and one was identified only in Hagrid with all other isolates being identical to the reference.

This was a small selection of isolates from across the full range of responses to fenpropimorph (table 1.2.1.1; figure 3.3.1.1). As there were no SNPs identified that correlated with the increased resistance phenotype, no further isolates were sequenced and no further work with *Erg2* was carried out.

3.3.4 Modelling the *Erg24* protein, analysing the locations of mutations, and docking fenpropimorph into the model

The *Bgt* ERG24 protein structure predicted by Phyre2 can be seen in figure 3.3.4.1A. It is a model based on the 3D structure of an integral membrane Δ^{14}-sterol reductase in *Escherichia coli*, and it had 100 % confidence with 41 % identity to the *E. coli* protein. This programme predicted that ERG24 is a transmembrane protein with ten transmembrane domains. When compared to the TMHMM output, it can be seen that both programmes predicted seven of the same transmembrane domains (S1, S3, S4, S7, S8, S9 and S10 in figure 3.3.4.2). In the TMHMM output,

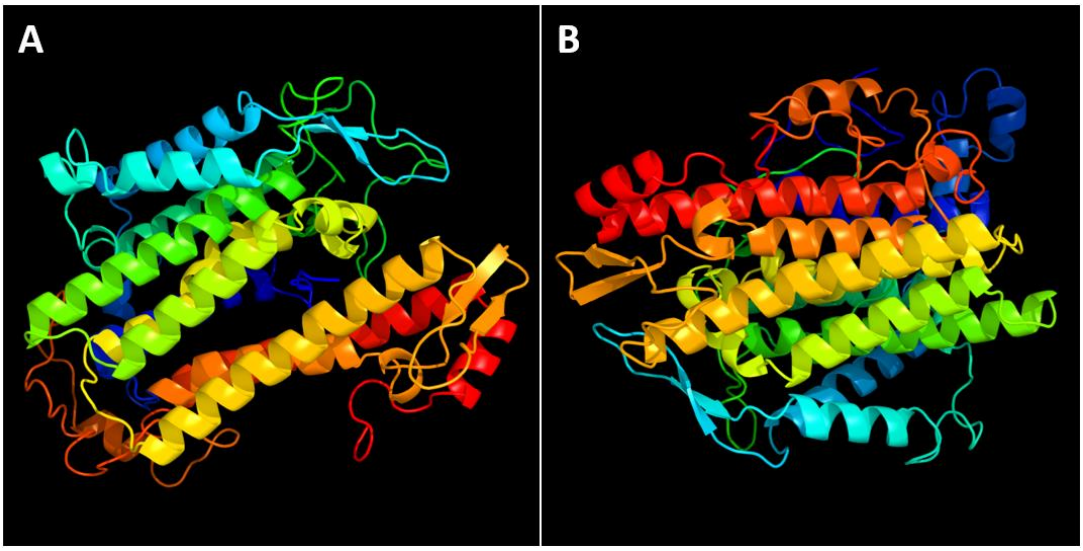

Figure 3.3.4.1: Predicted protein structures of Bgt *(A) and* Bgh *(B) ERG24 proteins from Phyre2.*

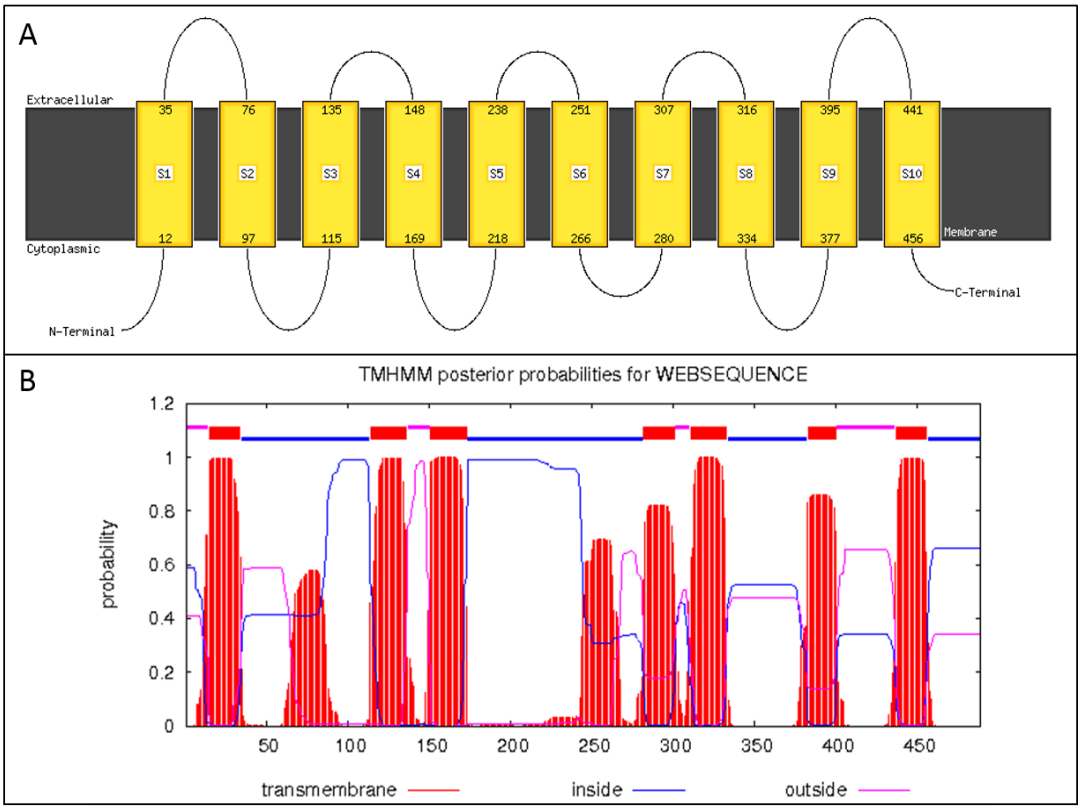

Figure 3.3.4.2: A: Predicted transmembrane domains in Bgt *and* Bgh *ERG24 proteins from Phyre2. Numbers at either end of each domain indicate the amino acid position. B: Predicted transmembrane domains in the* Bgt *ERG24 protein from TMHMM. Amino acid numbers are on the x-axis.*

domains S2 and S6 highlighted in the Phyre2 output also appear, but don't reach the threshold probability to be considered true transmembrane domains. The S5 domain predicted by Phyre2 was absent in the TMHMM output. The Phyre2 predicted domain locations were compared to the protein alignment from ten different organisms mentioned in section 3.2.3 and it was found that all ten of these domains are relatively conserved regions within those protein sequences.

The *Bgh* ERG24 protein structure can be seen in figure 3.3.4.1B. Phyre2 predicted the same transmembrane domains for *Bgh* as for *Bgt*. It also based the predicted structure on the same *E. coli* model with 100 % confidence and 40 % identity. With both *Bgt* and *Bgh*, 79 % of residues were modelled at >90 % confidence.

Protein models from Phyre2 were automatically submitted to 3DLigandSite for active site prediction. Amino acids predicted to be involved in binding were not the same in *Bgt* as they were in *Bgh*, but they were in a similar location suggesting the binding site is in approximately the same area. In *Bgt*, the amino acids predicted to form the binding site were W229, D233, V254, H258, Y299, S300, F301, Q302, and A303. In *Bgh*, the predicted amino acids were H376, Y379, D382, L454, R457, and D461. The locations of these amino acids within each protein have

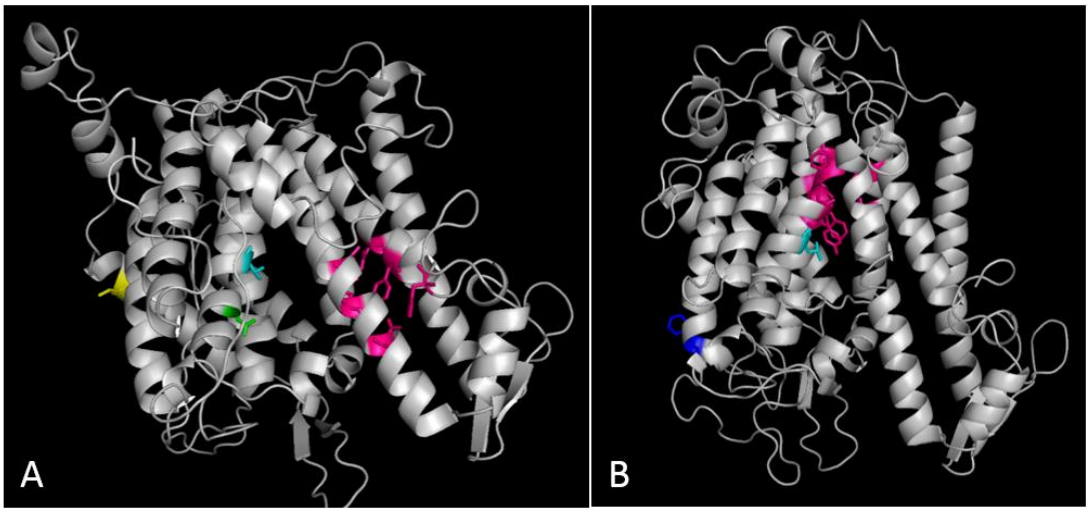

Figure 3.3.4.3: Amino acids predicted to form sterol-binding pockets in the Bgh *(A) and* Bgt *(B) ERG24 proteins have been highlighted in pink. Mutations identified from sequencing are coloured as follows. A: In* Bgh*, L77 is highlighted in yellow, D291 in green and V295 in light blue. B: In* Bgt*, F165 is highlighted in dark blue and L295 in light blue.*

been highlighted in the protein models and can be seen in figure 3.3.4.3. The locations of the predicted sterol-binding pockets are consistent with the existence of two openings in the homologous MaSR1 protein from the bacterium *Methylomicrobium alcaliphilum*[108]. They hypothesised that one of these openings faces the cytoplasm and allows the cofactor NADPH to enter the protein, and the other opening faces into the hydrophobic centre of the lipid bilayer where sterols can bind. This enzyme then brings the NADPH and sterol together and catalyses the reduction of the C14 double bond in the sterol substrate[108].

Locations of amino acid mutations identified from the gene sequence alignment were highlighted within the *Bgt* and *Bgh* ERG24 protein models and are also displayed in figure

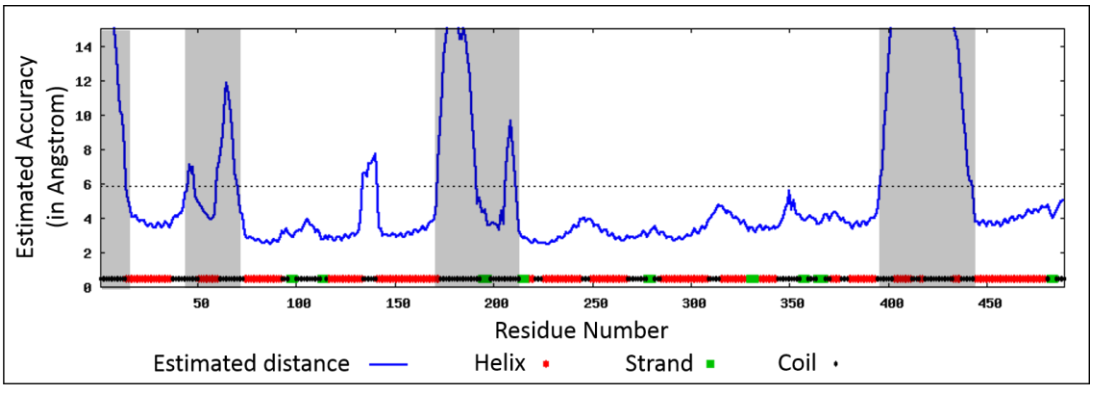

Figure 3.3.4.4: Output from I-TASSER server showing the estimated accuracy of the homology model derived from MaSR1 plotted as a function of residue number. The regions shaded in grey were deleted from the final model. Also shown along the bottom of the plot is the predicted secondary structure. Figure produced by Dr. Dave Lawson.

3.3.4.3. It was thus possible to decide whether it is likely that these mutations contribute to increased resistance to fenpropimorph or not. In *Bgh*, the L77F mutation is located on the opposite side of the protein to the predicted binding site, whereas the D291N and V295L mutations appear to face into the binding pocket. Likewise, in *Bgt*, the V295L mutation seems to be located directly next to the binding pocket, whereas the Y165F mutation found in *Bgt* isolates 96224 and CAW15S6320 is situated at the end of an α-helix which is not involved in forming the predicted binding site.

The homology modelling output generated from I-TASSER for molecular docking by Dr. Dave Lawson can be seen in figure 3.3.4.4. Sections with poor accuracy (highlighted in grey in figure

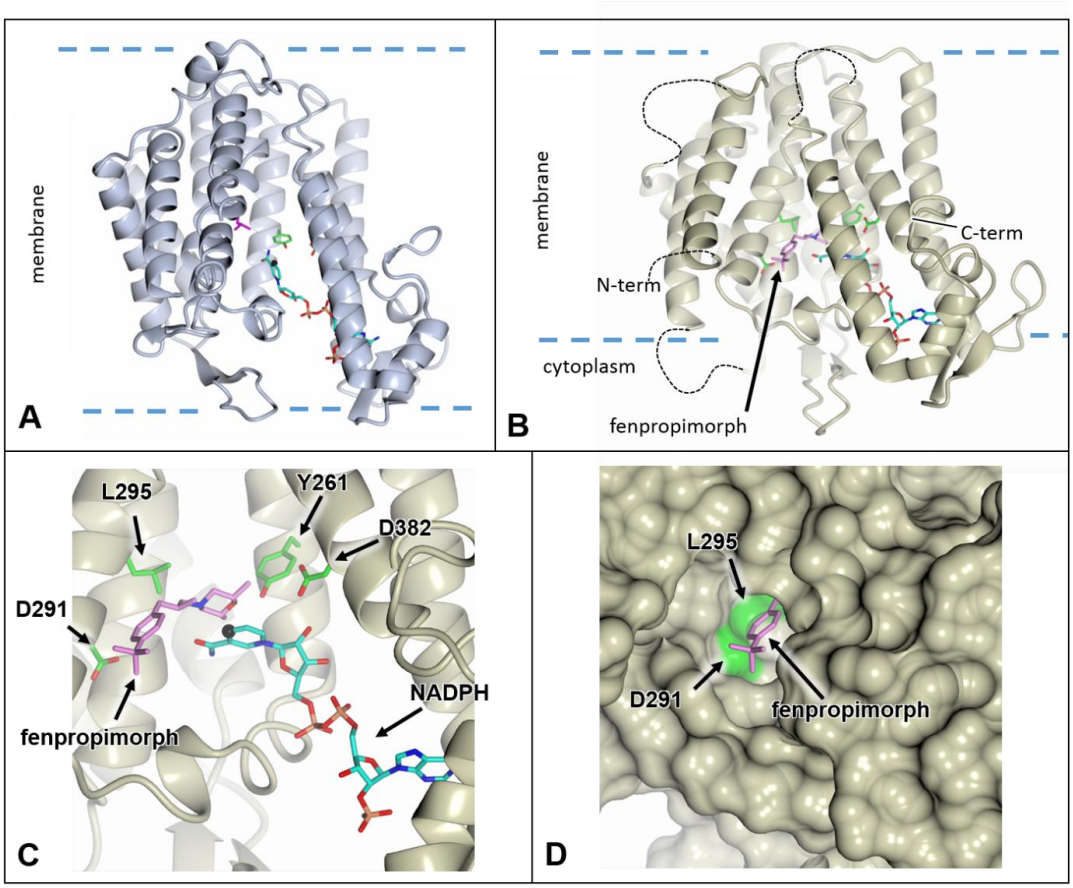

Figure 3.3.4.5: A cartoon representation of the ERG24 protein model showing the docked NADPH cofactor and key amino acids. A: In pink is L295. The green amino acids (Y261 and D382) are those identified by Li et al*. (2014) as being key catalytic residues. B: The dotted lines are low confidence surface regions deleted from the homology model. The purple molecule is fenpropimorph. C: A close-up view of the position of the fenpropimorph molecule shown relative to the D291 and L295 residues as well as the NADPH cofactor and key catalytic residues. D: A molecular surface view showing fenpropimorph docked into the active site. Figures produced by Dr. Dave Lawson.*

3.3.4.4) were deleted from the final model as they corresponded to surface regions and had bad geometry.

Molecular docking of the NADPH cofactor and fenpropimorph molecule into the ERG24 protein model suggests a role of the two openings into the active site in the interaction between the NADPH molecule, the sterol, and the protein as was found by Li *et al*. (2014). Figure 3.3.4.5 shows how NADPH enters the protein from the cytoplasmic opening and that the binding site is lined with conserved residues Y261 and D382 identified by Li *et al.* (2014) as potentially being catalytic residues (Y241 and D363 respectively in the MaSR1 structure). Figure 3.3.4.5B shows the updated model that has areas of low confidence removed and shows the fenpropimorph molecule docked.

Figure 3.3.4.6 A to F show a much closer view of the binding site of this protein. In 3.3.4.6 A and 3.3.4.6 D it is clear that NADPH enters from the cytoplasm and interacts with several amino acids

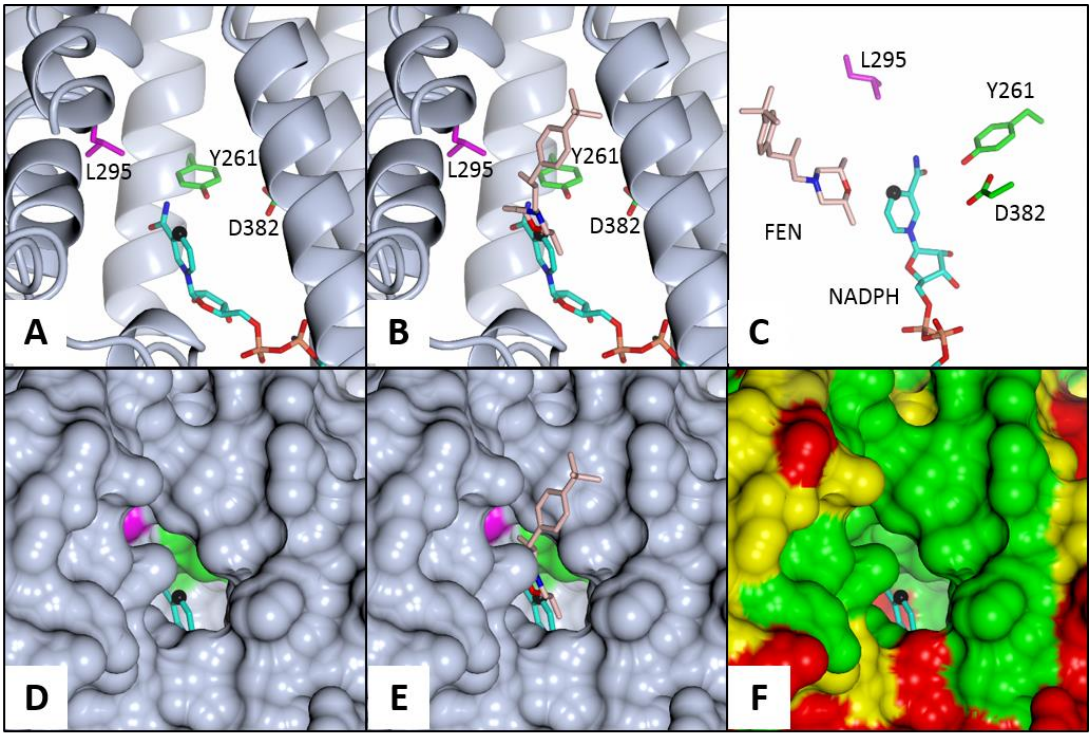

Figure 3.3.4.6: A: A closer view of the key amino acids and the docked cofactor. The black sphere is C4 of the nicotinamide in NADPH, i.e. the site involved in reduction. B: A closer view with fenpropimorph docked. C: A side view of the interaction between these amino acids and docked molecules without the cartoon structure. D: A molecular surface view of A showing the C4 faces towards the opening where sterols/fenpropimorph are likely to bind. E: A molecular surface view of B showing fenpropimorph entering through the side of the protein. F: A molecular surface view of A coloured according to level of conservation (green is highly conserved, red is not conserved). Figures produced by Dr. Dave Lawson.

in the pocket, including Y261, D382 and probably with L295, our mutation site of interest. 3.3.4.6 D also shows that the reactive carbon C4 in NADPH responsible for redox reactions clearly faces the second opening of the protein where the sterol substrate enters. 3.3.4.6 B and 3.3.4.6 E show that fenpropimorph, like the sterol substrate, enters the protein from the side pocket that faces the hydrophobic lipid bilayer and sits in close proximity to NADPH within the pocket. Finally, 3.3.4.6 F shows that the amino acids forming the binding pocket are highly conserved regions of the protein.

In the BASF product Corbel, both *S*- and *R*-enantiomers of fenpropimorph are present and are equally active within the mixture[51]. Both forms were docked into the protein model, but there was no preference for binding one enantiomer over the other so only the *S*-enantiomer is shown in these figures.

3.4 Discussion

By carrying out fungicide spray assays with *Bgt* isolates from the current UK population compared to an older UK isolate, it is clear that over time exposure to fenpropimorph has caused a reduction in sensitivity to this fungicide, but complete resistance currently does not occur and fenpropimorph remains partially effective against *Bgt* even after 35 years of use. This contrasts with other fungicides, such as QoIs (chapter 1 section 1.4), where a single mutation brought about complete resistance to this group of fungicides. Currently, the mutations that occur within *Bgt* and *Bgh* isolates confer a limited increase in resistance, but as was shown by the *Bgt* isolates collected after a second spray was applied, there is scope for greater resistance.

Fenpropimorph continues to provide moderately effective control of wheat powdery mildew even though it did not control *Bgt* effectively in the glasshouses in 2015. Loss of control can be due to other practical reasons rather than resistance to the chemical, for example the plants in the glasshouses were quite dense which may have prevented the fungicide spray from reaching all of the leaves, particularly those at the bottom in the middle of a group of plants. If the spray did not reach all leaves evenly, it could not effectively control the disease. Incomplete coverage of the foliage may therefore have selected the less-sensitive isolates (ED_{50} of $128.5 \pm 10^{(0.019)}$ mL/ha) which dominated the population in 2015 after a second spray of fenpropimorph had been applied.

It is also clear from these spray tests that *Bgt* and *Bgh* isolates respond slightly differently to fenpropimorph. *Bgt* isolates have a higher baseline tolerance to this fungicide than *Bgh* isolates do as the more resistant *Bgh* isolates CC148 and W4 were only as resistant as the sensitive *Bgt* controls. The number of *Bgh* isolates used in this study was very limited, therefore in order to fully understand the levels of resistance present in *Bgh*, a much larger sample size is needed as

well as a more appropriate dose range. As sequencing the *Erg24* gene showed many mutations between all *Bgt* and all *Bgh* isolates, it is possible that the protein structure in *Bgh* is subtly different from that in *Bgt* which may account for some of the difference in effectiveness. It is also possible that, as this fungicide would have been developed for control of *Bgh* not *Bgt*, the fungicide formulation may have been designed for most efficient uptake by barley rather than by wheat. As shown in previous studies, fenpropimorph may alter several general cellular metabolic pathways[100-102] so it is also possible that fenpropimorph is more effective in *Bgh* against these off-targets than it is in *Bgt*. As has been done with *Aspergillus*[102], an RNA-seq analysis of *Bgh* and *Bgt* isolates exposed to a sub-lethal dose of fenpropimorph could provide more insight into how fenpropimorph affects other cellular activities in each of these *formae speciales*.

By sequencing the *Erg2* and *Erg24* genes it can be concluded that increased resistance among the UK *Bgt* and *Bgh* populations is due to mutations within the *Erg24* gene rather than within *Erg2*. No mutations in *Erg2* were identified in *Bgt* that correlated with increased resistance, whereas two notable mutations in *Erg24* were discovered. This correlates with previous studies concluding that fenpropimorph's main target is Δ^{14}–reductase and that it may only partially affect $\Delta^{8} \rightarrow \Delta^{7}$-isomerase. It was previously shown that overexpression of the *Erg2* gene does not increase resistance to fenpropimorph[93], but this was not explored here. It is possible that mutations may occur outside of the *Erg2* open reading frame, but in the light of the results of previous work[93], they may not increase resistance to morpholines. It was also shown in previous studies that the loss of viability of *Erg24 S. cerevisiae* mutants could be recovered in *fen1* or *fen2* mutant backgrounds and that these genes also contribute to increased resistance to fenpropimorph[94,95]. Likewise, it has been suggested that there may be more than one gene that contributes to increased resistance to fenpropimorph in *Bgh* isolates[97]. As there were *Bgt* isolates collected from the glasshouses in 2015 which showed a further increase in resistance but did not have any additional mutations within *Erg24*, perhaps there are alterations in genes homologous to *fen1* or *fen2* or alterations elsewhere in the genome which contribute to this extra resistance. This, however, was not explored here.

According to the study by Li *et al*. (2014) and by modelling the protein, *Erg24* seems to be a transmembrane protein consisting of ten transmembrane α-helices and two small anti-parallel β-sheets. The structure of this protein also seems to be fairly well conserved in many organisms. The protein has two openings – one that faces the hydrophobic interior of the plasma membrane allowing the sterol substrate to bind, and one that faces the cytoplasm allowing NADPH to bind. It is likely that these two openings face into the same binding pocket where the sterol substrate and NADPH interact. By docking fenpropimorph into the model, it appears that the fungicide

molecule acts as a direct competitor of the sterol substrate and blocks the binding pocket. This seems probable as fenpropimorph is also extremely hydrophobic and so will remain within the membrane and not pass through to the aqueous cytoplasm, however this theory would need to be tested using appropriate biochemical assays.

By modelling the protein, predicting the sterol-binding pocket, and identifying mutations in the *Erg24* gene in resistant isolates, it was possible to predict that the D291N mutation in *Bgh* and the V295L mutation in both *Bgh* and *Bgt* are likely to interfere with fenpropimorph binding to the enzyme. Both of these amino acid positions are located within the predicted sterol-binding pocket which makes them excellent candidates for causing increased resistance to fenpropimorph, whereas the L77F mutation identified in *Bgh* and the Y165F mutation in *Bgt* are not associated with the sterol-binding pocket and are both in remote areas of the protein structure. This suggests that they are highly unlikely to affect substrates binding to the protein. As neither of the D291N or V295L mutations result in complete resistance to this fungicide, the interference caused is clearly not great enough to completely dislodge the fungicide but is enough to prevent full enzyme inhibition. It is possible that these mutations reduce the binding efficiency of fenpropimorph enough so that the sterol substrate exhibits more successful competition with the fungicide, but this would need to be demonstrated biochemically.

3.5 Epilogue

Following the work reported above, my colleague Dr. Laetitia Chartrain has used site-directed mutagenesis of *S. cerevisiae* strain S288C using CRISPR/Cas9-mediated gene editing[111] to confirm the involvement of the V295L mutation in ERG24 in increasing resistance to fenpropimorph. Three different guides were designed to target this mutation. The wild-type yeast had an ED_{50} of $2.97 \pm 10^{(0.12)}$ mM, mutants with guide 1 had an ED_{50} of $32.56 \pm 10^{(0.022)}$ mM, mutants with guide 2 had an ED_{50} of $40.87 \pm 10^{(0.022)}$ mM, and with guide 3 the ED_{50} was $41.87 \pm 10^{(0.025)}$ mM (figure 3.5.1; see Appendix I for ED_{50} ± standard error ranges). This shows an 11-fold increase in resistance between guide 1 mutants and the wild-type strain, a 13.8-fold increase between guide 2 mutants and wild-type, and a 14.1-fold increase between guide 3 mutants and wild-type. The same method can be used to test the role of the D291N mutation found in *Bgh*, which is close to the site of the V295L mutation in *Bgt*. Additionally, testing the responses of the CRISPR/Cas9-generated mutants to fenpropidin, tridemorph, and amorolfine (a morpholine used in medicine) would confirm if the V295L mutation also confers resistance to these fungicides.

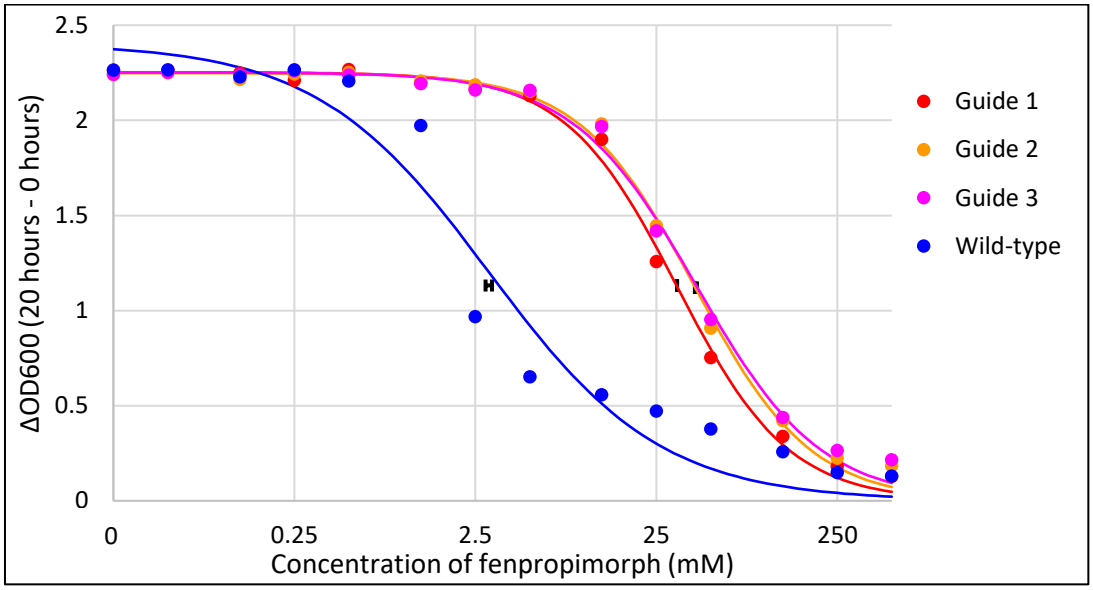

Figure 3.5.1: Fitted dose-response logistic curves for growth of wild-type S. cerevisiase *strain S288C, strains mutated with guide 1, guide 2, and guide 3 to increasing doses of fenpropimorph. Growth is represented as the change in OD600 readings (ΔOD) between 0 hours and 20 hours of growth. Three replicates were included for each of the four sets of strains. ED_{50} values for each set are included as black marks on the graph but as the error bars were so small, only the error bars are shown here.*

4 Resistance of *Blumeria graminis* f. sp. *tritici* to cyflufenamid and candidate modes of action

4.1 Introduction

There are many crop pathogens that are at high risk of developing resistance to fungicides, for example *Botrytis cinerea, Blumeria graminis,* and *Zymoseptoria tritici* have been found to have reduced sensitivity within a few years of several different fungicides being introduced to the field. For this reason, the agrochemical industry generally releases products with new modes of action as mixtures with other fungicides or recommends that they should only be used in a tank-mix with other fungicides in order to reduce the risk of selecting for resistant populations. An example of this is Aviator^{235} Xpro (Bayer AG) which is a mixture of bixafen (SDHI) and prothioconazole (azole) used to control multiple cereal crop pathogens, such as powdery mildew, and yellow and brown rust[79]. It is believed that if a fungicide mixture is used containing fungicides that have different modes of action then they will be effective for a longer period of time, extending the time over which the manufacturer can make a profit from sales of the compound[47].

Currently the main methods used to control the level of *B. graminis* on cereal crops are to spray with a rotation of fungicides, such as an azole followed by a morpholine, or fungicide mixtures, such as Aviator^{235} Xpro (SDHI and azole), and to use crop varieties with powdery mildew resistance genes. Figure 4.1.1 shows the results of fungicide performance trials. These trials are carried out regularly by the Agricultural and Horticultural Development Board (AHDB) as a continuous assessment of effective treatments for crop pathogens. These results showed that Tern (fenpropidin, a morpholine; Syngenta) and Proline (prothioconazole; Bayer AG) were moderately effective against powdery mildews, cutting the percent coverage by approximately 50 %[79]. Flexity (metrafenone, a benzophenone; BASF) and Talius (proquinazid, a quinazolinone; DuPont) were slightly more effective than Proline and Tern but were most useful as preventatives, applied before powdery mildew is visible. Cyflamid (cyflufenamid, an amidoxime; Nippon Soda), appeared to have a more potent effect on the mildew percentage, reducing it by over 80 %[79] therefore should be used in conjunction with another fungicide in order to reduce the risk of resistance development. It is important to continue to use mixtures and rotate fungicides in order to reduce the risk of fungicide resistance occurring in plant pathogen populations.

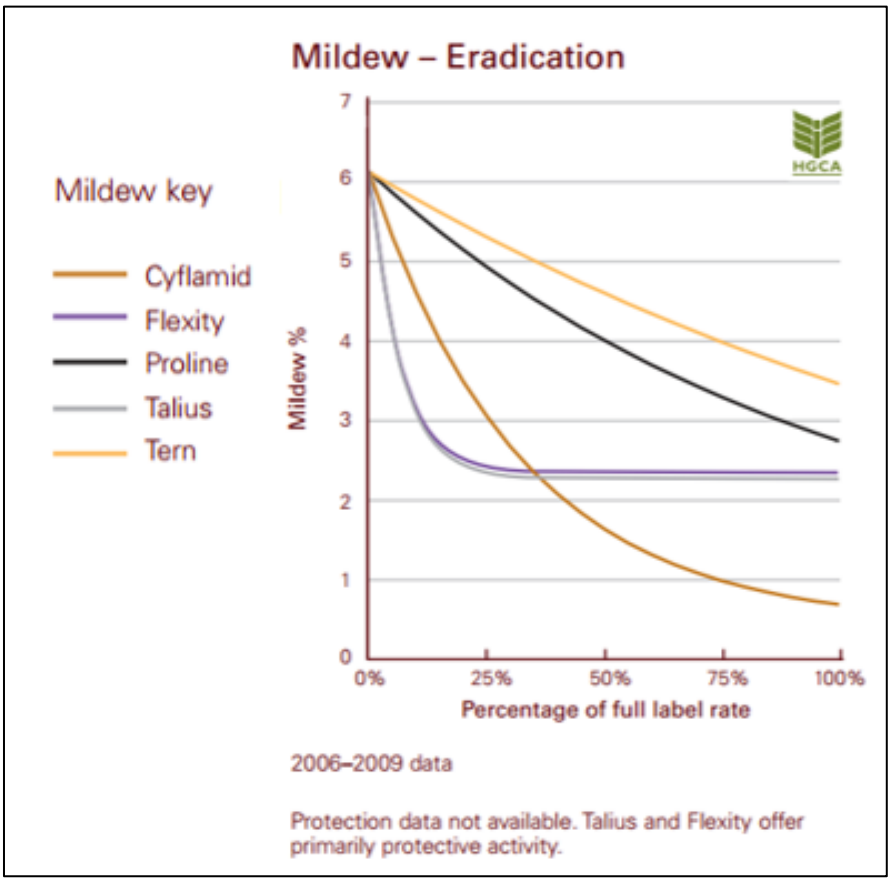

Figure 4.1.1: A graph showing the results of fungicide performance trials performed using five powdery mildew eradicants. Figure is taken from the 'Fungicide Activity and Performance in Wheat Information Guide' released by AHDB (2013).

At the time *B. graminis* f. sp. *tritici* (*Bgt*) isolates were collected from the JIC glasshouses in 2014, both Aviator[235] Xpro and cyflufenamid had been sprayed on cereals to control mildew. As already mentioned, cyflufenamid is able to control powdery mildew more effectively than the other fungicides tested in AHDB trials (see figure 4.1.1). As it has such a strong effect, it can be assumed that there is also a high risk of resistance development. Reduced sensitivity of powdery mildews to cyflufenamid has previously been described in Italy where cyflufenamid (formulated as Takumi, Certis) was applied four times every year between 2010 and 2013[112] while only two applications per year are permitted. A resistance factor greater than 100 was observed between wild isolates and isolates sprayed repeatedly with cyflufenamid[112]. There has also been a report of a less sensitive isolate of *Podosphaera fusca* (formerly *Sphaerotheca cucurbitae*) in Japan. The authors identified a *P. fusca* strain which could withstand 25 ppm cyflufenamid compared to a sensitive strain which only tolerated 8 ppm[113]. There have been no reports of resistance to cyflufenamid, however, when the fungicide has been used in accordance with the product label. These two reports demonstrate the potential for the development of resistance to this fungicide and that it is important to monitor its effectiveness in powdery mildews.

The mode of action of cyflufenamid is currently unknown, but a study using light microscopy and transmission electron microscopy (TEM) of *B. graminis* and *Monilinia fructicola* observed changes in fungal growth in the presence of cyflufenamid[114]. In *B. graminis*, cyflufenamid strongly inhibited colony, spore, and haustorium formation when applied at 0.2 ppm. In *M. fructicola*, elongation of germ tubes was halted 16 hours after cyflufenamid application, and at 24 hours swelling was seen at the tips of germ tubes as well as rupturing of germ tubes. The effects of cyflufenamid on *M. fructicola* growth were observed using TEM. Septa along the mycelia were thinner and smaller than in the untreated control and septal pores were larger. Ruptured hyphae and the formation of many vacuoles within hyphae could also be seen[114]. This study did not specify what the biochemical mode of action is, although the authors suggested that a membrane-associated protein or mechanism could be involved.

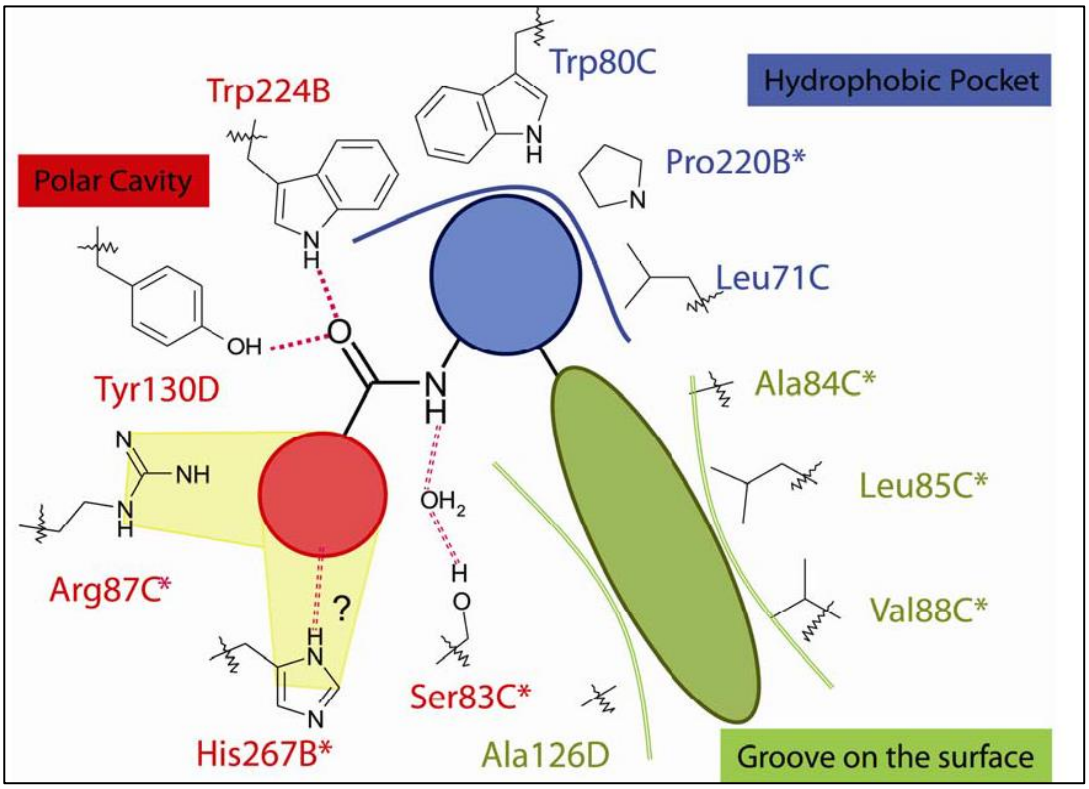

Figure 4.1.2: Diagram illustrating the sites of interaction between an SDHI molecule and the SDH protein complex. The letter (B, C or D) at the end of each amino acid indicates which subunit it resides in. The core part of the molecule in red interacts with residues in the polar cavity of the ubiquinone binding site, the linker part in blue interacts with a hydrophobic pocket in the binding site and the hydrophobic rest of the molecule in green interacts with a groove on the surface of the protein. The asterisks indicate amino acids that are commonly mutated in SDHI-resistant organisms. Taken from figure 1, Sierotzki and Scalliet (2013).

SDHIs are fungicides that target the succinate dehydrogenase (SDH) enzyme complex involved in the respiratory pathway. SDH is composed of four subunits: SDHA (flavoprotein), SDHB (iron-

sulphur subunit), SDHC (cytochrome b560 subunit), and SDHD (cytochrome *b* small subunit)[115]. SDHC and SDHD are integral membrane protein subunits which anchor the protein complex to the membrane, and SDHA and SDHB together are associated with this anchor. At the protein-protein interface between the SDHB, SDHC, and SDHD subunits lies the ubiquinone binding site where electrons released by the oxidation of succinate to fumarate bind to ubiquinone along with hydrogen ions for passage through the electron transport chain (ETC).

SDHI fungicides employed in protecting crops from pathogenic infections are designed so that the molecule binds to the ubiquinone binding site acting as a competitive inhibitor and preventing electrons passing into the ETC from succinate. A review by Sierotzki and Scalliet illustrates the binding interactions between an SDHI molecule and the three SDH subunits (see figure 4.1.2)[47].

Table 4.1.1: A summary of the amino acid substitutions identified within SdhB*,* SdhC *and* SdhD *genes of* Z. tritici*, induced by random UV mutagenesis. [a] indicates substitutions where fewer than ten colonies were formed when exposed to SDHI fungicides.* * *indicates mutations that were identified in both studies.*

Fraaije *et al*. (2012) study		**Scalliet *et al.* (2012) study**	
SdhB	C137R S221P*/T R265P* H267F/L*/N*/Y* I269V*	**SdhB**	S218F[a] P220T[a]/L[a] S221P[a]* N225H[a]/I[a] R265P[a]* H267L*/N*/Q[a]/Y* I269V* N271K[a]
SdhC	L85P* N86S*	**SdhC**	T79I[a] S83G[a] A84V/I[a] L85P[a]* N86K* R87C V88D[a] H145R[a] H152R
SdhD	I127V D129E/G/T*	**SdhD**	D129E[a]*/G[a]*/S[a]/T[a]*

Resistance to SDHIs has been reported in several organisms, such as *B. cinerea* and *Alternaria alternata*[47,116,117]. SDHI resistance has also been identified in laboratory isolates of *Z. tritici*, and is increasingly being identified in the field populations[48,118,119]. By mutating the *SdhB*, *SdhC*, and *SdhD* genes in a laboratory isolate of *Z. tritici* using UV mutagenesis, it was possible to identify

mutations that may confer fungicide resistance while maintaining the viability of the organism (see table 4.1.1)[48,118].

From this summary it is clear that several substitutions, such as S221P found in *SdhB* in both studies, are likely to arise in the future due to selection pressure from the use of SDHI fungicides[48,118]. Many of these substitutions have already been identified in field isolates of SDHI-resistant organisms, for example H277Y/R (equivalent to H267 in *Z. tritici*) was found in several boscalid-resistant *A. alternata* isolates[116], as was D123E (equivalent to D129E in *Z. tritici*)[117]. While monitoring the baseline sensitivity of *Z. tritici* field isolates to SDHIs in 2015 compared to older isolate collections from 2005-2010, a few isolates with reduced SDHI sensitivity were found which contain *SdhC* and *SdhD* mutations[119]. *SdhC* mutation N79T conferred a moderate level of resistance in one isolate. Two other isolates with high resistance to SDHIs contained mutations H152R in *SdhC* and R47W in *SdhD*. Out of 93 isolates, these were the only ones which showed significantly increased resistance to SDHIs, but as a whole, the ED_{50} value of the 2015 population had increased by 50 % compared to older populations (an increase from 0.163 mg/L to 0.26 mg/L). This shows that although the frequency of resistant *Z. tritici* isolates in the field population is low, the population as a whole is becoming slowly more tolerant of SDHIs[119].

The emergence and selection of resistance to fungicides is monitored by the Fungicide Resistance Action Committee (FRAC) who have reported the presence of reduced sensitivity to SDHIs in *Z. tritici* field populations in the UK, France, Germany, and Ireland. Amino acid substitutions identified included N225T, and T268I in SDHB, and T79N, W80S, N86S, and V166N in SDHC, most of which were not identified in the laboratory mutant isolates described above apart from N86S[120]. This suggests that although obtaining laboratory mutants of pathogens which have increased resistance to fungicides and characterising this resistance is useful, it may not necessarily reflect what happens in the field.

So far, there has only been one SDHI-resistant population reported in powdery mildews, in *P. fusca* on cucumber that had been sprayed with boscalid to control Corynespora leaf spot[121]. By sequencing a section of the *SdhB* gene in five resistant and five sensitive *P. fusca* isolates, an H267Y mutation was found in two of the five resistant isolates. However, in the other three resistant isolates included in the study, no mutations were identified compared to sensitive isolates. As only part of the *SdhB* gene was included in the study, it is possible that there were mutations present outside of the region sequenced. It is equally possible that there were mutations in the *SdhC* and/or *SdhD* genes conferring resistance, but this was not explored[121].

Currently, SDHIs are the newest group of broad-spectrum fungicides available for controlling plant pathogens but resistance has emerged in some pathogens, particularly amongst *Z. tritici*

populations. By being able to predict what mutations are likely to arise in response to fungicide pressure, newer SDHI molecules can be developed to target other areas of the binding pocket or protein complex. As soon as they are available for use they can be used in conjunction with currently available fungicides which have alternative modes of action in order to reduce the risk of fungicide-resistant pathogen populations emerging.

In the JIC glasshouses between September 2013 and November 2014, cyflufenamid and Aviator^{235} Xpro had been sprayed excessively to control wheat powdery mildew growth. Lack of mildew control suggested at least one of the three fungicides used in the glasshouses was not effectively controlling the spread of infection. This chapter tests the hypothesis that these *Bgt* isolates were resistant to at least one of these fungicides. It was found that *Bgt* with complete resistance to cyflufenamid had emerged in the glasshouses. RNA-seq was used to identify a candidate target gene for the fungicide as its mode of action is currently unknown. Increased resistance to prothioconazole within the UK *Bgt* field population compared to an older isolate was also found and, likewise, resistance to Aviator^{235} Xpro had increased despite no mutations within the *SdhB*, *SdhC*, and *SdhD* genes being present.

4.2 Methods

4.2.1 Determining the level of sensitivity of *Bgt* isolates to cyflufenamid and Aviator^{235} Xpro using fungicide-supplemented agar

Cyflufenamid was added to molten agar as described in chapter 2 (section 2.4). These fungicide agar tests were performed with an initial 10-fold dilution series from 0.0001 µg/mL to 10 µg/mL. As no colonies formed on the control leaves for UK field isolates, it was suspected that vapour from the higher doses were killing the spores. To find the minimum inhibitory concentration (MIC) for those isolates, the dose range was decreased until colonies were visible on the control leaves. The dose range required to see colonies from those isolates was a 10-fold series from 1 pg/mL to 100 pg/mL. These initial tests were performed with a small subset of isolates: four UK field isolates (EOW1501, EOW1502, AEW1504, TKW1504) and two 2014 glasshouse isolates (CAW14S6101 and CAW14S6312).

As there was a large differentiation between responses to cyflufenamid from resistant and sensitive isolates, it was possible to categorise them using a single critical dose of cyflufenamid in the agar tests. The same agar test method was used as with the large dose ranges except only one dose (0.01 µg/mL) per isolate was used that would distinguish between resistant and sensitive isolates. An untreated control was also included in the experiments. All isolates

described in chapter 2 (tables 2.1.1 to 2.1.6, excluding 2.1.3) were tested with a single critical dose and categorised as sensitive or resistant.

Aviator^{235} Xpro was added to molten agar to identify if isolates collected from the glasshouses were more resistant to bixafen compared to isolates from the UK field *Bgt* population. An initial 10-fold dose range from 0.01 to 100 µg/mL was used, then a more appropriate 2-fold dose range covering the range of ED_{50}s of isolates included was used from 0.625 to 10 µg/mL. These tests were performed with all 2014 glasshouse isolates and two UK field isolates (EOW1501 and EOW1502).

4.2.2 Determining the level of sensitivity of *Bgt* isolates to cyflufenamid and Aviator^{235} Xpro using a spray method

Fungicide spray tests were performed with Aviator^{235} Xpro and cyflufenamid separately as described in chapter 2 (section 2.5). For all fungicide tests, trays of Cerco seeds were used as only wheat powdery mildew was being tested. For spray tests using cyflufenamid, a 1.8-fold dose range up to and beyond the recommended field rate was applied. This included seven doses of 0, 86, 154, 278, 500 (recommended field rate), 900, and 1620 mL/ha. JIW11 and older European isolate Fel09 were used as sensitive controls in these tests. US isolates Harry, Ron, and Hagrid were also used as sensitive controls as they were sampled from areas where mildew had not been exposed to cyflufenamid. UK field isolates AEW1504, ASW1504, ASW1506, CMW1505, and TKW1503 were included as a comparison as they represent the baseline sensitivity in the current UK *Bgt* population. All 2014 and 2015 isolates in table 2.1.1, 2015 W.1 glasshouse isolates in table 2.1.2, and 2016 isolates in table 2.1.3 were tested for their levels of sensitivity to cyflufenamid.

For spray tests using Aviator^{235} Xpro, a 2-fold dose range up to the recommended field rate was applied. This included doses 0, 9.77, 19.53, 39.06, 78.13, 156.25, 312.5, 625, and 1250 mL/ha. Older UK isolate JIW11 was used as a sensitive control in this test, and three UK field isolates were included to represent the baseline sensitivity in the current UK *Bgt* population. All of the 2014 glasshouse isolates were tested for responses to Aviator^{235} Xpro. ED_{50} values were calculated according to the method in chapter 2 section 2.8.

4.2.3 RNA-seq analysis of cyflufenamid-resistant and -sensitive isolates to identify the mode of action of cyflufenamid

Isolates selected for RNA-seq analysis are summarised in table 4.2.3.1. Material collection, RNA extraction, and RNA quantification were performed as described in chapter 2 section 2.4. RNA from 20 isolates was extracted and quantified by my colleague Dr. Laetitia Chartrain. RNA

sequencing, alignment, and SNP calling were performed as described in chapter 2 section 2.5. For this analysis, access to the new version of the 96224 reference genome[67] was granted to us by Prof. Beat Keller, University of Zurich.

The non-synonymous SNPs identified at a minimum of 20x coverage were extracted for each isolate using custom Python scripts developed by Dr. Jitender Cheema along with the chromosome each SNP is located on, the nucleotide position in the chromosome, the gene identifier, the nucleotide at that position in the reference genome, and the nucleotide it has been mutated to in each isolate. These SNPs were then compared between resistant and sensitive isolates to identify mutations that occurred in all resistant isolates and none of the sensitive isolates. This included identifying positions that may have been mutated in both resistant and sensitive isolates as long as none of the sensitive isolates contained the same mutation as resistant isolates. It also included positions where different mutations may have occurred amongst the resistant isolates as long as none of those mutations were present in any of the sensitive isolates. In addition to this, the presence of multiple mutations at different bases within a gene which confer resistance was checked because different mutations within the same gene in different resistant isolates may have conferred resistance to cyflufenamid.

Table 4.2.3.1: Summary of Bgt *isolates used for RNA-seq analysis which aimed to identify candidate genes targeted by cyflufenamid. Lineages were determined using SSRs. "WC" indicates which isolates were exposed to a sub-lethal dose of cyflufenamid before epidermal peels were collected.*

Isolate	Group	Isolate	Group
CAW14S6303	Resistant – lineage 1	**CAW15S6343**	Sensitive
CAW14S6303 (WC)		**ASW1504**	
CAW15S6332		**CMW1502**	
CAW14S6313	Resistant – lineage 2	**EOW1501**	
CAW14S6330		**EOW1501 (WC)**	
CAW15S6309	Resistant – lineage 3	**JIW11**	
CAW14S6312		**Fel09**	
CAW14S6103	Resistant – lineage 4	**ASW1502**	
RBPT22	Resistant – lineage 6	**CMW1502 (rep)**	
CAW15S6320	Sensitive	**12 x US isolates**	
CAW15S6334		**2 x Swiss isolates**	

4.2.4 Sequencing of the *SdhB*, *SdhC,* and *SdhD* genes targeted by SDHI fungicides

The *SdhB* gene is 789 bp long containing two exons and one intron. Primers SDHB_1F and SDHB_1R were used to amplify the entire gene using PCR and were used to sequence the gene. *SdhC* is 737 bp long consisting of three exons and two introns. SDHC_1F and SDHC_1R were used

to PCR amplify and sequence the gene. *SdhD* is 661 bp long containing three exons and two introns. Primers SDHD_1F and SDHD_1R were used to amplify and sequence the entire gene. Primer sequences, annealing temperatures and PCR product sizes are shown in table 4.2.4.1. Positions of primers within each gene are shown in figure 4.2.4.1.

PCR for all three genes was performed in 20 µL reactions consisting of 1x HF buffer, 0.4 U Phusion® High-Fidelity DNA polymerase (New England Biolabs Ltd, UK), 200 µM dNTPs, 0.5 µM forward primer, 0.5 µM reverse primer, 3 % DMSO, 50 ng DNA, and made up to 20 µL with DNase-free water. To amplify the *SdhC* gene, thermocycling conditions began with an initial denaturation at 98 °C for 30 seconds, followed by 30 cycles of 98 °C for 1 minute, 67 °C for 1 minute, and 72 °C for 2 minutes, with a final elongation step at 72 °C for 7 minutes. To amplify the *SdhB* and *SdhD* genes, thermocycling conditions were as follows: initial denaturation at 98 °C for 10 seconds followed by 33 cycles of 98 °C for 10 seconds, 67.5 °C for 30 seconds, and 72 °C for 1 minute, with a final elongation step at 72 °C for 7 minutes.

Table 4.2.4.1: Primer sequences, annealing temperatures, and PCR product sizes for amplifying and sequencing the SdhB*,* SdhC*, and* SdhD *genes in* Bgt*.*

Primer name	Primer sequence (5' to 3')	Annealing temperature	PCR product size
SDHB_1F	TGCGCAGCAAAGCAGATTAT	67.5 °C	844 bp
SDHB_1R	AAGACCTCTCATGGCGCTTC		
SDHC_1F	ACTTTGTCGTGTGCCAAGCA	67 °C	1000 bp
SDHC_1R	GTACGGGAAACCATACGACTCT		
SDHD_1F	GAGCTTGTGGTCAGTGAACTT	67.5 °C	798 bp
SDHD_1R	CGTGCCGTTATTGCGATTCAA		

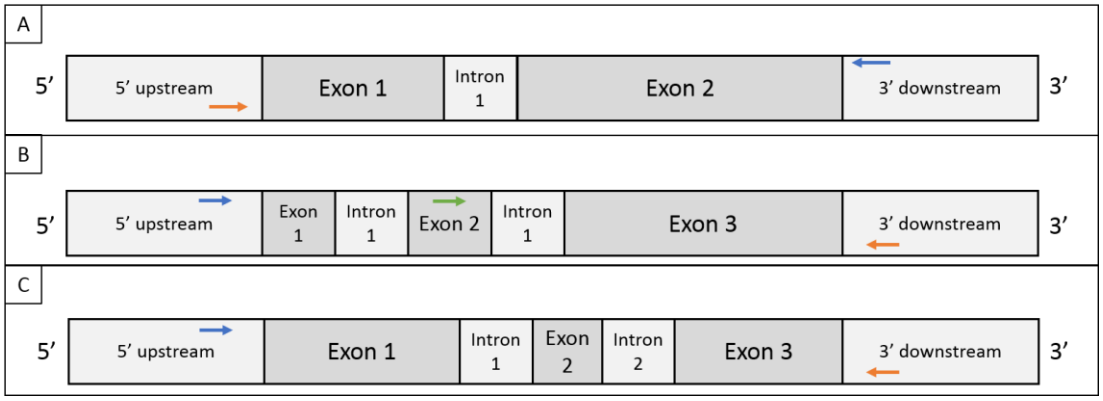

Figure 4.2.4.1: Diagram of the SdhB *(panel A),* SdhC *(panel B), and* SdhD *(panel C) genes in* Bgt *isolate 96224. Blue and orange arrows indicate forward and reverse primers used for PCR and sequencing. The green arrow in panel B shows an extra forward primer used for sequencing the middle section of* SdhC*.*

4.2.5 Amplifying simple sequence repeats in *Bgt* isolates to identify lineages

Primers developed by Parks *et al.* (2011) were used to amplify three simple sequence repeat (SSR) regions: Bgt-5, Bgt-8, and Bgt-10. Forward primers for Bgt-5 and Bgt-10 were M13-labelled in combination with the HEX fluorophore. The forward primer for Bgt-8 was M13-labelled in combination with the FAM fluorophore. All primer sequences are shown in table 4.2.5.1. PCR was performed in 6.2 µL volumes containing 1x HotStarTaq Master Mix (Qiagen Ltd, UK), 0.75 µM fluorolabelled adapter, 0.75 µM reverse primer, 0.05 µM forward primer with M13 tail, 10 ng DNA and made up to 6.2 µL with DNase-free water. Thermocycling conditions were 95 °C for 15 minutes, followed by 40 cycles of 95 °C for 1 minute, 58 °C (Bgt-5, Bgt-8) for 1 minute and 72 °C for 1 minute, and a final extension step at 72 °C for 10 minutes. Bgt-10 required a touchdown PCR programme consisting of 95 °C for 15 minutes, followed by 10 cycles of 95 °C for 1 minute, 65 °C to 56 °C for 1 minute decreasing by 1 °C every cycle and 72 °C for 1 minute, then 24 cycles of 95 °C for 1 minute, 55 °C for 1 minute, 72 °C for 1 minute with a final extension at 72 °C for 10 minutes.

Table 4.2.5.1: PCR primers designed by Parks et al*. (2011) to amplify SSRs in* Bgt*.*

Primer Name	Primer Sequence (5' to 3')
M13-Bgt-5F	TGTAAAACGACGGCCAGTGGAGAATGGAGGAACTTGTAT
Bgt-5R	CCACAGAATGAGGAAAGATAAT
M13-Bgt-8F	TGTAAAACGACGGCCAGTGGCATTCTGCTATATTCTATCCTA
Bgt-8R	TGCTGCCAATGTCAAGATGT
M13-Bgt-10F	TGTAAAACGACGGCCAGTCCAATCCTCAGGGTTCGGT
Bgt-10R	TGGATGTCACATGGTATCAGAGC

These three loci were amplified in all isolates from tables 2.1.1 to 2.1.4 and 2.1.6. Fragments were analysed on an ABI3730x1 DNA analyser with LIZ500 size standard. Results were analysed using GeneMapper 4.0 software and exported to Microsoft Excel.

4.2.6 PCR amplification of a section of the mitochondrial cytochrome *b* gene to identify the presence of a mutation involved in QoI fungicide resistance

Primers designed by Robinson *et al.* (2002) were used for allele-specific amplification of a portion of the mitochondrial cytochrome *b* gene. Resistance to QoI fungicides is very common amongst *Bgt* isolates in the UK as well as other countries[e.g.33,123,124]. Resistance is conferred by a

Table 4.2.6.1: PCR primer sequences designed by Robinson et al*. (2002) to amplify a portion of the cytochrome* b *gene.*

Primer Name	Primer Sequence (5' to 3')
CytbRF	GCAGATGAGCCACTGGGC
CytbSF	GCAGATGAGCCACTGGGG
Cytb11R	CATTCAGAGCTTGGCTAAGTCCG

single nucleotide mutation, G143A (chapter 1 section 1.4), which can be identified by a simple PCR amplification[33]. Two primer combinations were used: forward primer CytbRF and reverse primer Cytb11R to amplify QoI-resistant isolates containing nucleotide sequence GCN (alanine), and forward primer CytbSF and reverse primer Cytb11R to amplify QoI-sensitive isolates containing nucleotide sequence GGN (glycine). Primer sequences are shown in table 4.2.6.1. All isolates in tables 2.1.1 to 2.1.4 and 2.1.6 were included in these PCRs.

PCR was performed in 10 µL volumes containing 1x GoTaq® G2 Green Master Mix (Promega UK Ltd; GoTaq® G2 DNA Polymerase in 2X reaction buffer with 400 µM dATP, 400 µM dGTP, 400 µM dCTP, 400 µM dTTP and 3mM $MgCl_2$), 0.5 µM forward primer (either CytbRF or CytbSF), 0.5 µM reverse primer Cytb11R, 3 % DMSO, 10 ng/µL DNA, and made up to 10 µL with DNase-free water. Thermocycling conditions were as follows: 95 °C activation for 2 minutes followed by 32 cycles at 95 °C for 30 seconds, 66 °C for 30 seconds and 72 °C for 45 seconds, then a final elongation step at 72 °C for 3 minutes. Amplification with both primer pairs was performed separately for every isolate to determine if isolates were resistant or sensitive to QoI fungicides. PCR products were loaded into a 1.2 % agarose gel containing 0.4 µg/mL ethidium bromide and 1x TAE (Tris-acetate-EDTA) buffer and were electrophoresed at 90 V in 1x TAE buffer. Fragments were visualised and photographed using a UV transilluminator.

4.2.7 Using PCR to identify mating types of *Bgt* isolates

Pre-designed primers (Emily Meyers, North Carolina State University, personal communication) were used to amplify the MAT1 locus of the genome and can be found in table 4.2.7.1. MAT1_F1 and MAT1_R1 amplified the MAT1-1-1 idiomorph (mating type 1), while MAT2_F1 and MAT2_R1 amplified the MAT1-2-1 idiomorph (mating type 2) of the locus. Isolates producing amplicons with the MAT1 primers were considered to be of mating type 1, whereas those producing amplicons with the MAT2 primers were mating type 2. Both primer pairs were multiplexed in each PCR reaction and amplification should only occur with one pair or the other. PCR reactions were performed in 10 µL volumes consisting of 1x GoTaq® G2 Green Master Mix, 0.5 µM of each primer, 3 % DMSO, 20 ng DNA and made up to 10 µL with DNase-free water. Thermocycling conditions were 95 °C for 2 minutes, followed by 33 cycles of 95 °C for 30 seconds, 55 °C for 30 seconds and 72 °C for 30 seconds, with a final extension at 72 °C for 3 minutes. MAT1 amplicons were approximately 375 bp long and MAT2 amplicons were approximately 225 bp long so mating types could easily be distinguished from one another. PCR products were electrophoresed in a 1.2 % TAE-agarose gel with 0.4 µg/mL ethidium bromide and visualised using a UV transilluminator. All isolates in tables 2.1.1 to 2.1.4 and 2.1.6 were checked for their mating type.

4.2.8 Using differential pathology tests to obtain virulence profiles of individual *Bgt* isolates as a way of identifying isolates of the same lineage

The virulence profiles of isolates were obtained by inoculating detached leaves of a range of wheat cultivars with different resistance genes. Cultivars included in these tests were Ambassador (*Pm8*), Anfield (*Pm1*), Aquila (*Pm5*), Armada (*Pm4b*), Axona, Broom (*Pm3d*), Cerco (susceptible control), Chul (*Pm3b*), Galahad (*Pm2*), Holger (*Pm6*), Maris Dove (Pm2+*Mld*), Normandie (*Pm1*+*Pm2*+*Pm9*), Shamrock, Sicco and Wembley. The resistance genes present in each variety have been included in brackets. Those without named genes currently have uncharacterised resistance genes. All cyflufenamid-resistant *Bgt* isolates (identified using the single critical dose agar tests) were included in these tests. Reactions were scored based on their infection type on a scale of 0 – 4[125] with 0 meaning the plant is completely resistant to the pathogen, 1 – 2 meaning the pathogen is avirulent on the plant (presence of necrotic spots equal to or greater in size than colonies), and 3 – 4 meaning the plant is susceptible to the pathogen.

4.3 Results

4.3.1 Development of a single critical dose test to differentiate between resistant and sensitive *Bgt* isolates

To identify if a difference in sensitivity to either cyflufenamid or Aviator^{235} Xpro had emerged in glasshouse isolates compared to UK field isolates, both of these fungicide products were added to molten agar and the ends of detached leaves were sandwich between pieces of agar before being inoculated with *Bgt*. Agar tests with Aviator^{235} Xpro showed that there was no difference in response between 2014 isolates from the glasshouses and isolates from the UK field population. Figure 4.3.1.1 shows two representative 2014 glasshouse isolates (CAW14S6307 and CAW14S6309) and one UK field isolate (EOW1501), and their responses to increasing doses of Aviator^{235} Xpro added to the agar. All three isolates had an MIC of 5 µg/mL.

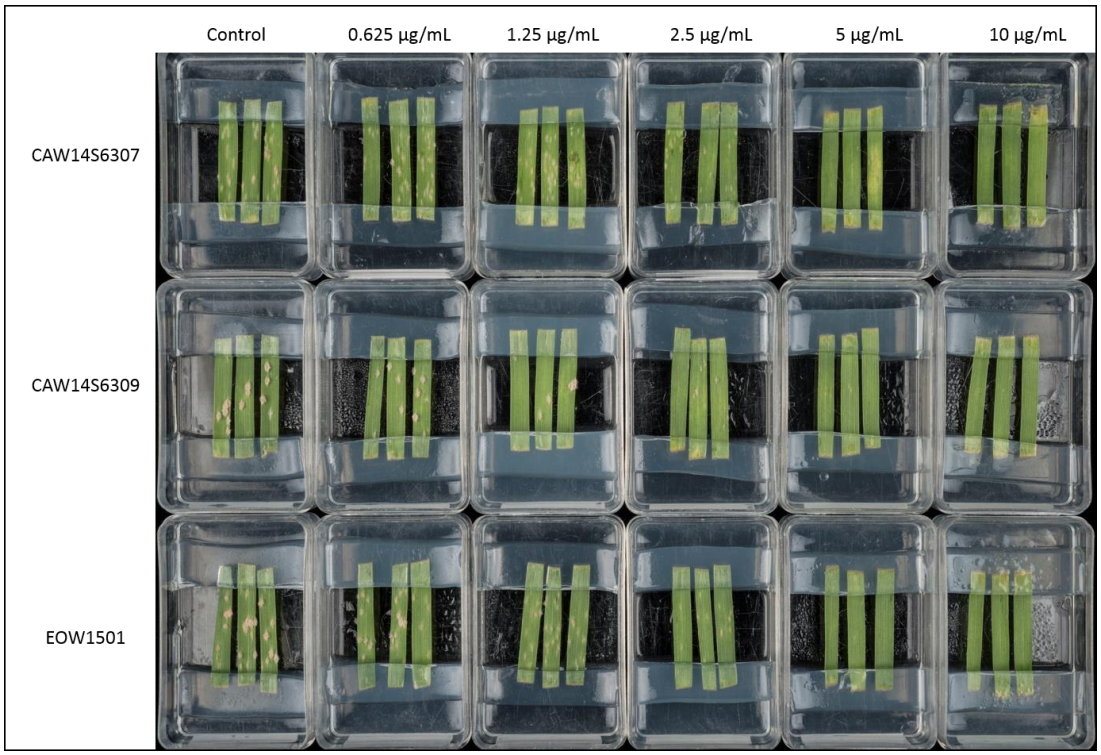

Figure 4.3.1.1: Responses of two 2014 glasshouse Bgt *isolates (CAW14S6307 and CAW14S6309) and one UK field isolate (EOW1501) to increasing doses of Aviator^{235} Xpro added to agar.*

The cyflufenamid fungicide agar tests showed that sensitive *Bgt* isolates only formed colonies at 1 pg/mL whereas isolates showing resistance were able to grow up to 1 µg/mL which is a one million-fold difference in sensitivity. There were no intermediate responses. This all-or-nothing response meant only a single dose was needed to categorise the isolates. Figure 4.3.1.2 summarises how many isolates from each group were categorised as being resistant or sensitive to cyflufenamid using the single critical dose test.

From this categorisation, it is clear that the number of resistant isolates present within the glasshouse *Bgt* population decreased over time after Cyflamid applications were stopped from mid-November 2014 onwards. The percentage of resistant isolates decreased from 100 % to 3 % between 2014 to 2016. These results illustrated that while there did not appear to be an increase in resistance to Aviator^{235} Xpro in *Bgt* in the glasshouses, resistance to cyflufenamid had occurred but when the spray was no longer applied, the resistant population rapidly declined.

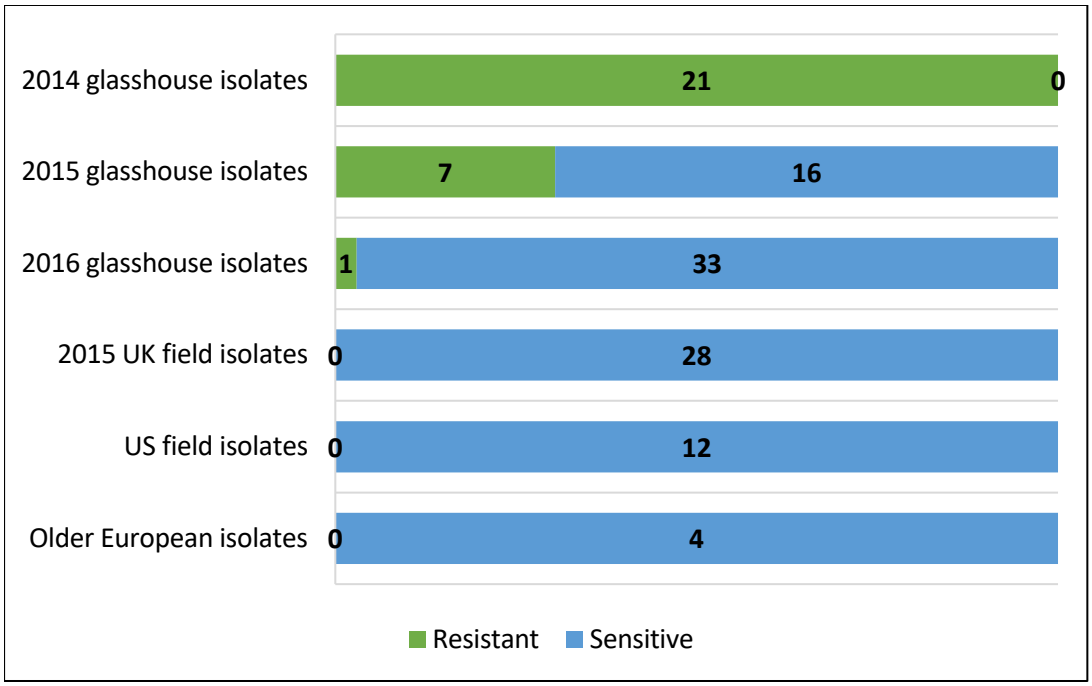

Figure 4.3.1.2: Bgt *isolates were tested with a single critical dose of cyflufenamid in order to categorise them as either resistant or sensitive to the fungicide. The numbers within the coloured bars represent how many isolates in each set were resistant (green bars) or sensitive (blue bars).*

4.3.2 *Bgt* responses to cyflufenamid and Aviator^{235} Xpro treatments

It is difficult to extrapolate from agar tests to spray applications, and the relevance of the million-fold difference between sensitive and resistant isolates to practical disease control is unclear. The fungicide was therefore applied to seedlings as a spray which is a more representative method of fungicide application in agriculture. Using this spray method, there was still a clear division between resistant and sensitive isolates. This can be seen in figure 4.3.2.1 which shows the responses to cyflufenamid from a selection of resistant and sensitive isolates.

Figure 4.3.2.2 summarises the results of the cyflufenamid spray test. The Y-axis shows the growth of isolates as a percentage of the maximum mean colony number. This is because there was inevitable variation in the distribution of *Bgt* spores over the leaves, therefore the maximum

growth seen was not necessarily on the untreated control. This meant that plotting growth as a percentage of the untreated control resulted in percentages higher than 100 %.

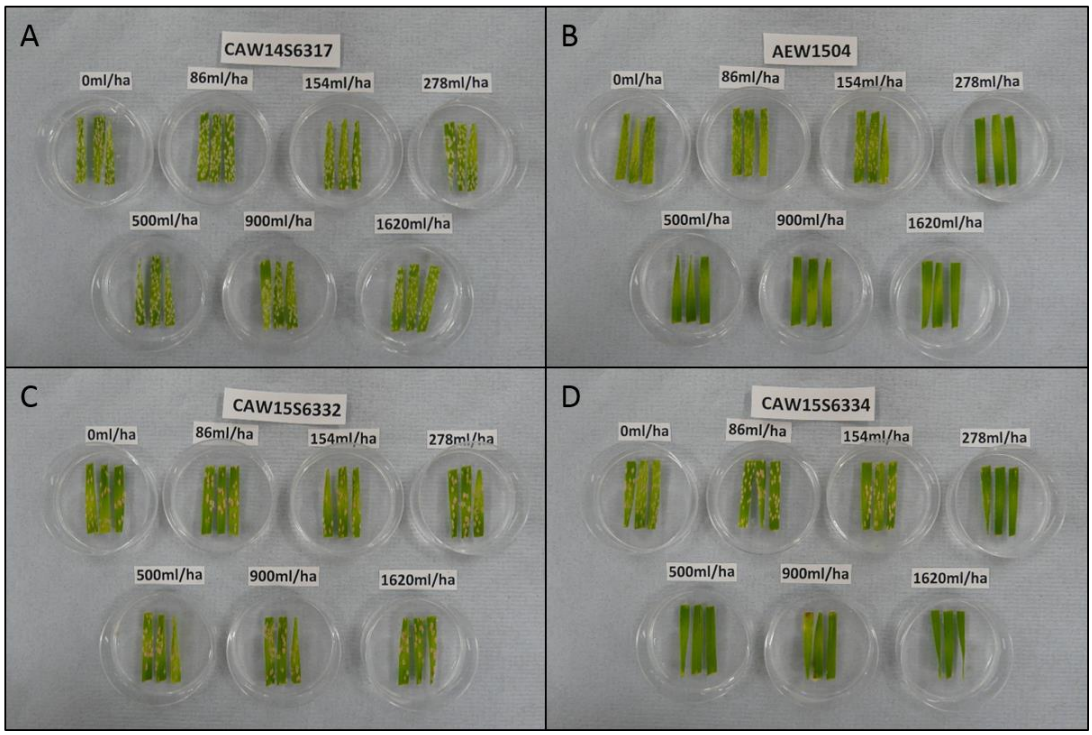

Figure 4.3.2.1: Responses of Bgt *isolates to increasing doses of cyflufenamid sprayed onto Cerco seedlings. A: a resistant isolate from the glasshouse in 2014. B: a sensitive isolate from the UK field population. C: a resistant isolate from the glasshouse in 2015. D: a sensitive isolate from the glasshouse in 2015. These are representative isolates from each of the resistant and sensitive categories. All isolates that are resistant, regardless of collection date or location, grow to the maximum dose (1620 mL/ha) and all sensitive isolates, regardless of their collection date or location, grow to 154 mL/ha or 278 mL/ha.*

A resistance factor for resistant glasshouse isolates from 2014 to 2016 could not be estimated as they were fully resistant to the maximum dose applied. As the recommended field rate of cyflufenamid is 500 mL/ha, it can also be seen that the cyflufenamid-resistant isolates survived doses more than 3-times this recommended rate. Sensitive isolates had an MIC usually of 278 or occasionally 500 mL/ha and an ED_{50} of 91.4 ± $10^{(0.017)}$ mL/ha (figure 4.3.2.3). Growth of UK field isolates was visible at 500 mL/ha in figure 4.3.2.2 due to one colony that formed from one isolate at this dose. Growth of 2015 sensitive glasshouse isolates was also visible at 500 mL/ha due to ten colonies that formed from two isolates.

As it was possible that the loss of control of *Bgt* in the glasshouses could have been due to resistance to SDHI fungicides occurring as is common with other pathogenic organisms, the effect of bixafen was studied on the 2014 glasshouse isolates compared to the UK field *Bgt*

population and JIW11. Figure 4.3.2.4 shows the responses of these isolates to increasing doses of Aviator^{235} Xpro and ED_{50} estimations.

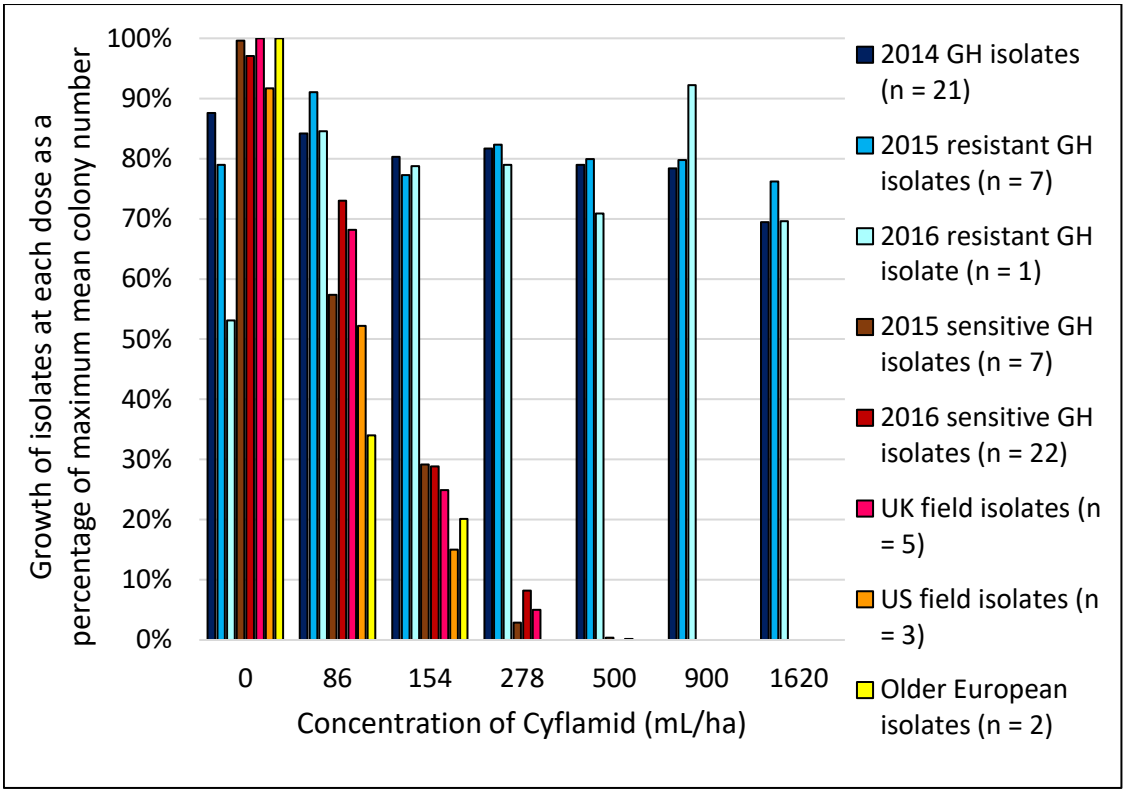

Figure 4.3.2.2: Responses of 58 Bgt *isolates from the glasshouses (GH) in 2014-16, five UK field isolates from 2015, three US isolates, and two older European isolates (JIW11 and Fel09) to increasing doses of cyflufenamid (Cyflamid). N values for each group are stated in parentheses.*

Apart from two out of 21 glasshouse isolates from 2014 that were able to form a total of four colonies at the highest dose, there appeared to be no significant difference in response to Aviator^{235} Xpro between the glasshouse isolates and isolates from the UK field population. However, by fitting a dose-response logistic curve to the data, the ED_{50} was estimated as 177.2 ± $10^{(0.024)}$ mL/ha for field isolates and 247.6 ± $10^{(0.017)}$ mL/ha for the 2014 glasshouse isolates, a resistance factor of 1.4 in glasshouse isolates. It can also be seen that the current *Bgt* population was 4-fold less sensitive to Aviator^{235} Xpro than JIW11 was. This was reflected in the ED_{50} estimations as the ED_{50} for JIW11 was 48.8 ± $10^{(0.27)}$ mL/ha. This meant there was a 3.6-fold increase in resistance in the field isolates and 5.1-fold increase in the 2014 glasshouse isolates compared to JIW11.

Overall, these spray tests showed that *Bgt* isolates collected from the glasshouses were more resistant to cyflufenamid than isolates from the field *Bgt* population as well as older UK isolate JIW11 and US isolates that have never been exposed to this fungicide. Additionally, there was a slight increase in resistance to Aviator^{235} Xpro between the 2014 glasshouse isolates and the field isolates, but most isolates were unable to grow at the recommended field application rate,

so complete resistance had not occurred even though the current UK *Bgt* population has reduced sensitivity compared to JIW11.

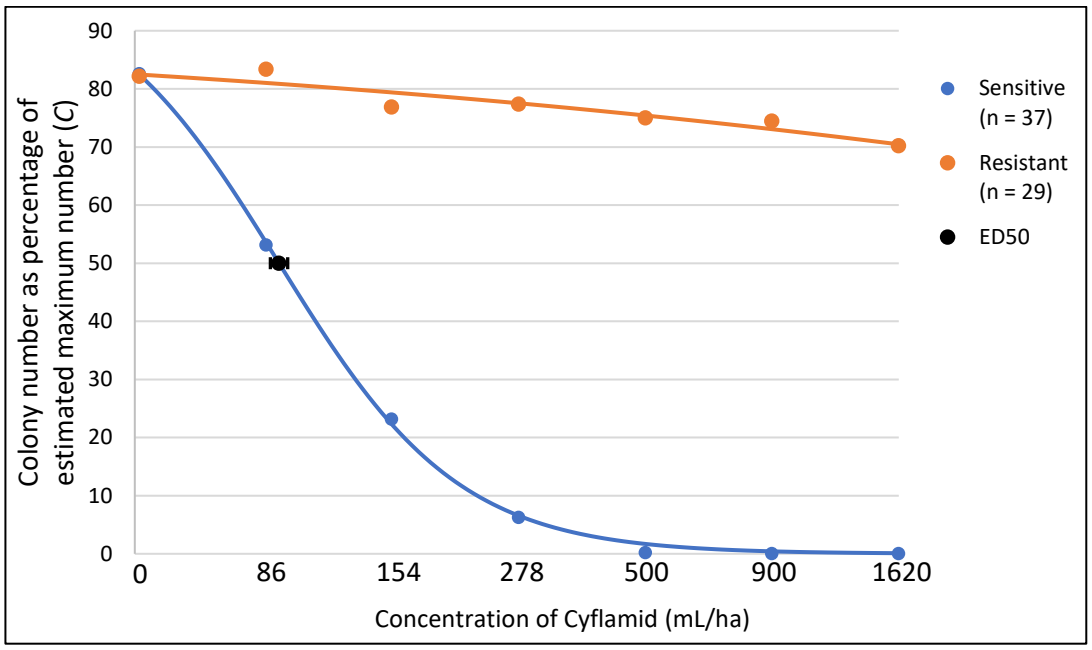

Figure 4.3.2.3: Fitted dose-response logistic curves for 37 sensitive isolates and 29 resistant Bgt *isolates to cyflufenamid (Cyflamid). The* ED_{50} *and standard error for sensitive isolates is shown in black. N values for each group are shown in parentheses.*

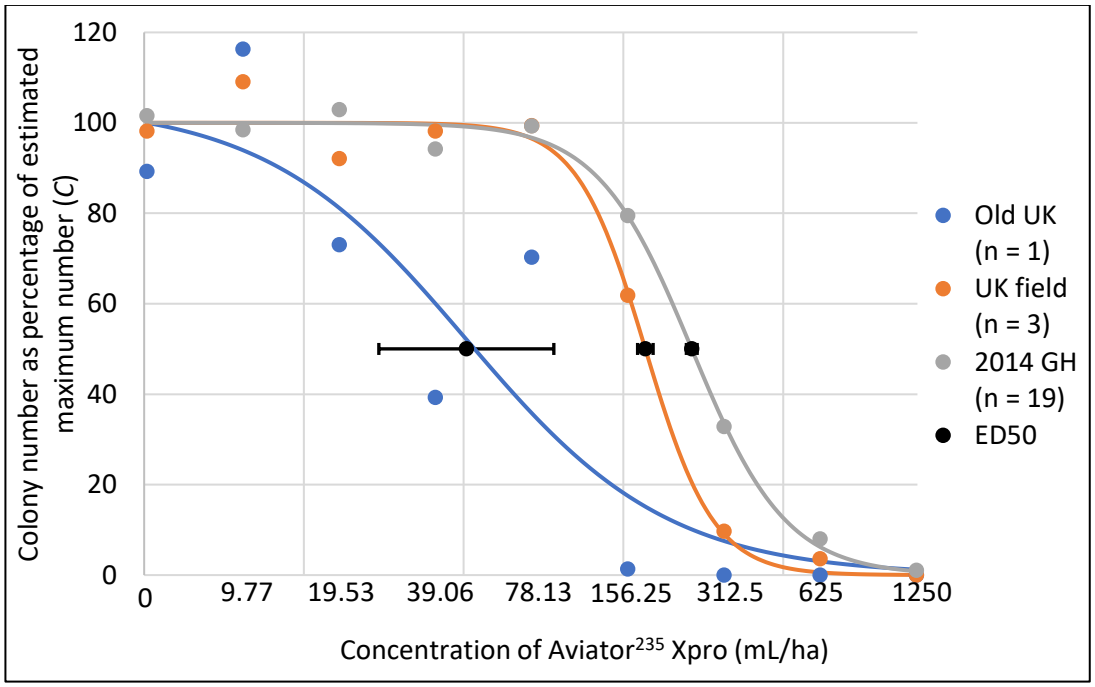

Figure 4.3.2.4: Fitted dose-response logistic curves for one old UK isolate, three UK field isolates, and 19 2014 glasshouse (GH) Bgt *isolates to Aviator*^{235} *Xpro. The* ED_{50} *values and standard errors are shown in black. N values for each group are shown in parentheses.*

4.3.3 *Sdh* gene sequencing shows that *Bgt* isolates lack mutations in *Sdh* genes

The SDHI fungicide bixafen included in the Aviator^{235} Xpro formulation targets the SDH protein complex. Mutations conferring resistance to SDHIs in other organisms have been found in the SDHB, SDHC, and SDHD proteins therefore the three genes encoding these proteins were sequenced in the 2014 glasshouse *Bgt* isolates and older UK isolate JIW11. When sequencing these genes, no mutations were identified in any of the open reading frames in any of the 2014 glasshouse isolates compared to the 96224 reference sequence. Additionally, no mutations were identified between any of the 2014 glasshouse isolates and older UK isolate JIW11 which suggested that the increased resistance to Aviator^{235} Xpro in the glasshouse isolates was either do to a mutation outside the open reading frames or that the SDHI bixafen did not control *Bgt* well anyway and the increased resistance to Aviator^{235} Xpro reflected responses to prothioconazole (discussed further in chapter 5).

4.3.4 Identification of several cyflufenamid-resistant isolate lineages

To classify cyflufenamid-resistant isolates into distinct lineages, for each *Bgt* isolate SSR fragment sizes, QoI resistance or sensitivity, mating type, cyflufenamid resistance or sensitivity, and whether isolates were mutant or wild-type at the Y136F position in the *Cyp51* gene (discussed in chapter 5) were considered; lineages 1 to 4 are shown in table 4.3.4.1. All 2014 isolates had the QoI-resistance allele.

The results showed that cyflufenamid-resistant isolates were clearly not all members of the same lineage. Several lineages were present, and resistance occurred in at least three separate parental isolates and spread through the glasshouses. As lineages 1 and 2 differed only at one SSR and it was only a 5 bp difference in size, it is possible that isolates from these 2 lineages are part of the same lineage, but for the analysis here they were considered as separate lineages. Table 4.3.4.2 shows the same summary for the 2015 glasshouse isolates. All 2015 isolates had the QoI-resistance allele. From these results, two of the lineages present in 2014 were also identified in 2015. The other two lineages were not detected either because they were not picked up during sampling or because they were no longer present. A fifth lineage of isolates was detected, but this was made up of cyflufenamid-sensitive isolates. All of the remaining 2015 isolates were very diverse and did not group into lineages.

Table 4.3.4.1: SSR analysis of 2014 Bgt *isolates identified as being resistant to cyflufenamid. SSR data along with mating type, cyflufenamid resistance, and genotype at the Y136F position in the* Cyp51 *gene allowed the isolates to be categorised into separate lineages. 'M' indicates missing data. 'Y/F' instead of Y136 or F136 in the* Cyp51 *gene indicates isolates that had both Y136 and F136 (discussed further in chapter 5).*

Lineage	Isolate	SSRs			Mating type	Cyflufenamid resistant (R) or sensitive (S)	*Cyp51* Y136F
		Bgt-5	Bgt-8	Bgt-10			
1	CAW14S6101	250	530	507	2	R	F136
	CAW14S6102	250	530	507	2	R	F136
	CAW14S6303	250	530	507	2	R	F136
	CAW14S6304	250	530	507	2	R	F136
	CAW14S6305	250	530	507	2	R	F136
	CAW14S6306	250	530	507	2	R	F136
	CAW14S6308	250	530	507	2	R	F136
	CAW14S6311	250	530	507	2	R	F136
	CAW14S6316	250	530	507	2	R	F136
	CAW14S6318	250	530	507	2	R	F136
	CAW14S6104	250	530	507	2	R	F136
	CAW14S6302	M	530	507	2	R	F136
	CAW14S6307	M	530	507	2	R	F136
	CAW14S6310	M	530	M	2	R	F136
2	CAW14S6301	250	535	507	2	R	F136
	CAW14S6313	250	535	507	2	R	F136
3	CAW14S6309	281	448	594	1	R	Y/F
	CAW14S6312	281	448	594	1	R	Y/F
	CAW14S6314	281	448	594	1	R	Y/F
	CAW14S6317	281	448	594	1	R	Y/F
4	CAW14S6103	M	448	594	1	R	F136

Table 4.3.4.2: SSR analysis of 2015 Bgt *isolates. SSR data along with mating type, cyflufenamid resistance or sensitivity, and genotype at the Y136F position in the* Cyp51 *gene allowed the isolates to be categorised into separate lineages. 'M' indicates missing data. 'Y/F' instead of Y136 or F136 in the* Cyp51 *gene indicates isolates that had both Y136 and F136 (dicussed further in chapter 5).*

Lineage	Isolate	SSRs			Mating type	Cyflufenamid resistant (R) or sensitive (S)	*Cyp51* Y136F
		Bgt-5	Bgt-8	Bgt-10			
1	CAW15S6332	250	530	M	2	R	F136
	CAW15W101	250	530	507	2	R	F136
	CAW15W102	250	530	507	2	R	F136
	CAW15W103	250	530	507	2	R	F136
	CAW15W104	250	540	507	2	R	F136
	CAW15W105	250	530	507	2	R	F136
2	CAW15S6330	250	535	507	2	R	F136
5	CAW15S6331	281	390	521	1	S	F136
	CAW15S6334	281	390	521	1	S	F136
	CAW15S6336	281	390	521	1	S	F136
	CAW15S6337	281	390	521	1	S	F136
	CAW15S6338	281	390	521	1	S	F136
	CAW15S6339	281	390	521	1	S	F136
	CAW15S6342	281	390	521	1	S	F136
	CAW15S6343	281	390	521	1	S	F136
Misc.	CAW15S6320	250	505	373	1	S	F136
	CAW15S6323	281	597	289	1	S	Y/F
	CAW15S6325	259	442	541	1	S	F136
	CAW15S6328	250	524	532	2	S	F136
	CAW15S6335	284	390	521	1	S	F136
	CAW15S6340	413	524	326	1	S	Y/F
	CAW15S6341	410	524	326	1	S	Y/F
	CAW15S6327	281	390	521	2	S	F136

This analysis was also performed with the 2016 glasshouse isolates (table 4.3.4.3). Only one isolate from 2016 was resistant to cyflufenamid and this was clearly from a different lineage to all of resistant isolates from 2014 and 2015. For the 2016 isolates, the mating type, resistance or sensitivity to QoIs, and sequence at the *Cyp51* Y136F base were not determined, but even so the SSRs and cyflufenamid response gave enough information to show that the frequency of cyflufenamid resistance in the glasshouses was declining.

SSR analysis was also performed with the UK *Bgt* field isolates which were all sensitive to cyflufenamid, but resistant to QoIs. There was huge SSR diversity among these isolates and none of them were from the same lineage. There was also a variety of isolates from both mating types – eleven isolates had mating type 1 and 17 had mating type 2. SSR analysis with Fel09, JIW11, 96224 and 94202 showed they were all from different lineages. Fel09 and 94202 had mating type 1 and the QoI-resistance genotype of Cyt *b*, while JIW11 and 96224 had mating type 2 and the QoI-sensitive genotype.

Table 4.3.4.3: SSR analysis of 2016 Bgt *isolates. SSR data along with cyflufenamid resistance or sensitivity allowed the isolates to be categorised into separate lineages. 'M' indicates missing data.*

Lineage	Isolate	SSRs			Cyflufenamid resistant (R) or sensitive (S)
		Bgt-5	Bgt-8	Bgt-10	
6	RBPT22	281	552	311	R
7	RBS54-14	259	547	311	S
	RBPTM60	259	547	311	S
Misc.	RBS57-3	281	390	M	S
	RBS57-6	281	390	521	S
	RBS54-3	281	390	521	S
	RBS54-8	281	390	521	S
	RBS54-9	281	390	521	S
	RBPT32	281	390	521	S
	RBPT33	281	390	521	S
	RBPT34	281	390	521	S
	RBPT35	281	390	521	S
	RBPT36	281	390	521	S
	RBPT39	281	390	521	S
	RBPTM3	281	390	521	S
	RBS54-1	281	396	521	S
	RBS54-11	281	406	521	S
	RBPT40	287	390	521	S
	RBPTM2	281	489	311	S
	RBPTM5	M	390	M	S
	RBPTM8	244	547	376	S
	RBPTM9	250	608	311	S
	RBPTM44	264	444	311	S

4.3.5 Differential pathology tests confirm presence of multiple lineages

All *Bgt* isolates resistant to cyflufenamid were virulent on Ambassador (*Pm8*), Aquila (*Pm5*), Armada (*Pm4b*), Cerco (susceptible control), Galahad (*Pm2*), Holger (*Pm6*), and Maris Dove (*Pm2+Mld*) regardless of lineage. All resistant isolates were avirulent on Anfield (*Pm1*), Chul (*Pm3b*), Normandie (*Pm1+Pm2+Pm9*), Sicco and Wembley (both with uncharacterised resistance). There was a lot of variation with Shamrock (uncharacterised) as it exhibited a strong hypersensitive response to most isolates. All resistant isolates in lineages 1 and 2 were virulent on Axona (uncharacterised) and Broom (*Pm3d*) whereas resistant isolates in lineages 3 and 4 were avirulent on these varieties. These differential pathology tests were in accordance with the separation of isolates into lineages by other traits and markers.

4.3.6 Identification of a candidate target gene for cyflufenamid using RNA-seq data

In order to identify potential candidate target genes of cyflufenamid, RNA-seq analysis was performed on eight resistant isolates from all five lineages and 23 sensitive isolates. Two candidate target genes were identified which were associated with increased resistance. The first candidate was annotated as being a hypothetical protein (GenBank accession EPQ65128.1) in *Bgt*, but a BLAST search showed it was annotated as a transcription factor in *Bgh* reference isolate DH14 (GenBank accession CCU81695.1). A C to G mutation was present at nucleotide 1734 in the coding sequence (excluding introns) in three out of five lineages, and a C to A mutation was found at the same position in the remaining two lineages. These mutations changed the codon from TTC to either TTG or TTA, both of which resulted in a phenylalanine to leucine substitution at amino acid 578. In four of the sensitive isolates, this codon was mutated from TTC to CTC which also resulted in an F578L mutation therefore this gene was discounted as a candidate.

The second candidate target gene was annotated as a coiled-coil protein in *Bgt* reference isolate 96224 (GenBank accession EPQ65469.1) and a BLAST search showed it was annotated as spindle assembly checkpoint component MAD1 in *Bgh* reference isolate DH14 (GenBank accession CCU74267.1). This gene is 2370 bp long consisting of two exons (117 and 2178 bp long) and one intron (75 bp long) and encodes a protein which is 764 amino acids long. In all five lineages of resistant isolates, a C at nucleotide 1678 was mutated to an A (codon CAG altered to AAG) resulting in a glutamine to lysine substitution (Q560K). Although MAD1 homologues are present in many organisms, no crystal structures from *Bgt* or any closely-related organisms were available, so a protein model could not be generated therefore it is currently unknown if this mutation is associated with the active site of the protein.

Three other candidate target genes were identified where mutations were present in four out of five lineages but in all three cases, isolate RBPT22 in lineage 6 did not have the mutation. In addition to this, another candidate gene was identified where isolates from two lineages had a mutation in one position and isolates from another two lineages had a mutation in a different position. As with the other three candidates just mentioned, isolate RBPT22 was not mutated at either of these positions. As one of the resistant isolates was not mutated in these four genes, they were not explored further.

4.4 Discussion

Here the first known occurrence of cyflufenamid-resistance in an organism other than *P. fusca*[112,113] is reported. The responses of *Bgt* isolates to cyflufenamid as a spray and in agar (figures 4.3.1.2 and 4.2.3.1-3) showed the same all-or-nothing difference in response between resistant and sensitive isolates with no intermediate responses. This differs from *P. fusca*, where resistant isolates had ED_{50} values from 0.23 to >50 µg/mL, suggesting they had a range of responses[112]. This suggests that in *Bgt* a single protein is targeted by this fungicide and that a single mutation, or small number of mutations in the same gene, may result in resistance. Sexually crossing resistant and sensitive isolates to test if this all-or-nothing response occurred in the progeny would test this hypothesis. If the progeny also exhibited this all-or-nothing response to cyflufenamid, then this would be further evidence to support the hypothesis that there is a single target. The presence of intermediate responses by progeny isolates would suggest that more than one gene is involved in resistance and the resistance alleles of each gene had been inherited independently of each other. Such crosses were attempted by co-inoculating one of each isolate with opposite mating types onto one plant. Unfortunately, chasmothecia were not produced so no progeny could be collected. This could have been due to the accumulation of resistances to QoI, triazole, morpholine, and cyflufenamid fungicides as it has been hypothesised that fungicide resistance may reduce fertility (Prof. James Brown, personal communication).

Even though the fungicide spray method is more representative of normal fungicide application in the field, using agar supplemented with cyflufenamid in the single critical dose tests was useful for quickly categorising isolates as resistant or sensitive, particularly when screening large glasshouse populations simply to monitor whether resistance is present or not. With regards to calculating the extent of increased resistance to a fungicide, the spray tests are more accurate.

As the glasshouses are relatively confined spaces compared to wheat fields, one would expect to find quite low diversity amongst *Bgt* isolates. It is therefore possible that resistance to cyflufenamid only occurred in one isolate and spores from that isolate were spread around the

two glasshouses sampled. By using three SSR loci along with the determination of mating type, isolate virulence profiles on a number of wheat lines, and identification of Y136 or F136 (or both) in the *Cyp51* gene, it was possible to identify that at least four lineages of cyflufenamid-resistant isolates were present in the glasshouses. This confirmed that there were some clonal isolates from the same lineages in the isolates collected, but also that resistance had occurred on at least four separate occasions. As mentioned in section 4.3.4, isolates from lineages 1 and 2 only differed at one SSR locus by 5 bp. As SSRs evolve at a relatively fast rate, it is possible that all isolates from these two lineages were actually part of the same lineage, but they are considered as two lineages in this thesis. The lack of variation in response to cyflufenamid among the different lineages of these resistant isolates further suggests that there is only a single target. If there was more than one target, one may have expected to see some degree of variation in response from isolates of different lineages.

SSR analysis of glasshouse isolates collected in 2015 and 2016 was useful in showing the disappearance of cyflufenamid-resistant isolates, especially as cyflufenamid was no longer being sprayed from 2015 onwards. The SSRs also showed that sensitive isolates in 2014-6 were from different lineages to resistant isolates. Both of these factors suggest that when removing the selection pressure by not spraying cyflufenamid, the resistant isolates did not lose the resistance phenotype, but instead were replaced by sensitive isolates from an external source. Not only does this suggest that resistance is brought about by a mutation in the DNA rather than a change in gene expression potentially due to DNA methylation alterations, but also that there may be a fitness penalty associated with cyflufenamid-resistance. By identifying that all 2014 and 2015 glasshouse isolates (regardless of their level of sensitivity to cyflufenamid) were resistant to QoIs, contained the Y136F mutation in the *Cyp51* gene associated with increased triazole resistance (discussed in chapter 5), and showed reduced sensitivity to fenpropimorph (discussed in chapter 3), it is possible that the addition of a fourth fungicide resistance to cyflufenamid led to an accumulated fitness penalty that impeded the isolates' sexual and asexual reproduction. This could explain why the proportion of resistant isolates present in the glasshouses in 2015 had halved within a single year of removing the selection pressure.

As already discussed, it is important to know what a fungicide's mode of action is and to understand mechanisms of resistance so appropriate fungicide rotation programmes can be put in place as well as understanding toxicity in non-target organisms, assessing off-target effects on other proteins, and aiding resistance monitoring in pathogen populations. Cyflufenamid's mode of action is currently unknown so RNA-seq analysis was carried out with a number of resistant and sensitive isolates which aimed to identify candidate target genes and mutations involved in resistance. The evidence suggests that cyflufenamid is a single-site inhibitor and by

comparing non-synonymous SNPs in resistant isolates from five separate lineages with those from 23 sensitive isolates, a candidate target gene was identified. Based on a BLAST search, this gene is annotated as encoding a spindle assembly checkpoint component, MAD1, which is conserved between many eukaryotic organisms, including yeast (*Saccharomyces cerevisiae* S288C, sequence ID: NP_011429.3, 31% identity, E-value: 3^{-24}), and even humans (*Homo sapiens*, sequence ID: NP_001291452.1, 24% identity, E-value: 1^{-18}). As a crystal structure of this protein is not available from any fungus, modelling of the protein was unsuccessful therefore it was not possible to hypothesise if the mutation was associated with the protein's active site. However, DNA of cyflufenamid-resistant and sensitive cucurbit powdery mildew in Italy[112] could be sequenced to test if the mutation is also present there. It would also be possible to perform UV mutagenesis on cyflufenamid-sensitive *Bgt* isolates, inoculate the exposed spores on detached leaves that have been sprayed with cyflufenamid in order to select for new resistant isolates, and sequence the *MAD1* gene in those isolates. To identify any other potential candidate target genes of cyflufenamid, the abundance of mRNA species within the resistant isolates compared to sensitive isolates could be examined using the RNA-seq data. If there is a significant increase or decrease in abundance of a particular RNA sequence, or absence of a particular sequence from the resistant isolates, this would indicate another potential target of cyflufenamid.

Initial agar tests supplemented with the two fungicides showed that the 2014 *Bgt* glasshouse isolates were no more resistant to Aviator^{235} Xpro than isolates from the UK field population, whereas they were one million-fold more resistant to cyflufenamid. As the isolates were not completely resistant to Aviator^{235} Xpro, one would expect this fungicide to have controlled the growth of *Bgt* even though cyflufenamid did not, particularly as there was a huge increase in resistance to cyflufenamid, but not to Aviator^{235} Xpro, showing that they do not have the same modes of action. By examining the results from the Aviator^{235} Xpro spray tests (figure 4.3.2.4), it could be suggested that this fungicide mixture was not very effective against *Bgt* in the first place as two isolates were able to grow at the recommended application rate, and most other isolates could grow at half that strength. In this case, the complete lack of control could have been amplified by poor spraying practice. If the plants were densely packed in the glasshouse and not spread out for fungicide application, then the spray was unlikely to have evenly reached all of the leaves. This would result in sub-optimal application and present the opportunity for *Bgt* to continue to grow.

The Aviator^{235} Xpro spray tests showed that there was a 1.4-fold increase in resistance between UK field isolates and the 2014 glasshouse isolates (figure 4.3.2.4). They also showed that the UK *Bgt* population as a whole has become less sensitive to a mixture of bixafen and prothioconazole than the older isolate JIW11 by a factor of 3.6. To test this hypothesis, the responses of more UK

Bgt isolates from older populations to Aviator[235] Xpro should be tested but given the trend of reduced sensitivity occurring with many fungicides and many organisms, for example with *Z. tritici* and SDHIs[119], it is likely that this conclusion is correct. Unfortunately for this thesis, only JIW11 was available to include as an older UK *Bgt* isolate in these experiments, but for future experiments, the US field isolates used elsewhere in this thesis could be included as sensitive isolates as they have never been exposed to SDHIs.

The results from the Aviator[235] Xpro and cyflufenamid spray tests along with *Sdh* gene sequencing indicates that the lack of *Bgt* control in the glasshouses in 2014 was mostly due to poor spraying practice as well as the development of resistance to cyflufenamid rather than resistance to bixafen and prothioconazole (Aviator[235] Xpro). The UK *Bgt* population appears to have an increased tolerance to Aviator[235] Xpro compared to older isolate JIW11, but this is not due to mutations in the *SdhB*, *SdhC*, or *SdhD* genes. It is possible that bixafen is not particularly effective against *Bgt* and the difference in response seen here is due to increased resistance to prothioconazole (discussed in more detail in chapter 5), but as bixafen is not available as a single product, this is difficult to test. It is still possible for increased resistance to bixafen to be present without mutations in these genes as this has been seen in *Z. tritici*[126], but alternative mechanisms of resistance have yet to be identified. Although bixafen may not control the growth of *Bgt* particularly well, experiments testing the responses of *Bgt* isolates to other SDHI fungicides should be performed to identify those that do control it well.

Between September 2013 and November 2014, both Aviator[235] Xpro and cyflufenamid had been sprayed in one JIC glasshouse a total of eleven times. Between August and November 2014, both fungicides had been applied in a second glasshouse nine times. During these time periods, it is likely that some plants would have been removed and fresh plants put into the glasshouses, but some plants infected with *Bgt* would have remained which could then have allowed *Bgt* spores to inoculate the fresh plants. This means that although the plant population was not constant, the *Bgt* population likely was and so would have been exposed to all of these individual applications. This is an excessive amount of fungicide application and greatly exceeds the permitted number of applications (two per crop of both Cyflamid and Aviator[235] Xpro).

From the experiments carried out here, it is possible to confirm that resistance to cyflufenamid had occurred in the JIC glasshouses in 2014. Since restricting the use of cyflufenamid and improving glasshouse management, resistant isolates in the glasshouses have been replaced by sensitive isolates. These experiments also showed that resistance to SDHIs had not occurred specifically in these glasshouses, but the general UK *Bgt* population is less sensitive to SDHIs and triazoles than older *Bgt* isolates are which follows the trend seen in other organisms, such as *Z. tritici*[119,126-128].

5 Mechanisms of resistance of *Blumeria graminis* f. sp. *tritici* to sterol C14-demethylation inhibitor fungicides

5.1 Introduction

Sterol de-methylation inhibitor (DMI) fungicides are the largest group of fungicides used to control many crop and human pathogens[129]. Within this group, triazoles are the largest and most commercially significant sub-group and have been used worldwide since the 1970s to control powdery mildew fungi on crops[130]. DMIs inhibit sterol C-14 α-demethylase, a key enzyme in the ergosterol biosynthesis pathway (chapter 1, figure 1.4.1) encoded by the *Cyp51* gene in powdery mildew fungi[49] and *Cyp51* or *Erg11* in other organisms. Resistance to triazole fungicides has gradually emerged over time. Currently, there are four known mechanisms of resistance that have developed in several fungi which include increased *Cyp51* (or equivalent) gene copy number, increased expression of the *Cyp51* gene, increased expression of ATP-binding cassette (ABC) transporter genes, and mutations within the C-14 α-demethylase (CYP51) enzyme. These mechanisms also lead to cross-resistance between triazoles. Isolates of various pathogens have frequently been found to contain combinations of these resistance mechanisms rather than relying on only one[131-135].

Amino acid mutations within the CYP51 protein have been identified in many organisms showing a range in degree of resistance to triazoles[103,132,133,136]. *Blumeria graminis* ff. spp. *hordei* (*Bgh*) and *tritici* (*Bgt*) isolates with a very high level of resistance to triadimenol (a triazole-like fungicide) and propiconazole contained the Y136F mutation. This mutation was also found in isolates that had low levels of resistance. Additional mechanisms of resistance must be present in isolates with Y136F that have higher resistance. Additionally, *Bgh* isolates with very high resistance contained a K147Q mutation[103]. The Y136F mutation was also identified in *Uncinula necator* by cloning and sequencing the *Cyp51* gene and is predicted to increase the hydrophobicity of the DMI binding site[137]. *U. necator* isolates containing this mutation were more resistant to triadimenol, but as with *B. graminis* the level of resistance was variable therefore indicating the presence of alternative resistance mechanisms in some isolates[137]. Additionally, the Y136F mutation was found in three French DMI-resistant *Bgh* isolates but was absent in four Swiss DMI-sensitive *Bgh* isolates which were used for comparison[138].

A study of DMI-resistant *Zymoseptoria tritici* isolates identified a wider range of mutations in the *Cyp51* gene that have emerged in response to newer triazole fungicides, such as epoxiconazole[132]. It was found that DMI-resistant isolates often had combinations of mutations rather than one individual mutation. The Y137F mutation (homologous to Y136F in *B. graminis*) was commonly found in isolates resistant to older triazoles but has been lost in more recent

populations of *Z. tritici* possibly because it causes a significant fitness cost[139]. Most isolates containing this mutation also had an S524T mutation. The *Z. tritici Cyp51* gene sequence was introduced into *Saccharomyces cerevisiae* on a vector that was able to suppress the native *S. cerevisiae Cyp51* gene from being expressed when grown in the presence of doxycycline[140]. The wild-type *Z. tritici Cyp51* gene was able to complement the function of the *S. cerevisiae* gene so it was possible to study the effects of mutations on protein function and cell fitness. When the Y137F mutation was introduced into the *Z. tritici* CYP51 protein, it was unable to complement the function of the native protein therefore no cell growth was seen, however when both Y137F and S524T were introduced, protein function was partially restored and cells were able to grow, but not to the same extent as with the wild-type protein[132]. This suggests why Y137F and S524T are commonly found together in *Z. tritici* field isolates and why Y137F alone is no longer found in the field. However, S524T was not identified alone in any field isolates[132].

Several other mutations were identified in *Z. tritici* in this study. The effects of several combinations of mutations were observed by introducing them into *S. cerevisiae* using the complementation assay described above. These effects are summarised in table 5.1.1. This table also includes mutations identified in *Z. tritici* from other studies that have not already been discussed[141-143].

It was found that the accumulation of mutations caused a greater increase in resistance to a broader range of DMI fungicides than the presence of only one or two mutations[132]. This study proceeded to model the wild-type *Z. tritici* CYP51 protein and compared the wild-type model to one containing the L50S, D134G, V136A, Y461S, and S524T mutations. This showed that the introduction of these mutations resulted in the loss of two β-sheets which contribute to the structure of the protein's active site. This results in the active site having a more open conformation causing DMI fungicide molecules to bind with a lower affinity. The looser conformation means there are fewer amino acids that can come into contact with the fungicide at any one time. The protein model also showed that amino acids D134, Y137, and Y461 are likely to be involved in forming the active site[132].

DMI fungicides are not only used in agriculture but are also used in medicine to control fungal infections. Amino acid Y137 in *Z. tritici* is equivalent to Y132 in the CYP51 protein of *Candida albicans* which was one of the amino acids found to be mutated in fluconazole-resistant isolates[136]. In two *C. albicans* isolates showing more than a 64-fold increase in minimum inhibitory concentration (MIC), Y132 was mutated to a histidine residue. One of these two isolates also had an S504F mutation which, when present alone in four other isolates, conferred a 4-fold increase in fluconazole MIC. The second isolate also contained G464S and R467K. These two mutations were found together in two other isolates and resulted in an 8-fold relative

fluconazole MIC increase. The G464S mutation was found in another isolate alongside G129A resulting in a 32-fold increase in fluconazole MIC[136].

Table 5.1.1: A summary of mutations identified in field isolates of Z. tritici *and their effects on DMI resistance and protein function when introduced into* S. cerevisiae*. The asterisk marks mutations studied by Cools* et al*. (2011).*

Mutation(s)	Effects on protein function and DMI resistance
I381V[141,142]	Resistance to tebuconazole Unique to *Z. tritici*
V136A[143]*****	Destroyed protein function in *S. cerevisiae* Resistance to prochloraz in *Z. tritici* Unique to *Z. tritici*
Y137F + S524T*	S524T partially restored protein function Reduced sensitivity to epoxiconazole, tebuconazole, triadimenol, prochloraz, and propiconazole
L50S + Y461S*	Reduced sensitivity to epoxiconazole, tebuconazole, triadimenol, prochloraz, and propiconazole
L50S + Y461S + S524T*	Substantially reduced sensitivity to epoxiconazole, tebuconazole, triadimenol, prochloraz, prothioconazole, and propiconazole
L50S + V136A + Y461S*	Destroyed protein function in *S. cerevisiae*
L50S + V136A + Y461S + S524T*	S524T partially restored protein function
L50S + D134G + V136A + Y461S*	D134G fully restored protein function Reduced sensitivity to epoxiconazole, tebuconazole, triadimenol, prochloraz, prothioconazole, and propiconazole
L50S + D134G + V136A + Y461S + S524T*	D134G fully restored protein function Substantially reduced sensitivity to epoxiconazole, tebuconazole, triadimenol, prochloraz, prothioconazole, and propiconazole

A second mechanism of resistance employed to overcome the effects of DMIs is to overexpress the *Cyp51* gene. Overexpression of *Cyp51* has commonly been associated with mutations within the promoter region of the gene. An example of this is with *Penicillium digitatum* where 126 bp of the promoter region was found to be tandemly-repeated five times in three DMI-resistant isolates whereas it was only present once in three DMI-sensitive isolates[144]. A fourth isolate which was derived from one of the resistant isolates showed more sensitivity than its parent but was not as sensitive as the DMI-sensitive isolates. In this isolate, the 126 bp region was present twice in tandem. It was suggested that this region may be involved in binding a transcription activator therefore having multiple copies of this region results in increased transcription of the gene. As expected, isolates containing more repeats of the 126 bp region had higher levels of

Cyp51 mRNA which was unaltered in the presence of DMIs suggesting expression was constitutive[144].

In *Blumeriella jaapii*, overexpression of *Cyp51* was achieved in DMI-resistant isolates by the presence of one of four large insertions in the promoter region[145]. These four insertions were 2120, 2224, 2461, and 5585 bp in length. Each of the three shorter insertions contained one retrotransposon open reading frame (ORF) while the larger insertion contained two retrotransposon ORFs, but all of these retroelements were found to be truncated compared to similar retroelements in other organisms. While these insertions were associated with a 5- to 12- fold increase in *Cyp51* gene expression, there was no particular association of increased expression with any one size of insertion[145]. A 553 bp promoter region insertion was also found in DMI-resistant *Venturia inaequalis* isolates and was associated with the highest increase in *Cyp51* (*CYP51A1* in *V. inaequalis*) gene expression[146].

In field isolates of *Puccinia triticina*, several mechanisms of resistance were present in isolates exposed to epoxiconazole[131]. Five out of 110 isolates contained the Y134F mutation homologous to Y136F in *B. graminis* and Y137F in *Z. tritici*. Two of these isolates showed a slightly increased resistance to DMIs, but the other three isolates had ED_{50}s (the dose needed to reduce growth by 50 %) within the normal range of all other isolates included in the study. Additionally, several isolates were identified as having increased expression of the *Cyp51* gene, but it was not determined which mechanism caused the increased expression and overexpression was also identified in a highly sensitive isolate so was not strongly correlated with increased resistance. It was shown that *Cyp51* gene expression in resistant and sensitive isolates was constitutive and was not altered by exposure to different concentrations of epoxiconazole. Interestingly, some isolates showed increased resistance to epoxiconazole, but had neither the Y134F mutation nor increased *Cyp51* expression suggesting another mechanism of resistance was causing resistance in these isolates[131].

In some organisms, *Cyp51* overexpression was achieved by increasing the *Cyp51* gene copy number[147,148]. In *Candida glabrata*, DNA hybridisation probes were used to calculate the quantity of *Cyp51* genes in comparison to the *ACT1* gene encoding actin which was constant across all isolates[147]. The *Cyp51*:*ACT1* gene hybridisation intensity ratio was 3.7-fold higher in DMI-resistant isolates than in sensitive isolates. Likewise, ratio of hybridisation intensity for *CYP51* mRNA compared to *ACT1* was 8-fold higher in DMI-resistant isolates than it was in sensitive isolates. It was found that in isolates with an increased number of *Cyp51* genes, not only had the gene itself been duplicated, but the entire chromosome it was situated on was duplicated. This not only resulted in up-regulation of *Cyp51* gene expression, but also altered the regulation of 100 other genes. After sub-culturing the resistant isolates 40 times in DMI-free medium, the

chromosome duplication along with DMI-resistance was lost. This suggested that without the selection pressure from the fungicide, this duplication was too costly for the organism to maintain[147].

Duplication of the *Cyp51* gene has been identified in *Erysiphe necator* which causes grapevine powdery mildew[148]. Two to 14 copies of the *Cyp51* gene containing the Y136F mutation were found in *E. necator* isolates from vineyards that had been treated with fungicides. From the untreated vineyards, only one copy of the *Cyp51* gene containing the wild-type Y136 allele was present. Overall, 94% of isolates containing multiple copies of the gene also had the Y136F mutation. Additionally, increased copy number was associated with increased *Cyp51* gene expression[148].

In additional experiments, three genotypes were identified amongst *E. necator* isolates[133]. These included wild-type isolates with Y136 (codon TAT), mutated (TTT) isolates with F136, and mixed-genotype (TWT) isolates with both alleles. As *E. necator* is a haploid organism, the presence of both alleles clearly indicated a gene duplication event had occurred and this was associated with increased *Cyp51* gene expression as well as with the highest levels of DMI resistance. TTT and TWT isolates showed a 6- to 19-fold increase in gene expression compared to TAT isolates showing that the Y136F mutation in conjunction with copy number variation were responsible for the quantitative DMI resistance found in *E. necator*[133].

In organisms where no alterations to the CYP51 protein, gene expression or copy number were identified, increased resistance to DMIs was found to be associated with the up-regulation of genes encoding ABC transporters[134,149,150]. In *C. albicans*, increased resistance was associated with a reduced level of accumulated fluconazole in the cytoplasm compared to sensitive strains[134,135]. This was correlated with increased expression of major facilitator gene *BEN*^{r} in one resistant isolate and of the ABC transporter gene *CDR1* in the remaining resistant isolates[134]. This was also found in *B. cinerea* where the overexpression of ABC transporter gene *BcatrD* resulted in reduced oxpoconazole accumulation in the cytoplasm and increased resistance to DMIs[149]. Likewise, when *BcatrD* was knocked-out in *B. cinerea*, the accumulation of oxpoconazole in the cytoplasm exceeded that in wild-type sensitive strains and resulted in increased sensitivity to DMIs[149].

The CDR1 protein in *C. albicans* is a homolog of the Sts1 transporter in *S. cerevisiae* which also confers azole resistance[151]. By introducing CDR1 into a *Δsts1 S. cerevisiae* mutant, resistance to fluconazole, ketoconazole, and itraconazole was restored showing the involvement of CDR1 in DMI resistance[134]. Interestingly, introducing BEN^r into *S. cerevisiae* cells increased resistance to fluconazole, but did not confer resistance to ketoconazole or itraconazole showing the

specificity of this transporter[134]. In *Z. tritici*, the up-regulation of ABC transporters MgAtr1 and MgAtr2 was stimulated by the presence of cyproconazole[150]. When the *MgAtr1* gene was disrupted in several DMI-resistant isolates, the accumulation of cyproconazole in the cytoplasm matched that of the sensitive isolates confirming the role of ABC transporters in increased DMI resistance by active efflux of toxic chemicals[150]. Using ABC transporters to detoxify the cytoplasm is a useful alternative mechanism of resistance to DMIs, particularly as it has been shown that mutations within the CYP51 protein have been associated with a fitness cost[152,153]. An example of this is in *Monilinia fructicola* where azole-resistant isolates containing the Y136F mutation grew slower than wild-type sensitive isolates, produced smaller lesions, and also had an impaired ability to produce spores[152]. A fitness cost was also seen in *C. albicans* isolates where the T315A mutation conferred increased resistance to DMIs by reducing the binding affinity, but also resulted in a 57 % reduction in enzyme function[153].

As has already been alluded to, cross-resistance can occur between DMI fungicides resulting in organisms being resistant to chemicals they have not previously been exposed to[103,130,132,147]. A correlation was shown in *Bgh* between increased resistance to triadimenol and cross-resistance to four other DMI fungicides[130]. In *Z. tritici*, the combination of mutations Y137F and S524T were associated with an increased resistance to triadimenol as well as five other DMIs[132]. In *C. glabrata*, isolates showing increased resistance to fluconazole also showed resistance to ketoconazole, itraconazole, terbinafine, and amorolfine. Interestingly, when these isolates were grown in media without selection pressure they regained sensitivity to itraconazole, but not to the other three fungicides confirming the utilisation of multiple resistance mechanisms[147].

Resistant alleles, such as the *Cyp51* F136 allele, can be used to monitor the presence of potential resistance to fungicides within a pathogen population and thus predict the usefulness of the fungicide at controlling that pathogen. It is also important to understand what resistance mechanisms occur so new fungicides can be designed which avoid targeting the same part of the protein or the same resistance mechanism. For example, the use of particular ABC transporters for detoxifying the cells has been discussed here, but it appears that specific transporters have an affinity for particular fungicides in many organisms, so fungicides should be designed to avoid these particular ABC transporters. In this chapter I explore the effectiveness of two commonly used triazole fungicides at controlling wheat powdery mildew in relation to the sequence, copy number, and expression of the *Cyp51* gene. As described above, reduced sensitivity to DMIs has already been observed in powdery mildew fungi, therefore I investigate which mechanisms of resistance are present in isolates from the UK and US *Bgt* populations.

5.2 Methods

5.2.1 Determining the level of sensitivity in *Bgt* isolates to prothioconazole and tebuconazole using spray tests

Table 5.2.1.1: UK and US Bgt *isolates tested for responses to prothioconazole.*

Isolate	Category	Isolate	Category	Isolate	Category
CAW14S6101	2014 glasshouse F136	CAW14S6313	2014 glasshouse F136	CAW15S6323	2015 GH Y136/F136
CAW14S6102		CAW14S6316		ADW1501	UK field Y136/F136
CAW14S6103		CAW14S6318		ASW1502	
CAW14S6104		EOW1502	UK field F136	CMW1502	
CAW14S6301		ADW1503		JBW1504	
CAW14S6302		AEW1503		TKW1504	
CAW14S6303		ASW1505		EOW1501	
CAW14S6304		CMW1503		AEW1504	
CAW14S6305		JBW1502		JIW11	Older UK Y136
CAW14S6306		TKW1506		Fel09	European F136
CAW14S6307		CAW14S6309	2014 GH Y136/F136	Harry	US Y136
CAW14S6308		CAW14S6312		Ron	
CAW14S6310		CAW14S6314		Hagrid	US F136
CAW14S6311		CAW14S6317			

All fungicide spray tests were performed as described in chapter 2 section 2.5. Trays of Cerco seedlings were used in these tests. For spray tests using prothioconazole (Proline), a 2-fold dose range up to 720 mL/ha (recommended field rate) was used. This included six doses at 22.5, 45, 90, 180, 360, and 720 mL/ha, and water as a no-fungicide control. Isolates included in these tests were 24 UK F136 isolates, twelve UK Y136/F136 isolates, UK Y136 isolate JIW11 (triazole-sensitive control), European F136 isolate Fel09 (triazole-resistant control), two US Y136 isolates, and one US F136 isolate. Isolates were categorised as 'F136', 'Y136/F136', or 'Y136' based on the Y136F sequencing described in section 5.2.2. All isolates used in this experiment are shown in table 5.2.1.1.

For tebuconazole (Folicur) spray tests, a 1.9-fold dose range up to the 750 mL/ha recommended field rate was used. Seven doses at 16, 30, 58, 109, 208, 395, and 750 mL/ha were used as well as water for the no-fungicide control dose. These spray tests were performed using twelve UK Y136/F136 isolates, 13 UK F136 isolates, and old UK Y136 isolate JIW11 (triazole-sensitive control). All isolates used in this experiment are shown in table 5.2.1.2.

Table 5.2.1.2: UK Bgt *isolates tested for responses to tebuconazole.*

Isolate	Category	Isolate	Category
CAW14S6301	2014 glasshouse F136	CAW14S6309	2014 glasshouse Y136/F136
CAW14S6303		CAW14S6312	
CAW14S6304		CAW14S6314	
CAW14S6308		CAW14S6317	
CAW14S6311		CAW15S6323	2015 glasshouse Y136/F136
CAW14S6318		EOW1501	UK field Y136/F136
EOW1502	UK field F136	ADW1501	
ADW1503		AEW1504	
AEW1503		ASW1502	
ASW1505		CMW1502	
CMW1503		JBW1504	
JBW1502		TKW1504	
TKW1506		JIW11	Older UK Y136

5.2.2 Identifying mutations within the *Cyp51* gene

Identification of the Y136F mutation in Bgt isolates

Primers were designed by Nicola Cook (Ph.D. student, John Innes Centre) using the *Cyp51* gene sequence from the National Centre for Biotechnology Information (NCBI) genetic sequence database GenBank (GenBank ID AJ578751.1, *Bgt* isolate JIW24) to PCR-amplify the gene and sequence it. The gene was split into six overlapping amplicons with a forward and reverse primer designed for each amplicon. Primer sequences and melting temperatures are shown in table 5.2.2.1. Locations of primers within the gene are shown diagrammatically in figure 5.2.2.1.

Table 5.2.2.1: Primers used for amplification and sequencing of the Bgt Cyp51 *gene.*

Primer name	Primer sequence (5' to 3')	Melting temperature (°C)
Blumeria_CYP51_Amp1.1	ATGGGAAAACCAGAAAGCT	59.75
Blumeria_CYP51_Amp1.2	TAACATCCCTCAGTTTTCCA	59.25
Blumeria_CYP51_Amp2.1	TTTCACTTTCATATTACTGGGTAA	58.86
Blumeria_CYP51_Amp2.2	TGAAGCGGTATATATCGTAATTTC	59.32
Blumeria_CYP51_Amp3.1	AAATAAATGCGACGATTTTCG	58.69
Blumeria_CYP51_Amp3.2	GCGATCATCATATGTGCAAT	58.94
Blumeria_CYP51_Amp4.1	TATCATGTGGCAATTAATGCG	59.61
Blumeria_CYP51_Amp4.2	GGGAATGGGTCTTAGGTATT	59.17
Blumeria_CYP51_Amp5.1	GAAAAGTAAAGAATCCAATGCC	58.72
Blumeria_CYP51_Amp5.2	TAATTGTAACTAATTGCACCGTT	59.59
Bg_CYP51Amp6.1R	AAAATTCGATTATGGGTATGGAT	58.92
Bg_CYP51Amp6.2R	AGTAAACTTAACACTCCGTTTT	58.96

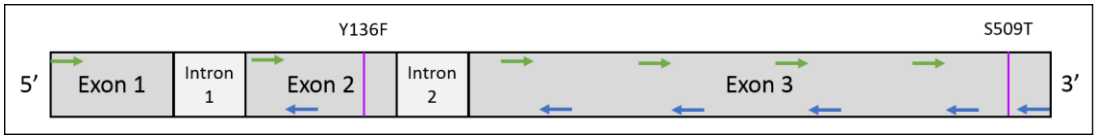

Figure 5.2.2.1: Diagrammatic representation of the Cyp51 *gene showing approximate locations of the primers within the gene. Green arrows represent forward primers in order from 1.1 to 6.1. Blue arrows show reverse primers in order from 1.2 to 6.2. Purple lines show approximate locations of the two key mutations.*

PCR and sequencing were used initially to identify the presence of the common Y136F mutation in most *Bgt* isolates from our collection (chapter 2 tables 2.1.1, 2.1.2, 2.1.4, 2.1.5, and 2.1.6). PCR was performed in 25 µL reactions containing 1x Q5® reaction buffer, 200 µM dNTPs, 0.5 µM forward primer Blumeria_CYP51_Amp2.1, 0.5 µM reverse primer Blumeria_CYP51_Amp2.2, 0.5 U Q5® High-Fidelity DNA polymerase (New England BioLabs Inc., UK), 3 % DMSO, 30 ng DNA, and made up to 25 µL with water. Primers for amplicon 2 were used as the Y136F locus lies within this amplicon. Thermocycling conditions were 98 °C for 30 seconds, followed by 35 cycles of 98 °C for 10 seconds, 60 °C for 15 seconds, and 72 °C for 20 seconds, with a final extension at 72 °C for 2 minutes. PCR products were electrophoresed on a 1.2 % TAE-agarose gel containing 0.4 µg/mL ethidium bromide and visualised using a UV transilluminator. PCR products were then purified using a QIAGEN QIAquick PCR Purification Kit according to the manufacturer's instructions, quantified using a NanoDrop2000 Spectrophotometer, and diluted appropriately for sequencing using primer Blumeria_CYP51_Amp2.1. Purified PCR products were sent to Eurofins Genomics for DNA sequencing. Sequences were trimmed and aligned to the GenBank JIW11 sequence (ID AJ578749.1) using Vector NTI ContigExpress.

Cloning of the Cyp51 gene

The whole *Cyp51* gene was PCR-amplified in four 2014 glasshouse isolates (CAW14S6309, CAW14S6312, CAW14S6314, and CAW14S6317) and two UK field isolates (ADW1501 and EOW1501) as above except with primers Blumeria_CYP51_Amp1.1 and Bg_CYP51Amp6.2R. Thermocycling conditions were 98 °C for 30 seconds, followed by 33 cycles of 98 °C for 10 seconds, 57 °C for 20 seconds, and 72 °C for 50 seconds, with a final extension at 72 °C for 2 minutes. PCR products were then purified using a QIAGEN QIAquick PCR Purification Kit. For cloning, A-overhangs needed to be added to PCR products. A-tailing reactions were performed per sample by adding 5 µL PCR product to 1 µL 10x standard Taq reaction buffer, 2 µL dATP (final concentration 2 mM), 1 µL Taq DNA polymerase (New England BioLabs Inc., UK; total of 10 units), and 1 µL water. These reactions were incubated at 70 °C for 30 minutes. PCR products were ligated into the pGEM®-T easy vector (Promega UK) in 11 µL reactions containing 1x rapid

ligation buffer, 25 ng pGEM®-T easy vector, 1.5 U T4 DNA ligase, 2 µL unpurified A-tailing reaction, and made up to 11 µL with water. The unpurified A-tailing reaction was substituted for control insert DNA provided with the pGEM®-T easy vector system I kit as a positive control and was substituted for additional water as a negative background control. Reactions were incubated at room temperature for 1 hour then overnight at 4 °C.

To transform the ligated PCR products and vector into bacterial cells, 50 µL competent DH5α *Escherichia coli* cells were gently mixed with 10 µL of the ligation reaction and incubated on ice for 30 minutes. The cell-ligation mix was heated at 42 °C for 20 seconds in a heat block then returned to ice for 2 minutes. 950 µL SOC (pre-warmed to 37 °C) was added to the cells which were then incubated at 37 °C for 1 hour. Cells were centrifuged at 6000 rpm for 3 minutes to form a pellet, 500 µL of the supernatant was removed, and cells were resuspended in the remaining volume. Cells were spread onto LB agar plates supplemented with ampicillin, XGal, and IPTG made from InvivoGen *E. coli* Fast Media sachets (125 µL cells per plate), left to dry, and incubated overnight at 37 °C. Individual white colonies were picked with a sterile toothpick which was then placed in 5 mL LB with 200 µg/mL carbenicillin. Liquid cultures were incubated overnight in a 220 rpm shaker at 37 °C. DNA was isolated from individual liquid cultures using a QIAGEN QIAprep Spin Miniprep Kit according to the manufacturer's protocol, quantified using a NanoDrop2000 spectrophotometer, and diluted appropriately. Samples were sent to Eurofins Genomics for sequencing with primers Blumera_CYP51_Amp1.1, -2.2, -3.1, Bg_CYP51Amp6.1R, and Bg_CYP51Amp6.2R. Four clones per 2014 glasshouse isolate, nine ADW1501 clones, and seven EOW1501 clones were sequenced all the way through the gene.

Identifying the presence or absence of the S509T mutation

Several samples containing only the F136 allele and some containing the Y136 allele were checked for the presence of the S509T mutation. The selection of samples containing only the F136 allele were three 2014 glasshouse isolates (CAW14S6301, CAW14S6303, CAW14S6318), seven UK field isolates (EOW1502, ADW1503, AEW1503, ASW1505, CMW1503, JBW1502, TKW1506), and Hagrid. Samples containing only the Y136 allele were JIW11, Harry, and Ron. PCR was performed in 25 µL reactions using primers Blumeria_CYP51_Amp1.1 and Bg_CYP51Amp6.2R as described in the 'cloning of the *Cyp51* gene' section above. PCR products were visualised, purified, diluted, and sequenced with primer Bg_CYP51Amp6.2R as already described.

5.2.3 Identifying mutations within the *Cyp51* promoter region

PCR and sequencing of the Cyp51 promoter region

The *Cyp51* promoter region was sequenced in a selection of isolates up to 2131 bp upstream of the start codon. The isolates sequenced were nine 2014 F136 glasshouse isolates, three 2014 Y136/F136 glasshouse isolates, one 2015 Y136/F136 glasshouse isolate, two 2015 F136 glasshouse isolates, seven UK field F136 isolates, six UK field Y136/F136 isolates, JIW11 (Y136 isolate), Fel09 (F136 isolate), 96224 (Y136/F136 isolate), 94202 (Y136 isolate), US Y136 isolates Harry and Ron, and US F136 isolate Hagrid. Primers were designed based on the 96224 *Cyp51* gene sequence deposited in the EnsemblFungi database (ID: BGT96224_A21131). Primer sequences are shown in table 5.2.3.1 and locations of the primers in relation to the *Cyp51* gene are shown in figure 5.2.3.1.

Table 5.2.3.1: Primers designed to amplify and sequence the Cyp51 *promoter sequence in* Bgt *isolates.*

Primer name	Primer sequence (5' to 3')
cyp51-promoter-F1	ATACGAGTTGAGCCCCATGT
cyp51-promoter-R1	GATCGGTGGCTCATTTGGAT
cyp51-promoter-F2	GTGGATTGTCGTGCATGTGT
cyp51-promoter-R2	TGCGATAAGGACGGAAAATGG
cyp51prom_Y136F	GCTGCTTTCATGAACTGTGC
cyp51-promoter-F3	AAGTATTCCGATTAGATACAT

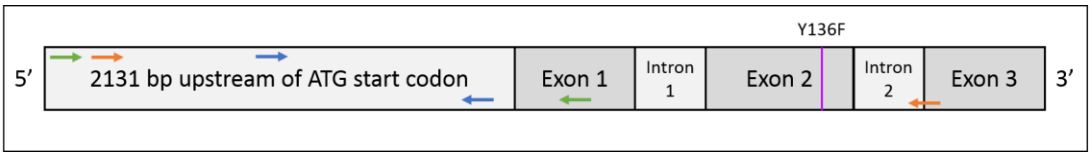

Figure 5.2.3.1: Diagrammatic representation of the Cyp51 *gene showing approximate locations of the primers within the gene and promoter region. Green arrows represent forward and reverse primers F1 and R1. Blue arrows show forward and reverse primers F2 and R2 used to sequence the middle section of the promoter region. Orange arrows show forward primer F3 and reverse primer cyp51prom_Y136F. The purple line shows the approximate location of the Y136F mutation.*

PCR was performed in 20 µL reactions containing 1x Q5® reaction buffer, 200 µM dNTPs, 0.5 µM forward primer cyp51-promoter-F1, 0.5 µM reverse primer cyp51-promoter-R1, 0.4 U Q5® High-Fidelity DNA polymerase, 30 ng DNA, and made up to 20 µL with water. Primers -F1 and -R1 were used to amplify the 2131 bp region upstream of the start codon as well as the first 162 bases of the gene. Thermocycling conditions were as follows: 98 °C for 30 seconds followed by 33 cycles at 98 °C for 10 seconds, 69 °C for 20 seconds, and 72 °C for 75 seconds, then a final

elongation step at 72 °C for 2 minutes. PCR products were electrophoresed, purified, diluted, and sequenced as already described. Samples were sequenced with primers F1, R1, F2, and R2.

With Y136/F136 isolate CAW15S6323, additional PCR was performed with forward primer cyp51-promoter-F1 and reverse primer cyp51prom_Y136F to check that the promoter region of both alleles was being amplified and sequenced correctly. As only the Y136 allele was amplified, a new forward primer (F3) was designed to amplify both alleles in Y136/F136 isolates using the promoter sequence alignment from Y136 and F136 isolates. This alignment was used to design a primer that would be within a conserved region of the promoter where no SNPs had been found. PCR amplification of the promoter region in Y136/F136 isolates was performed in 20 µL reactions as described above using the two new primers. Thermocycling was performed as described above with an annealing temperature of 67.5 °C. PCR product visualisation, purification, quantification, and sequencing was performed as already described, and the sample was sequenced using reverse primer cyp51prom_Y136F.

Identifying promoter region sequences in the 96224 reference genome isolate

Raw DNA sequencing reads for both the 2014 and 2017 versions of the 96224 reference genome were obtained from Prof. Beat Keller (University of Zurich, Switzerland). A reference sequence containing 2131 bp of the JIW11 *Cyp51* promoter region and the first 561 bp of the gene was used to map raw DNA reads using the Burrows-Wheeler Alignment (BWA) tool[154] version 0.7.12 and SAMtools version 1.2[86]. SAMtools was then used to sort and index the mapped reads before identifying SNPs. The SNP calling pipeline identified the nucleotide present at each position in comparison to the reference sequence and the proportion of reads which contained that nucleotide.

5.2.4 Estimating *Cyp51* gene copy number

Conidia were harvested from two Y136 isolates (JIW11 and 94202), five F136 isolates (Fel09, CAW14S6101, CAW15S6330, EOW1502, ASW1506), and five Y136/F136 isolates (AEW1504, CAW14S6312, CAW14S6314, CAW15S6341, CMW1502). Conidia were then ground using a pestle, mortar, a small amount of sand, and liquid nitrogen. DNA was then extracted using a QIAGEN DNeasy Mini Plant Extraction Kit according to the manufacturer's protocol. DNA extractions were quantified using a Qubit 3.0 fluorometer.

Droplet digital PCR (ddPCR)[155] was used to estimate *Cyp51* copy number using β-tubulin (*Tub2*; GenBank accession JQ268163.1) as a reference gene. *Tub2* has been shown to be a single copy gene in *B. graminis* f. sp. *hordei*[156].The *Cyp51* and *Tub2* PCRs were performed on each sample separately and two replicates per gene were included for each sample. For a more precise copy

number estimation, restriction enzyme NcoI-HF® (New England BioLabs Inc., UK) was added to the PCR mix to digest the DNA before PCR commenced to separate any potentially tandem copies. The quantity of DNA required for PCR was calculated by first estimating the mass of the genome size (M) using the following calculation:

$$M = (genome\ size\ in\ bp)(1.096 \times 10^{-21})$$

$$M = (158{,}000{,}000)(1.096 \times 10^{-21})$$

$$M = 1.73168 \times 10^{-13}\ g$$

$$M = 0.17\ pg$$

From this, the number of copies of the genome present in 1 ng DNA was calculated:

$$0.17\ pg = 0.00017\ ng$$

$$Genome\ copies\ in\ 1\ ng = \frac{1}{0.00017}$$

$$Genome\ copies\ in\ 1\ ng = 5882.35$$

This means that for 1 ng DNA, there are 5882 copies of the genome present, thus there are 5882 copies of the *Tub2* gene assuming one copy per genome. As the range of ddPCR is 0.25 – 5000 copies per µL PCR (5 – 100,000 per 20 µL PCR), the above calculation suggested only a small amount of DNA was needed for each PCR. ddPCR was initially performed with 1, 2, 4, 8, 10, and 12 ng DNA to find the optimal quantity based on this calculation. This showed that between 2 and 4 ng gave the best separation between positive and negative droplet signals therefore 3 ng DNA was used in the final experiment.

PCR was set up in 22 µL reactions containing 1x QX200™ ddPCR™ EvaGreen Supermix (BIO-RAD UK), 200 nM forward primer, 200 nM reverse primer, 5 U NcoI-HF®, and 3 ng DNA. Forward and reverse primer sequences and product sizes for both genes are shown in table 5.2.4.1. Approximate locations of primers within the genes are shown in figure 5.2.4.1.

Table 5.2.4.1: Primer sequences and PCR product sizes for estimating Cyp51 *copy number using* Tub2 *as a reference gene.*

Target gene	Primer sequence 5' to 3'	Product size
Cyp51	TTTCATGCTTCACTGGGCAC	116 bp
	CAGTTTCTTTCTGCGTCCGA	
Tub2	AGAACATGATGGCAGCCTCC	88 bp
	GCATGCGTATAAAACGTGCAG	

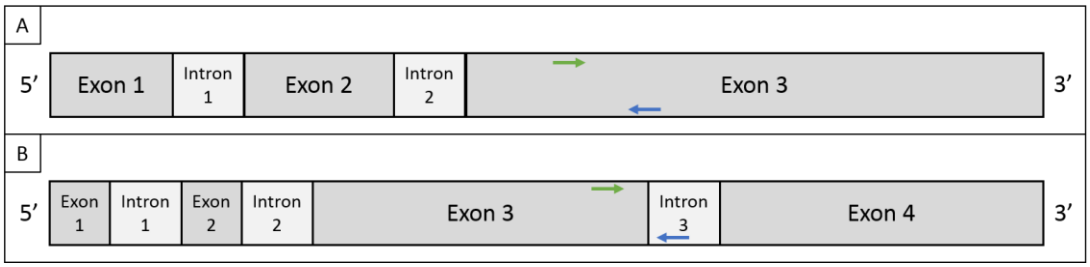

Figure 5.2.4.1: Diagrammatic representation of the Cyp51 *gene (panel A) and partial* Tub2 *gene (panel B). Green and blue arrows represent forward and reverse primers, respectively. Exons and introns are numbered in the* Tub2 *gene, but may be incorrect as only a partial sequence has been deposited in GenBank.*

ddPCR was performed according to the BIO-RAD QX200™ ddPCR™ EvaGreen Supermix protocol. 20 µL of the reaction mixture was loaded into a DG8 Cartridge rather than 22 µL to avoid introducing bubbles into the cartridge. 70 µL of QX200™ Droplet Generation Oil for EvaGreen was loaded into each oil well in the cartridge. Cartridges were covered with DG8™ gaskets, placed into the BIO-RAD QX200™ Droplet Generator, and 35 µL of each sample was subsequently loaded into a 96-well plate. Once all samples were loaded into the plate, the plate was sealed with a BIO-RAD pierceable PCR foil seal using an Eppendorf heat seal machine. Thermocycling proceeded as follows: 95 °C for 5 minutes, followed by 40 cycles of 95 °C denaturation for 30 seconds, and 60 °C annealing/extension for 1 minute. This was followed by a signal stabilisation step at 4 °C for 5 minutes then 90 °C for 4 minutes. After thermocycling, the 96-well plate was placed in a BIO-RAD QX200™ Droplet Reader for absolute quantification of each reaction using BIO-RAD QuantaSoft™ software. A medium threshold was applied to separate negative and positive droplets (figure 5.2.4.2). As there were two readings per gene for each sample, a ratio of *Cyp51*/*Tub2* was calculated for every combination of the two readings from each gene (e.g. *Cyp51* reading 1/*Tub2* reading 1, *Cyp51* reading 2/*Tub2* reading 1, etc.). An average of these ratios as well as the standard deviation was calculated giving an estimate of *Cyp51* copy number relative to *Tub2*.

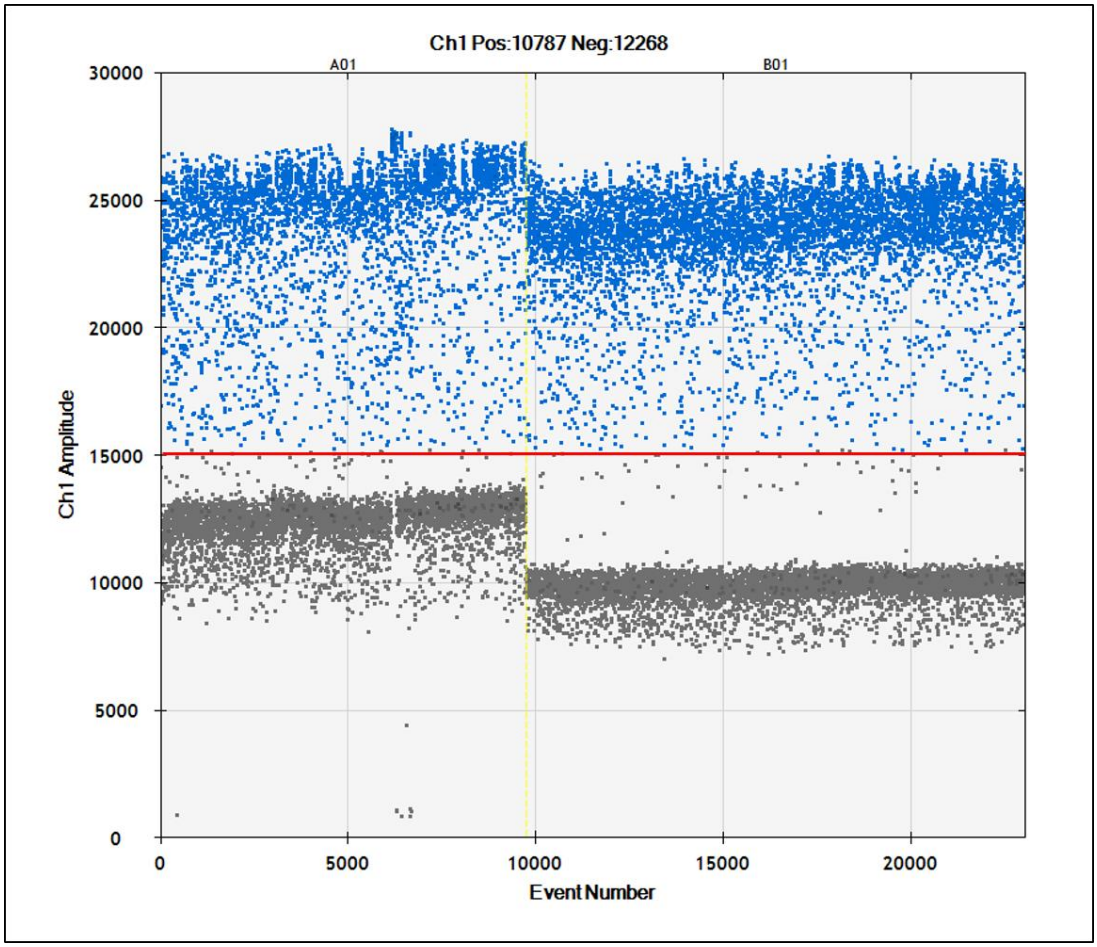

Figure 5.2.4.2: ddPCR output from two samples showing a positive signal cloud in blue, a negative signal cloud in grey, and a red line showing a manually-imposed medium threshold.

5.2.5 Quantifying *Cyp51* gene expression using qRT-PCR

For qRT-PCR *Cyp51* gene expression assays, epidermal peels were collected from a selection of isolates and RNA was extracted according to the method described in chapter 2 section 2.4. Isolates and the number of replicates collected are summarised in table 5.2.5.1. Isolates with only one replicate grew poorly and were difficult to collect epidermal peels from. The first ten samples (ADW1501 x3, ADW1503 x3, AEW1503 x3, and AEW1504 x1) were extracted in the first batch using buffer RLT, but this produced a large gelatinous pellet during the process and resulted in low yields, so all other samples were extracted using buffer RLC.

RNA samples were subjected to a double TURBO™ DNase (Invitrogen, UK) treatment. 20 µL RNA was added to 3 U TURBO DNase and 1x TURBO™ DNase buffer, mixed gently, and incubated for 30 minutes at 37 °C. Another 3 U TURBO™ DNase was added to the reaction, mixed gently again, and incubated for another 30 minutes at 37 °C. 0.2 volumes DNase inactivation reagent was added to the reaction which was then vortexed and incubated at room temperature for 5

minutes, vortexing briefly every minute. Reaction tubes were centrifuged for 1.5 minutes at 10'000 xg then the supernatant was transferred to a clean Eppendorf tube leaving the pellet behind. RNA was quantified using a NanoDrop2000 spectrophotometer.

Table 5.2.5.1: Isolates used for Cyp51 *gene expression assays.*

Group	Isolate name	Number of biological replicates	Group	Isolate name	Number of biological replicates
UK field Y136/F136 isolates	ADW1501	3	UK field F136 isolates	ADW1503	3
	AEW1504	3		AEW1503	3
	ASW1502	3		ASW1505	3
	CMW1502	3		CMW1503	1
	EOW1501	4		EOW1502	3
	TKW1504	3		TKW1506	3
Glasshouse Y136/F136 isolates	CAW14S6309	3	Glasshouse F136 isolates	CAW14S6301	1
	CAW15S6323	3		CAW14S6303	1
Old UK Y136 isolate	JIW11	4		CAW14S6318	4

For cDNA synthesis, a QIAGEN QuantiTect Reverse Transcription Kit was used according to the manufacturer's protocol. The DNA removal step was performed in 14 µL reactions consisting of 500 ng RNA, 1x gDNA wipeout buffer, and RNase-free water. Reactions were mixed gently, incubated for 2 minutes at 42 °C then placed immediately on ice. The reverse-transcription step was performed in 20 µL reaction volumes by mixing the entire DNA removal reaction with 1 µL RT primer mix, 1 µL Quantiscript reverse transcriptase, and 1x Quantiscript RT buffer. The reaction was mixed gently then incubated for 15 minutes at 42 °C. The reverse transcriptase enzyme was inactivated by incubating the reaction for 3 minutes at 95 °C. Assuming the cDNA synthesis was 100 % efficient, cDNA was diluted to 2 ng/µL based on the RNA NanoDrop readings.

To assess the levels of *Cyp51* gene expression in Y136/F136 isolates compared to F136 and Y136 isolates, qRT-PCR was performed using primers designed to amplify the *Cyp51*, *Tub2*, and *Actin* genes. *Tub2* and *Actin* were used as housekeeping genes to standardise the level of *Cyp51* expression within a sample before it was compared to other samples. Primers were designed so that the forward primers were located over exon splice sites to make them cDNA-specific. This was to reduce the amount of amplification of any possible contaminating DNA. Primer sequences, PCR product sizes, primer annealing temperatures, and primer efficiencies are shown in table 5.2.5.2. Locations of primers within the three genes are shown in figure 5.2.5.1.

Table 5.2.5.2: Primer sequences, PCR product sizes, annealing temperatures, and primer efficiencies for qRT-PCR with the Tub2*,* Actin*, and* Cyp51 *genes.*

Target gene	Primer name	Primer sequence (5' to 3')	Product size	Annealing temperature	Efficiency
Tub2	TUBb_x12a_F	ACATGCTCTGCTATTTTCCG	105 bp	58 °C	1.93
	TUBb_1a_R	TGGAATCCACTCAACAAAGT			
Actin	ACT_x12a_F	CGAGCTGTTTTCCCATC	125 bp	54 °C	1.93
	ACT_2a_R	TATCTAAGAGTCAGAATACCA			
Cyp51	cyp51_x12b_F	GAATCCCAAGCCAAGTAC	122 bp	60 °C	1.97
	cyp51_x_splice_R	GCATTAACATCCCTCAGTT			

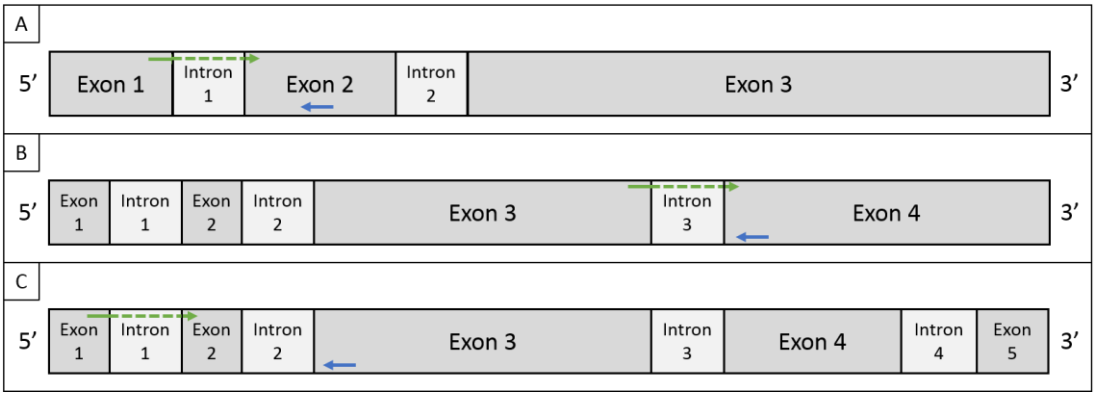

Figure 5.2.5.1: Diagrammatic representation of the Cyp51 *gene (panel A), partial* Tub2 *gene (panel B), and* Actin *gene (panel C). Green and blue arrows represent forward and reverse primers, respectively. The dotted portion of the green arrows shows where forward primers lie over splice sites within the gene.*

To calculate the primer efficiency of *Tub2* primers, a 10-fold dilution series of one cDNA sample (from 46.8 ng/µL to 0.0468 ng/µL) was used. To calculate primer efficiencies of *Actin* and *Cyp51* primers, a 5-fold dilution series of a second cDNA sample (from 6.88 ng/µL to 0.055 ng/µL) was used due to availability of cDNA. qRT-PCR primer efficiency assays were performed in 10 µL reaction volumes including 2 µL diluted cDNA, 1x SsoAdvanced™ universal SYBR® Green supermix, 0.3 µM forward primer, 0.3 µM reverse primer, and made up to 10 µL with water. Thermocycling was performed in a BIO-RAD CFX96 Real-Time System C1000 Thermal Cycler using the following programme: 95 °C for 30 seconds, 40 cycles of 95 °C denaturation for 5 seconds then the appropriate annealing temperature (table 5.2.6.2) for 30 seconds with a plate read at the end of every cycle. After cycling, a melt-curve was produced by increasing the temperature from 65 °C to 95 °C in 0.5 °C increments with 5 seconds allowed per increment. A plate read was taken at every increment. Standard curves and efficiencies were calculated using the BIO-RAD CFX Manager 3.1 software.

After determining that primer efficiencies were within the acceptable range (90-105 %), qRT-PCR was performed with cDNA from all samples in table 5.2.5.1. PCR was performed with the same reaction component quantities as with primer efficiencies except 4 ng cDNA was used per reaction instead of a dilution series. Two technical replicates per biological replicate were included in the assays. Quantitation cycle (Cq) values were calculated automatically using the BIO-RAD CFX Manager 3.1 software. JIW11 was the only isolate with the Y136 allele included in these assays and this was used as the standard level of *Cyp51* gene expression to compare all other isolates to. The Pfaffl method was used to calculate relative *Cyp51* gene expression between Y136, F135, and Y136/F136 isolates[157]. Firstly, the mean Cq value for each biological replicate was calculated by averaging the *Cyp51* Cq values from each of the two technical replicates (see equation 1 below). As JIW11 is a Y136 isolate (i.e. wild-type), this was used as the control so the mean Cq values from all four biological replicates of this isolate were averaged to give one Cq value for *Cyp51* (equation 2). The ΔCq value for each biological replicate was calculated by subtracting the mean Cq value per replicate from the JIW11 mean Cq (equation 3). The primer efficiency was then taken into account as shown in equation 4.

1) $Mean\ Cq = \frac{(Cq1+Cq2)}{2}$

   Cq1 and Cq2 mean Cq values from technical replicates 1 and 2 respectively.

2) Calculate the average Cq value across all mean JIW11 Cq values to give "average JIW11 Cq value".

3) $\Delta Cq = mean\ Cq - average\ JIW11\ Cq\ value$

4) $E^{\Delta Cq}$

   E represents the primer efficiency value (table 5.2.5.2).

These four steps were repeated for both *Tub2* and *Actin* Cq values. The values obtained from equation 4 for *Tub2* and *Actin* were averaged per biological replicate per isolate. The ratio of *Cyp51* gene expression to reference gene expression was calculated by dividing the *Cyp51* $E^{\Delta Cq}$ value by the mean reference gene $E^{\Delta Cq}$ value. This ratio was then averaged across all biological replicates per isolate. The average ratio values for F136 isolates and Y136/F136 isolates, and the standard deviations of these two groups were calculated. Average ratios were plotted on a graph and standard deviation bars were added to show any differences between *Cyp51* gene expression in Y136, F136, and Y136/F136 isolates as a whole.

In-house custom Python scripts were used to perform analysis of variants (ANOVA) statistical analyses between *Cyp51*:reference gene expression ratios from Y136, F136, and Y136/F136 isolates. R was used to perform Kruskal-Wallis statistical analysis for comparisons between all three groups of isolates using the dplyr package. The Wilcoxon statistical test was used for pairwise comparisons between groups, i.e. comparing Y136 and Y136/F136, Y136 and F136, and Y136/F136 and F136 separately. R was also used to plot the results using the ggplot and ggpubr packages showing both pairwise comparison p-values from the Wilcoxon test and the global p-value from the Kruskal-Wallis test.

5.2.6 Quantifying *Cyp51* gene expression using RNA-seq data

The RNA-seq data collected in chapter 4 contained a selection of Y136, Y136/F136, and F136 isolates from both the UK and the US therefore proved to be a useful resource to look at *Cyp51* gene expression. Trimmomatic version 0.33 was used to trim adapter sequences and low-quality bases from the ends of the raw reads[158]. HISAT2 version 2.1.0 was used to index the *Bgt* reference genome and map the reads to the reference[159]. SAMtools version 1.5 was used to pair reads together and was then used in conjunction with StringTie version 1.3.4 to assemble the mapped reads into transcripts and estimate transcript abundances, i.e. expression levels, as FPKM (fragments per kilobase of transcript per million mapped reads) values[159]. In-house custom Python scripts were then used to extract the *Cyp51* FPKM values and for performing ANOVA statistical analyses between US Y136 and F136 isolates, UK Y136, F136, and Y136/F136 isolates, as well comparing US Y136 isolates with UK Y136 isolates, and US F136 with UK F136 isolates. Here the UK Y136 isolates group included JIW11 and Swiss isolate 94202 (labelled collectively as "UK" for ease). The UK Y136/F136 isolates group also included Swiss isolate 96224 and German isolate Fel09.

5.3 Results

5.3.1 *Bgt* responses to prothioconazole and tebuconazole

Fungicide spray tests using prothioconazole were performed to see if there was any phenotypic difference in response to triazoles by Y136, F136, and Y136/F136 *Bgt* isolates (see section 5.3.2). These tests showed that isolates containing the Y136F mutation had a higher resistance to this fungicide than wild-type isolates. US Y136 isolates had a mean MIC of 360 mL/ha while UK Y136 isolate JIW11 had an MIC of 720 mL/ha. Three F136 isolates had an MIC of 720mL/ha and the remaining 23 F136 and Y136/F136 isolates grew at the top dose (figure 5.3.1.1). ED_{50} values were calculated as described in chapter 2 section 2.8 for Y136, F136, and Y136/F136 isolates (with UK and US Y136 isolates grouped together, and UK, US, and old EU F136 isolates grouped together).

Logistic dose-response curves were fitted to colony number data from each group (figure 5.3.1.2). See Appendix I for ED_{50} ± standard error ranges as standard errors were calculated from $\log_{10}$(dose) so are on a logarithmic scale. Y136 isolates had an estimated ED_{50} of $103.7 \pm 10^{(0.47)}$ mL/ha while F136 isolates had an ED_{50} of $443 \pm 10^{(0.31)}$ mL/ha showing a 4.3-fold increase in resistance. As the maximum dose did not effectively control the Y136/F136 isolates, the ED_{50} could not be accurately estimated. The 90 mL/ha dose was removed from both figures as the leaves wilted after spraying and colonies could not be counted.

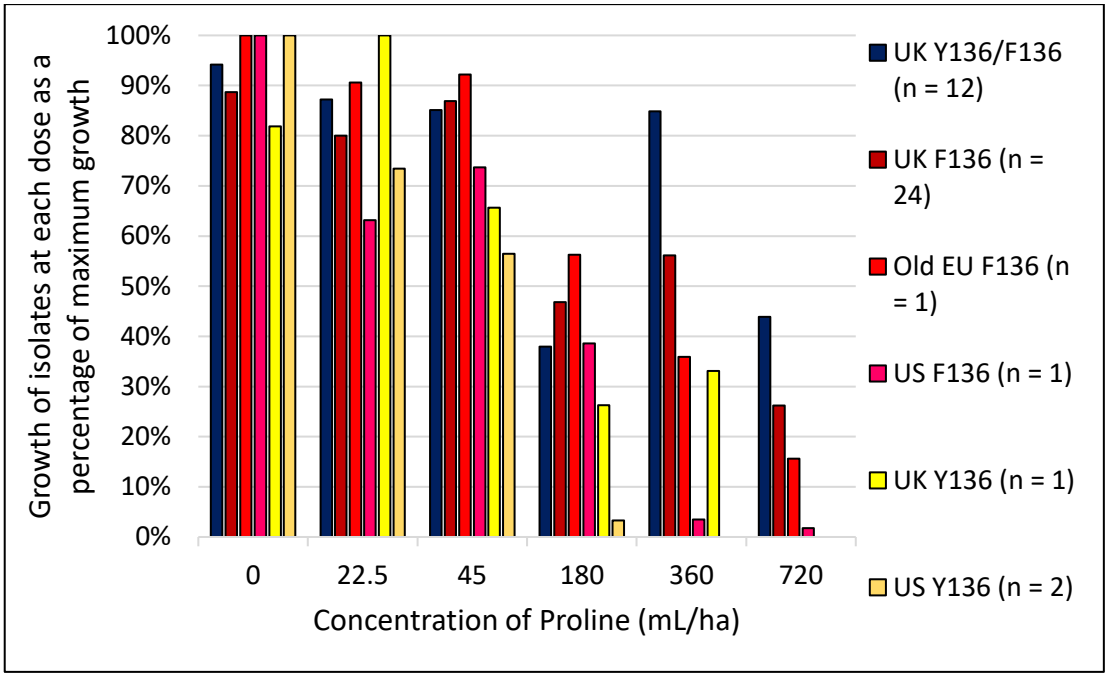

Figure 5.3.1.1: Responses of two US Y136, one US F136, one UK Y136, 24 UK F136, twelve UK Y136/F136 Bgt *isolates, and one older European F136 isolate to increasing doses of prothioconazole (Proline) up to the recommended field application rate. N values for each group are shown in parentheses.*

As most isolates grew at the highest prothioconazole dose, UK isolates' responses to a second triazole, tebuconazole (Folicur), were tested. ED_{50} values were calculated for Y136, F136, and Y136/F136 isolates and logistic dose-response curves were fitted to colony number data (figure 5.3.1.3).

UK Y136 isolate JIW11 had an ED_{50} of $22.7 \pm 10^{(0.043)}$ mL/ha, and F136 isolates had an ED_{50} of $102.6 \pm 10^{(0.075)}$ mL/ha which is approximately 4.5-fold more resistant than JIW11. Y136/F136 isolates had an ED_{50} of $179.6 \pm 10^{(0.04)}$ mL/ha which showed a 1.75-fold increase in resistance compared to F136 isolates, and a 7.9-fold increase in resistance compared to JIW11.

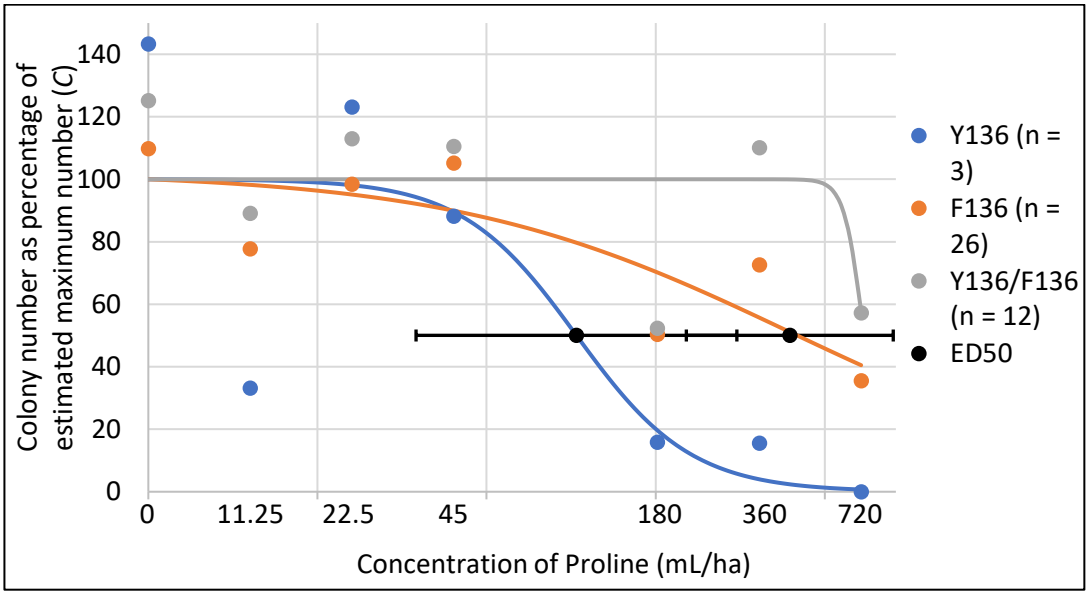

Figure 5.3.1.2: Fitted dose-response logistic curves for three Y136, 26 F136, and twelve Y136/F136 Bgt *isolates to prothioconazole (Proline). ED_{50}s and error bars for Y136 and F136 isolates are shown in black. N values for each group are shown in parentheses.*

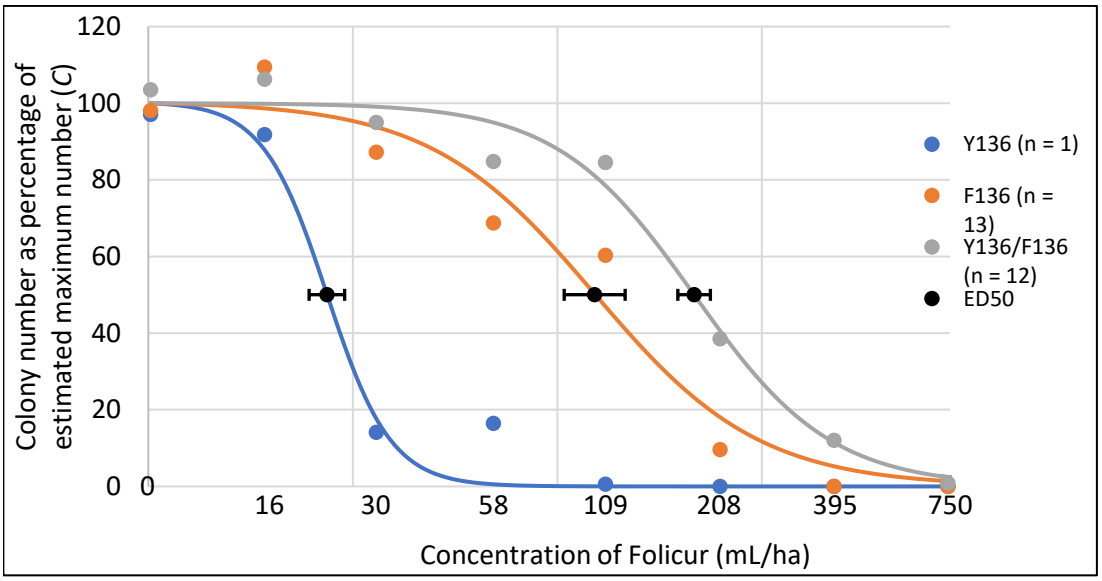

Figure 5.3.1.3: Fitted dose-response logistic curves for one Y136, 13 F136, and twelve Y136/F136 Bgt *isolates to tebuconazole (Folicur) concentration. ED_{50} estimations are shown in black with error bars. N values for each group are shown in parentheses.*

5.3.2 Mutations in the *Cyp51* gene sequence

Amplicon 2 of the *Cyp51* gene was sequenced to identify isolates containing the common Y136F mutation associated with increased resistance to triazole fungicides. This sequencing identified isolates carrying the Y136 allele or the F136 allele, but unexpectedly also identified isolates

carrying both alleles. These isolates were categorised as 'Y136/F136' and were referred to as 'heteroallelic'. A summary of isolates included in the F136, Y136, or Y136/F136 categories can be found in table 5.3.2.1.

Table 5.3.2.1: Isolates categorised as Y136, F136, or Y136/F136 based on sequencing of the Cyp51 *Y136F locus.*

F136 isolates					
2014 glasshouse isolates	CAW14S6101	2015 glasshouse isolates	CAW15S6320	2015 glasshouse isolates	CAW15W104
	CAW14S6102		CAW15S6325		CAW15W105
	CAW14S6103		CAW15S6327	2015 UK field isolates	EOW1502
	CAW14S6104		CAW15S6328		ADW1503
	CAW14S6301		CAW15S6330		AEW1501
	CAW14S6302		CAW15S6331		AEW1503
	CAW14S6303		CAW15S6332		ASW1505
	CAW14S6304		CAW15S6334		ASW1506
	CAW14S6305		CAW15S6335		CMW1503
	CAW14S6306		CAW15S6336		CMW1505
	CAW14S6307		CAW15S6337		CMW1506
	CAW14S6308		CAW15S6338		JBW1502
	CAW14S6310		CAW15S6339		JBW1503
	CAW14S6311		CAW15S6342		JBW1505
	CAW14S6313		CAW15S6343		TKW1502
	CAW14S6316		CAW15W101		TKW1506
	CAW14S6318		CAW15W102	US isolates	Hagrid
Old EU isolate	Fel09		CAW15W103		McGonagall
Y136 isolates		**Y136/F136 isolates**			
Old UK isolate	JIW11	2014 glasshouse isolates	CAW14S6309	2015 UK field isolates	AEW1505
Swiss isolate	94202		CAW14S6312		ASW1502
US isolates	Snape		CAW14S6314		ASW1504
	Ginny		CAW14S6317		CMW1502
	Harry	2015 glasshouse isolates	CAW15S6323		CMW1504
	Hermione		CAW15S6340		JBW1504
	Malfoy		CAW15S6341		JBW1506
	Moody	2015 UK field isolates	EOW1501		TKW1501
	Ron		ADW1501		TKW1503
	Sirius		ADW1506		TKW1504
	Dumbledore		AEW1504	Swiss isolate	96224

To ensure that Y136/F136 isolates were pure and not a contaminated mixture of Y136 and F136 isolates, one Y136/F136 isolate (CAW15S6323) was reduced to seven single-spore colonies, each colony was grown into a separate culture, and the Y136F locus was sequenced from each culture

individually. All seven cultures were identified as Y136/F136 isolates showing that there was no contamination and that at least two copies of the *Cyp51* gene were present in these isolates.

Four Y136/F136 glasshouse isolates (CAW14S6309, CAW14S6312, CAW14S6314, and CAW14S6317) and two UK field Y136/F136 isolates (ADW1501 and EOW1501) were selected for cloning of the *Cyp51* gene to sequence the two alleles separately. Four clones from each glasshouse isolate, nine ADW1501 clones, and seven EOW1501 clones were sequenced all the way through the *Cyp51* gene. Two of each of the glasshouse isolate clones were wild-type (Y136) and two were mutated (F136). Five ADW1501 and EOW1501 clones were mutated, four ADW1051 clones were wild-type, and two EOW1501 clones were wild-type. Cloning the entire gene in Y136/F136 isolates also revealed that in the mutated F136 allele the S509T mutation was present. This mutation was not present in the Y136 allele of Y136/F136 isolates and was also absent in F136 isolates.

5.3.3 Identification of alterations in the *Cyp51* promoter region sequence

The *Cyp51* promoter region was sequenced in Y136, F136, and Y136/F136 *Bgt* isolates to see if there was any association between promoter region sequences and gene expression levels. Sequencing 2131 bp of the upstream region of *Cyp51* revealed nine SNPs present in UK F136 isolates that were absent in UK wild-type Y136 isolates.

Table 5.3.3.1: A summary of SNPs found in the Cyp51 *promoter region in UK and US* Bgt *isolates and the reference genome 96224 (both A and B versions), and their nucleotide locations relative to the ATG start codon compared to UK Y136 isolate JIW11.*

Y136F	**Nucleotide number upstream of start codon**											
	1830	1315	1310	1161	928	875	737	696	404	298	174	114
UK Y136	T	C	G	T	G	G	A	T	A	T	C	T
UK Y136/F136	T	C	G	T	G	G	A	T	A	T	C	T
UK F136	G	A	C	C	T	A	A	G	T	T	T	T
US Y136	G	C	C	C	T	A	G	G	A	A	T	C
US F136	G	C	C	C	T	A	G	G	A	A	T	C
96224	G	C	C	T	G	A	A	G	A	T	C	T

In contrast to this, US Y136 and F136 isolates had identical promoter sequences to each other. Oddly, both US Y136 and F136 isolates had the same nucleotides as UK F136 isolates at seven out of nine SNP positions and the remaining two nucleotides (positions 1315 and 404, table 5.3.3.1) were identical to the UK Y136 isolates. US Y136 and F136 isolates also had three additional SNPs 114, 298, and 737 bp upstream of the start codon that were C, A, and G, respectively in US isolates, but were T, T, and A in all UK isolates. A summary of SNPs and their nucleotide position upstream of the start codon can be found in table 5.3.3.1. By aligning the

raw DNA sequencing reads from both the 2014 (A) and 2017 (B) versions of the 96224 reference genome assembly to the JIW11 promoter region sequence (including 2131 bp upstream of the start codon and the first 561 bp of the gene), the nucleotides present at all twelve positions were identified and are also shown in table 5.3.3.1.

Table 5.3.3.2: Extrapolated wild-type and mutant allele promoter region sequences within Y136/F136 isolates.

	Nucleotide number upstream of start codon											
	1830	1315	1310	1161	928	875	737	696	404	298	174	114
Y136 allele	T	C	G	T	G	G	A	T	A	T	C	T
F136 allele	G	C	C	T	G	A	A	G	A	T	C	T

Initially, this sequencing showed that Y136/F136 isolates did not have a mixture of the Y136 and F136 allele promoter sequences as expected but had a single sequence identical to the wild-type sequence in Y136 isolates. However, PCR and sequencing with the cyp51prom_Y136F reverse primer showed that only the Y136 allele was being amplified thus the sequence shown in table 5.3.3.1 is only that of the Y136 allele promoter. By comparing the sequence identified in the 96224 reference genome reads (which is a Y136/F136 isolate) with this wild-type sequence, the potential wild-type and mutant allele promoter sequences within Y136/F136 isolates were extrapolated (table 5.3.3.2). In this table, the discrepancies between the UK Y136 isolate promoter sequence and the 96224 reference promoter sequence are highlighted in pink which show the potential SNPs between Y136 and F136 allele promoters in Y136/F136 isolates. Unfortunately, sequencing of the mutant allele promoter in Y136/F136 isolates was unsuccessful so this could not be confirmed.

5.3.4 Estimating *Cyp51* copy number using ddPCR

ddPCR was used to estimate *Cyp51* gene copy number in Y136, Y136/F136, and F136 isolates as sequencing results showed that in Y136/F136 isolates at least two copies of the gene were present. Assuming *Tub2* was a single copy gene as it is in *B. graminis* f. sp. *hordei*, comparing the ddPCR output for *Cyp51* with *Tub2* gave the number of *Cyp51* copies within the genome of each sample included. A summary of the results is shown in figure 5.3.4.1.

The ddPCR results showed that both Y136 isolates, 94202 and JIW11, had two copies of the *Cyp51* gene. They also showed that four out of five Y136/F136 isolates had three copies of the gene. Y136/F136 isolate CAW15S6341 had 4.7 (therefore possibly five) copies of the gene, more than the other Y136/F136 isolates. F136 isolates had between three and five copies of the gene.

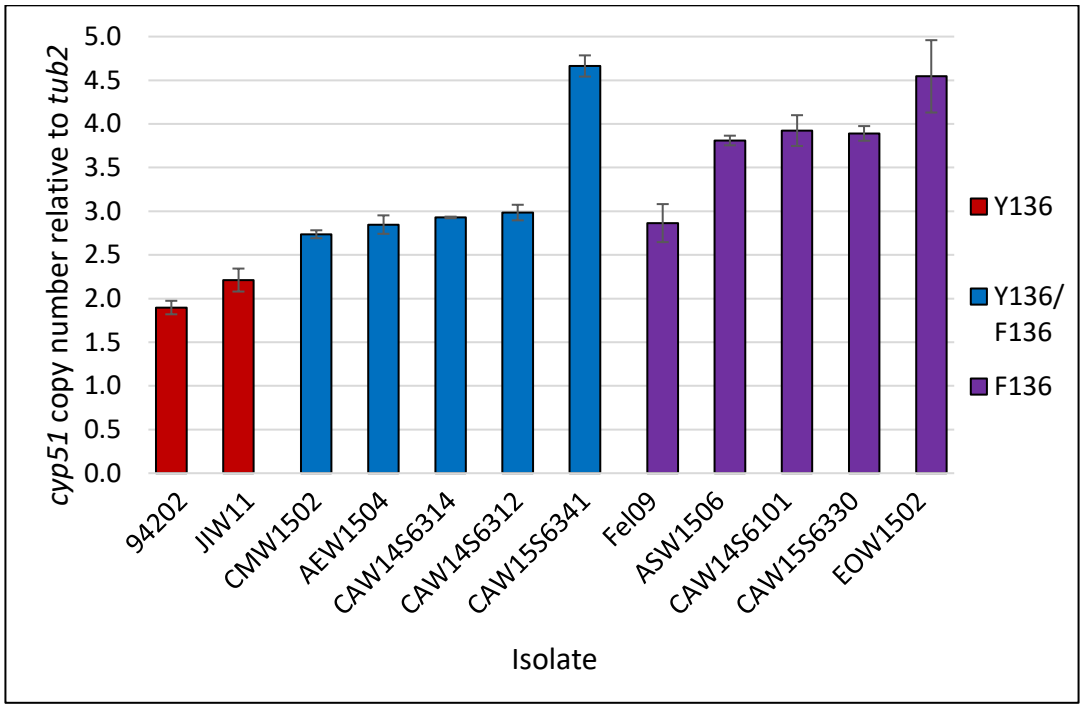

Figure 5.3.4.1: Cyp51 *copy number estimations in two Y136 isolates, five Y136/F136 isolates and five F136 isolates compared to* Tub2 *using droplet digital PCR. Error bars show the standard deviations.*

5.3.5 Using qRT-PCR to identify differences in *Cyp51* gene expression in Y136, Y136/F136, and F136 isolates

qRT-PCR was used to examine *Cyp51* gene expression in Y136/F136 and F136 isolates compared to Y136 isolate JIW11. Box and whisker plots representing the ratio of *Cyp51* to reference gene expression from Y136, Y136/F136, and F136 isolates are shown in figure 5.3.5.1. On average, Y136/F136 isolates expressed *Cyp51* 1.6 times more strongly than Y136 isolate JIW11 did. F136 isolates showed an average of 5.4-fold increase in *Cyp51* gene expression compared to JIW11, and a 3.4-fold increase compared to Y136/F136 isolates.

Pairwise comparisons between the groups using an ANOVA test showed a statistically significant difference in *Cyp51* gene expression between F136 and Y136/F136 isolates. As only one UK Y136 isolate was available for testing, it was not possible to make robust conclusions about its *Cyp51* expression relative to F136 and Y136/F136 isolates. As more than two groups of data were being compared, p-values were adjusted using a Benjamini-Hochberg correction. Original and adjusted p-values can be seen in table 5.3.5.1.

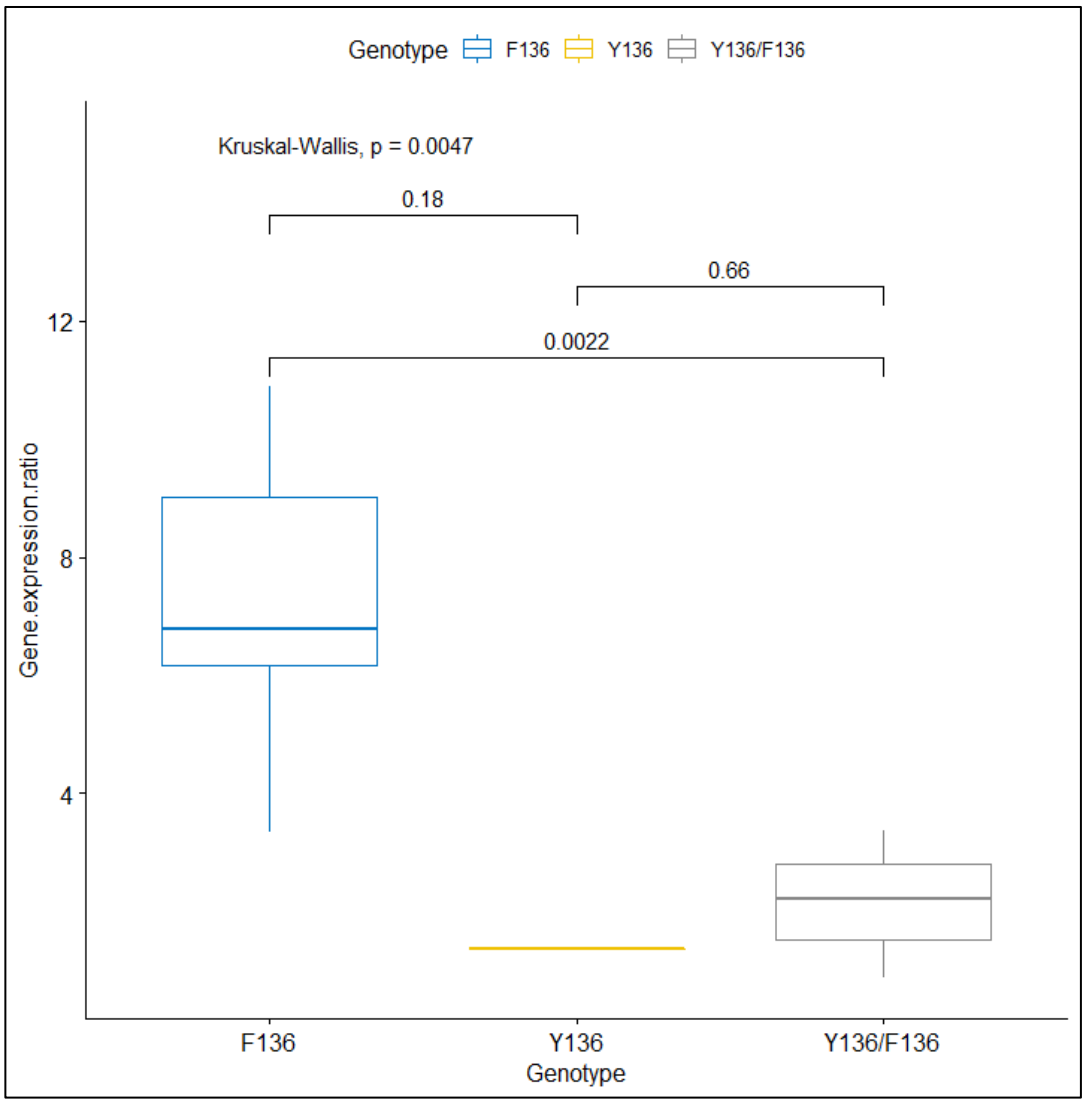

Figure 5.3.5.1: Graphical representation of mean gene expression ratios in one UK Y136 isolate, nine UK F136 isolates, and eight UK Y136/F136 isolates between Cyp51 *and two housekeeping genes* Tub2 *and* Actin *using Y136 isolate JIW11 as a control. Pairwise comparison p-values between groups are shown above the plot with bars indicating which*

Table 5.3.5.1: Summary of p-values and adjusted p-values from pairwise comparisons of Cyp51 *qRT-PCR expression ratios in UK* Bgt *Y136, F136, and Y136/F136 isolates using an ANOVA test and Benjamini-Hochberg correction.*

Genotype 1	**Genotype 2**	**p-value**	**Adjusted p-value**	**Significance**
F136	Y136/F136	0.0001	0.0004	***
F136	Y136	0.05	0.08	ns
Y136/F136	Y136	0.5	0.5	ns

5.3.6 Using RNA-seq data to identify differences in *Cyp51* gene expression between US and UK *Bgt* isolates

Using the RNA-seq data collected in chapter 4, *Cyp51* gene expression levels between US Y136 and F136 isolates, and UK Y136, Y136/F136, and F136 isolates could be compared. Figure 5.3.6.1 shows *Cyp51* FPKM (fragments per kilobase of transcript per million mapped reads) values of individual isolates with US isolates shown in two shades of red and UK isolates shown in three shades of blue. An average of 4.7-fold up-regulation of *Cyp51* was apparent in US F136 isolates compared to US Y136 isolates, however UK Y136 isolates showed similar levels of gene expression to those US F136 isolates. UK Y136/F136 and F136 isolates showed a large range in levels of *Cyp51* gene expression, with UK Y136/F136 isolate CAW14S6309 and Swiss Y136/F136 isolate 96224 showing similar levels of expression as the UK Y136 isolates and US F136 isolates. On average, UK Y136/F136 isolates (including Swiss isolate 96224) showed a 2.1-fold increase in expression compared to the Y136 isolates JIW11 and 94202. Likewise, UK F136 isolates showed an average of 5.7-fold expression increase compared to those Y136 isolates. Additionally, *Cyp51* expression in F136 isolates averaged at 2.7-fold higher than in Y136/F136 isolates. Y136 isolates JIW11 and 94202 had a 4.4-fold higher expression than US Y136 isolates, and UK F136 isolates had a 5.4-fold increase compared to US F136 isolates.

Table 5.3.6.1: A summary of p-values, adjusted p-values and level of statistical significance calculated between various combinations of UK and US isolate groups using an ANOVA test on FPKM values. Stars represent the level of statistical significance between two groups; ns means not significant.

Country	Genotype 1	Genotype 2	p-value	Adjusted p-value	Significance
UK	F136	Y136/F136	0.0002	0.0005	***
	F136	Y136	0.01	0.02	*
	Y136/F136	Y136	0.2	0.2	ns
US	F136	Y136	2×10^{-8}	N/A	****

ANOVA tests were performed separately with FPKM values from the US and UK isolates to see if the differences in expression levels were statistically significant. P-values and adjusted p-values (using Benjamini-Hochberg correction) from UK Y136, F136, and Y136/F136 comparisons and a US Y136 and F136 comparison are shown in table 5.3.6.1. The UK ANOVA tests with FPKM values showed there was a statistically significant difference in *Cyp51* gene expression in Y136 vs F136 isolates and Y136/F136 vs F136 isolates, however, there was no significant difference between Y136 and Y136/F136 isolates. US ANOVA tests showed a statistically significant difference in expression between Y136 and F136 isolates.

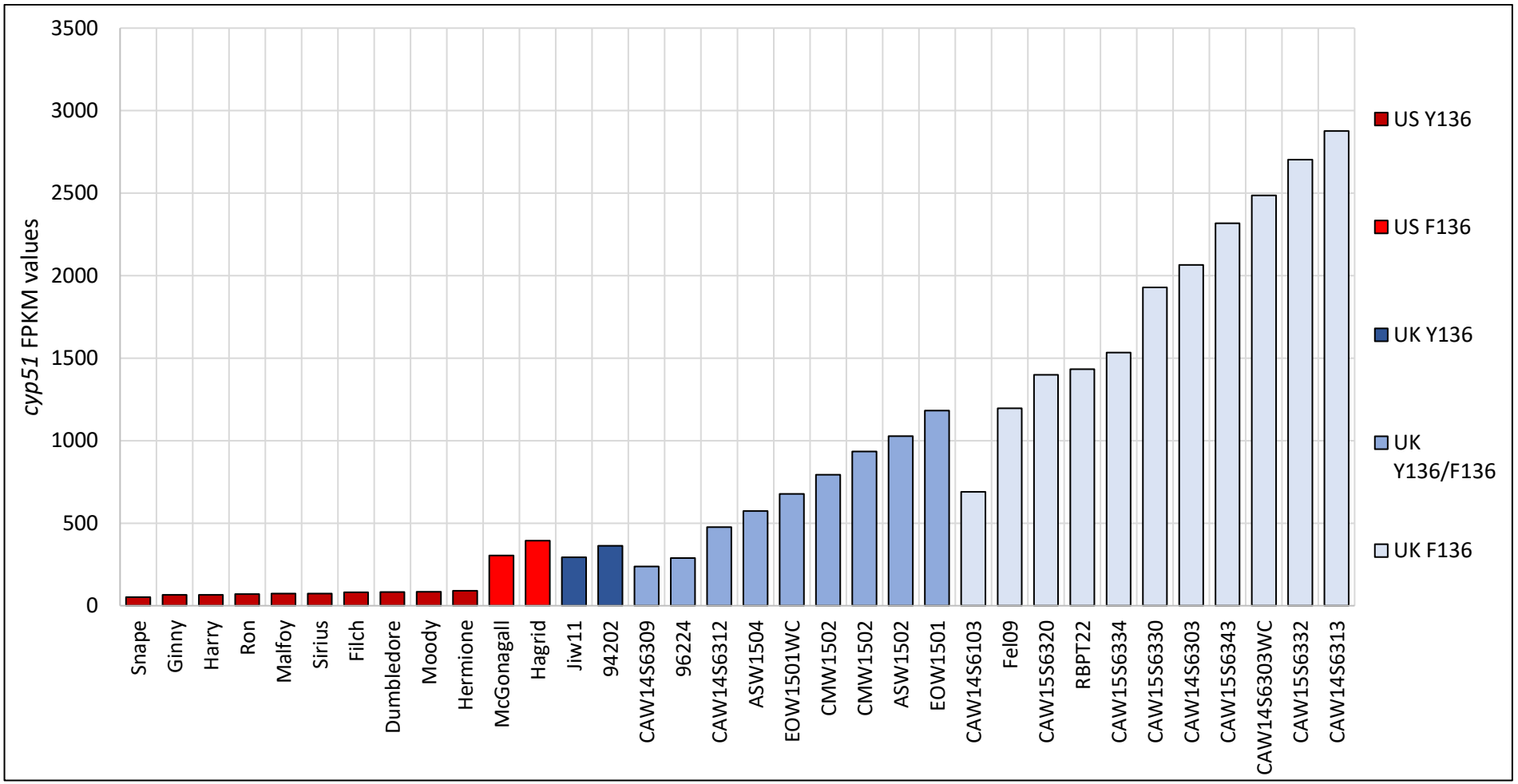

Figure 5.3.6.1: Graphical representation of Cyp51 *gene expression FPKM values from ten US Y136 isolates, two US F136 isolates, UK Y136 isolate JIW11, Swiss Y136 isolate 94202, Swiss Y136/F136 isolate 96224, eight UK Y136/F136 isolates, and eleven UK F136 isolates.*

ANOVA tests were also performed between US and UK Y136 isolates as well as US and UK F136 isolates using FPKM values. The results from these two comparisons are shown in table 5.3.6.2. Both of these tests showed a statistically significant difference in *Cyp51* gene expression between US and UK isolates.

Table 5.3.6.2: Results from ANOVA tests comparing US and UK Y136 and F136 isolates using FPKM values.

Genotype 1	Genotype 2	p-value	Significance
US Y136	UK Y136	9.66×10^{-9}	****
US F136	UK F136	0.011	*

5.4 Discussion

From the experiments performed in this chapter, it is clear that resistance to triazole fungicides in the UK and US *Bgt* populations has been increased through the evolution of a complex combination of several resistance mechanisms. Sequencing the *Cyp51* gene in *Bgt* isolates collected from the JIC glasshouses and from around Norfolk in 2014-15 revealed that isolates in the current UK *Bgt* population have either one allele containing the Y136F mutation or have both the mutated and wild-type alleles. Isolates containing only the wild-type allele could still be present in the population, but they were not present in the samples collected therefore are likely to be at a very low frequency, if present at all. The presence of both mutated and wild-type alleles has not been found in individual *Bgt* isolates before. Interestingly, the mutated allele in "heteroallelic" or "Y136/F136" isolates always had the S509T mutation as well as Y136F, whereas F136 isolates containing only the F136 allele did not have this second mutation.

The effects of the presence of two alleles within an isolate compared to only having the wild-type allele was examined using fungicide spray tests. With prothioconazole, no distinction between Y136/F136 and F136 isolates was seen as many of these isolates were able to grow at the highest dose, i.e. at the recommended field rate. This showed that prothioconazole was unable to effectively control *Bgt* isolates containing the Y136F mutation. With a second triazole, tebuconazole, F136 isolates had an ED_{50} of $102.6 \pm 10^{(0.075)}$ mL/ha and were approximately 4.5-fold more resistant than wild-type Y136 isolate JIW11 which had an ED_{50} of $22.7 \pm 10^{(0.043)}$ mL/ha. Y136/F136 isolates were even more resistant than F136 isolates as they had an ED_{50} of $179.6 \pm 10^{(0.04)}$ mL/ha. This is a 7.9-fold increase in resistance compared to JIW11 and a 1.75-fold increase compared to F136 isolates. The added resistance in Y136/F136 isolates could be due to the presence of both wild-type and mutated alleles, the addition of S509T, or a combination of both.

The advantage of retaining the wild-type allele is unclear, but it is possible that the wild-type protein has a higher affinity for the fungicide than the mutated protein does and acts as a bait which sequesters the fungicide molecules leaving the mutated protein free for demethylation

activity. This mechanism would only be advantageous when the fungicide concentration is not high enough to saturate all CYP51 molecules. In *S. cerevisiae*, the Y136F mutation was lethal to protein function and the addition of S509T partially restored function[132]. It is possible that a similar but not identical effect happens in Y136/F136 isolates of *Bgt*, so the mutated protein with both F136 and T509 acts as the functional form while the wild-type protein sequesters fungicide molecules, thus enabling the isolate to overcome fungicide inhibition whilst retaining near-normal demethylation activity. This could be a reason for why F136 isolates had markedly greater expression of *Cyp51* compared to Y136 and Y136/F136 isolates as this could overcome the effects of reduced enzyme activity from the Y136F mutation alone. It is also possible that possessing both wild-type and mutant alleles had no effect on the level of resistance compared to only having the mutant allele and that the increased resistance seen in these UK Y136/F136 isolates was due to the added S509T mutation instead. In US Y136/F136 and F136 isolates, there appears to be no difference in response to triazole fungicides, but those Y136/F136 isolates are also lacking the S509T mutation (personal communication with Emily Meyers, Ph.D. student, North Carolina State University).

The 96224 promoter region sequence showed four potential SNPs between the UK Y136 and F136 allele promoter sequences (positions 1830, 1310, 875, and 696, tables 5.3.3.1-2). The SNPs present in the F136 allele, however, were identical to those found in the US Y136 and F136 isolates therefore are unlikely to have increased gene expression as all US isolates had lower gene expression on average than UK Y136/F136 isolates (figure 5.3.6.1). It is interesting that the promoter region sequences in US Y136 and F136 isolates were identical to each other as the RNA-seq *Cyp51* gene expression data showed an up-regulation of expression in US F136 isolates (figure 5.3.6.1). It is also interesting that the US isolates had identical sequences to the UK F136 isolates at seven out of nine SNP locations as there was significantly greater (5.4-fold) *Cyp51* expression in UK than US F136 isolates (figure 5.3.6.1, table 5.3.6.2). The much lower expression in US isolates could be associated with the three SNPs that were only present in US isolates, but the critical regions of the promoter for gene expression are currently unknown.

The presence of SNPs in the *Cyp51* promoter region in UK F136 isolates compared to UK Y136 isolate JIW11 is reflected in the 5.4- and 5.7-fold increase in gene expression in the qRT-PCR and RNA-seq data, respectively (figures 5.3.5.1 and 5.3.6.1). There was SNP variation between the F136 promoter region and both the predicted Y136 and F136 allele promoter sequences in Y136/F136 isolates at positions 1315 and 404. As F136 isolates had the highest levels of *Cyp51* gene expression, it is possible that these two SNPs were responsible for that up-regulation. On average, Y136/F136 isolates had a 1.6- to 2.1-fold increase in *Cyp51* expression compared to Y136 isolate JIW11, whereas F136 isolates had a 5.4- to 5.7-fold increase in expression according

to qRT-PCR and RNA-seq data. It is likely that the increase seen in Y136/F136 isolates compared to Y136 isolates was due to an increase in gene copy number whereas the increase in F136 isolates was more likely due to the alterations in promoter region but could also have been increased by copy number. Unfortunately, only one UK Y136 isolate was available for this gene expression study, and US Y136 isolates had US-specific SNPs in the promoter region which, as discussed, may have an effect on gene expression and skew the data.

It is interesting that there was very little difference in gene expression between UK Y136 isolate JIW11 and Swiss Y136 isolate 94202, and UK Y136/F136 isolate CAW14S6309 and Swiss Y136/F136 isolate 96224. ddPCR was used to estimate *Cyp51* copy number in two Y136, five Y136/F136, and five F136 isolates. This experiment showed that both JIW11 and 94202 contained two copies of the gene correlating with the elevated gene expression in these isolates compared to US isolates. This experiment also showed that four out of five Y136/F136 isolates included had three copies of the gene, while the fifth Y136/F136 isolate had 4.7 (possibly five) copies, and F136 isolates had between three and five copies. These results correlate with the slightly increased levels of expression in Y136/F136 isolates and larger increase in F136 isolates compared to Y136 isolates. Although adequate quantities of DNA could not be obtained from 96224 spores to include this isolate in the ddPCR, DNA sequencing reads from this isolate were made available by Prof. Beat Keller. Aligning the raw DNA reads from the two versions of the 96224 reference genome (the already-available genome data and the new version I was given access to) to the *Cyp51* gene showed a ratio of 0.54(Y136):0.46(F136) reads. This suggested that there were two copies of the *Cyp51* gene present, one wild-type and one mutated. Unfortunately, performing allele-specific copy number assays for this gene is difficult as the Y136F mutation lies in an AT-rich region. Designing primers and probes that have a high-specificity whilst reaching the required melting temperatures is difficult therefore the ratio of mutated to wild-type genes could not be confirmed experimentally (data not shown).

The presence of both Y136 and F136 alleles in one isolate has previously been identified in *Erysiphe necator*[133,148]. With *E. necator*, Y136/F136 isolates also showed a further increase in resistance to triazoles than F136 isolates as was seen here with *Bgt*. However, with *E. necator*, Y136/F136 isolates also had the highest levels of *Cyp51* gene expression[133]. Information about the presence of SNPs in the *Cyp51* promoter region of those isolates is currently unavailable so it could be possible that *E. necator* Y136/F136 isolates also have mutated promoter regions or that F136 isolates have wild-type promoters. As discussed in the introduction, many organisms also use ABC transporters to detoxify the cells. The use of ABC transporters has not been explored here in *Bgt* isolates, but it would be greatly beneficial to investigate this in future

studies using RNA-seq data to observe changes in gene expression or biochemical assays to look at fungicide concentration within hyphae of resistant isolates in comparison to sensitive isolates.

6 General Discussion

6.1 Implications of this thesis

As the world's population increases, so does the demand for food. The United Nation's Food and Agricultural Organisation estimated that by 2050, the world's population will have increased by 34 % and that food production will need to increase by 70 % to meet the demand[160]. There are many ways in which food production could be increased and there is a large variety of research being conducted to work towards this goal, for example a new comprehensive wheat genome has recently become available which is a valuable tool for improving wheat performance in drought and warmer climates[161]. One method of enhancing a crop's yield is by improving the efficiency of plant growth and grain, seed, or flower production. Another method is to control and reduce plant diseases. This can be achieved by either improving the plant's immune system so it has a better defence against pathogens or by applying pesticides. Extensive research into plant *resistance* (*R*) genes, such as nucleotide-binding domain and leucine-rich repeat (NB-LRR) proteins[162], and the development of technologies, such as resistance gene enrichment sequencing (RenSeq)[163], have boosted our understanding of the plant immune system and have opened new avenues of increasing resistance to pathogens. Although this is a valuable method for increasing resistance in plants, the introduction of individual *R* genes into plants is only a short-term solution as pathogens evolve relatively quickly and overcome these resistances. An example of this is in wheat where *R* gene *Sr31* was commonly used to protect against wheat stem rust caused by *Puccinia graminis* f. sp. *tritici* until a new race (Ug99) evolved which showed complete resistance to this gene[5]. Because of this problem, breeders try to select for partial resistance using field trials while researchers are exploring the use of gene stacks consisting of several *R* genes that can be introduced into a crop variety at once thereby reducing the risk of virulent pathogens evolving. As mutations conferring resistance evolve by random chance, the probability of multiple virulences evolving in a short space of time is low thus the more *R* genes that can be "stacked" and introduced at once, the more durable the resistance should be. Of course, much research remains to be done on the effects of introducing several *R* genes into a plant at once on the fitness, yield, and potential trade-offs in the plant, but it is currently a promising solution.

Applying pesticides to control plant pathogens is not necessarily an alternative to improving the plant's immune system but can be used in conjunction with it. As *R* genes target the virulence proteins used by a pathogen to overcome the plant's immune system, pesticides are designed to target essential biochemical pathways within the pathogen, for example succinate dehydrogenase inhibitors (SDHIs) target the respiratory pathway and triazoles target the

ergosterol biosynthesis pathway. As is well understood, using several pesticides with different modes of action is a more durable and effective way of controlling pathogens than using a single mode of action alone. It is a strong argument that, at least in the short term, using several different pesticides along with plant *R* genes could help keep pathogens at bay. Unfortunately, the variety of pesticides available for use to control plant pathogens is shrinking as pathogens are developing resistance to them in addition to the tight regulatory restrictions on the marketing and use of pesticides. This problem is exacerbated by broad-spectrum fungicides being used too frequently to control multiple groups of pathogens thus selecting for resistance. This thesis has examined the emergence of resistance to four examples of fungicides from three different groups with different modes of action and highlighted the importance of using pesticides responsibly to maintain their efficacy and reduce the risk of resistance developing.

6.1.1 Technology for studying fungicide resistance

The use of genomics has proved to be a powerful tool for identifying potential mechanisms of resistance and testing their involvement in increased resistance to fungicides. RNA-seq in particular has proved useful in many ways in this thesis, but the most powerful use of this technology was to identify the candidate target, MAD1, of cyflufenamid in chapter 4. Additionally, the use of RNA-seq data was fruitful with observing alterations in *Cyp51* gene expression between *Bgt* populations in the US and the UK/Switzerland as well as with identifying the presence of Y136, F136, or both alleles in individuals where reduced sensitivity to triazole fungicides is common amongst the population. This shows the application of this technology for screening populations to identify the presence and prevalence of multiple resistance mechanisms to fungicides.

Chapter 3 showed how simple sequencing techniques can also be useful for identifying mutations which may confer resistance to fungicides as sequencing the *Erg24* gene showed the presence of a V295L mutation in *Bgt* isolates and D291N in *Bgh* isolates with increased resistance to fenpropimorph. The hypothesis that V295L in ERG24 confers an increased resistance to fenpropimorph was tested by introducing this mutation into *S. cerevisiae* using the modern CRISPR/Cas9 technology. CRISPR/Cas9 is an excellent method for testing such hypotheses and has been proven here, and in many other studies, to be an extremely valuable tool for gene editing and has many more applications to test the results found in this thesis.

An example of this is the discovery of multiple *Cyp51* gene copies within *Bgt* (chapter 5). Between 3 and 5 copies of this gene were identified in heteroallelic (Y136/F136) isolates and at least one of those copies contained the Y136F and S509T mutations while at least one of the other copies was wild-type at both positions. As the value of retaining a wild-type copy of the

gene while having at least one mutated copy remains unknown, I hypothesised that the wild-type protein is used to sequester fungicide molecules while the mutated protein is used for its usual demethylation activity. The availability of a reliable CRISPR/Cas9 method in *S. cerevisiae* presents the opportunity to test this hypothesis as it allows a variety of *Cyp51* allele combinations to be introduced into *S. cerevisiae* to study their effects on resistance to triazoles. The initial combinations to test would be to introduce the wild-type *Bgt Cyp51* gene alone under a yeast promoter (and suppress the native gene) to use as a baseline as it is not identical to that in *S. cerevisiae*, then to introduce Y136F alone, Y136F and S509T together, wild-type and Y136F alleles together, and wild-type and Y136F + S509T alleles together.

Although using CRISPR/Cas9 in *S. cerevisiae* is valuable for testing these hypotheses, it is not particularly closely-related to *Blumeria* therefore the development of a CRISPR/Cas9 method for use with powdery mildew fungi, or other biotrophic fungi, would be even more valuable. In the context of this thesis, being able to edit the *MAD1* gene in cyflufenamid-sensitive *Bgt* isolates to introduce the Q560K mutation hypothetically involved in increased resistance to cyflufenamid would be desirable. It is unlikely that cyflufenamid would be able to inhibit the growth of *S. cerevisiae* as it has been shown that this fungicide can only control a limited range of organisms[114] therefore being able to perform CRISPR/Cas9 with a more closely-related organism, or with *Blumeria* itself, would be beneficial to test this hypothesis. Adding to this, it would be more beneficial to test the effects of *Cyp51* mutations and copy number on the levels of resistance to triazoles in *Blumeria* rather than in *S. cerevisiae* as suggested above.

6.1.2 Molecular evolution of resistance

Fungicide spray tests and sequencing technologies, such as RNA-seq, have given an insight into how resistance to fungicides can evolve in *Blumeria*. The results from this thesis have shown that resistance can evolve in a number of ways from acquiring a single mutation in a gene, as with ERG24 and morpholines, to accumulating more complex combinations of mechanisms, as with triazoles, but why more complex mechanisms have evolved is not necessarily clear. The most obvious reason for multiple resistance mechanisms accumulating in *Bgt* isolates to confer increased triazole resistance is that single mutations within the target CYP51 protein itself may result in a significantly high fitness cost which is unfavourable for the pathogen's survival. Although it has been shown in *S. cerevisiae* that acquiring the Y136F mutation destroyed CYP51 protein function[140], CYP51 function is not affected to the same extent in *Blumeria* or other wheat pathogens. However, this does show that acquiring mutations in the protein's active site can drastically affect protein function which could explain why other mutations, besides S509T, have not appeared which confer complete resistance.

Likewise, with ERG24, only one mutation was identified in *Bgt* which was shown, using gene-editing in *S. cerevisiae*, to confer increased but not complete resistance to morpholines. This morpholine resistance appears to be a much simpler situation than with triazoles, but there was a small range of isolates which had a further increase in resistance, the cause of which remains unexplained. It is possible that alternative mechanisms similar to those used with triazoles have evolved which confer this further increase in those isolates, but those possibilities were not explored here. It is also possible that, as only a small local sample of isolates were included in this study, this is not representative of how morpholine resistance has occurred in the wider UK *Bgt* population.

One question that should be addressed is why has fenpropimorph remained effective for longer than many of the triazole fungicides when they all target the same biosynthetic pathway? It could be that the fenpropimorph molecule interacts with key amino acids within the ERG24 active site that are vital for protein function and mutation of those amino acids would result in a high fitness cost. It could also be because triazole fungicides are single-site inhibitors whereas fenpropimorph, although it mostly targets ERG24, also has a low affinity for ERG2. The research performed here shows how resistance to a fungicide may appear to have evolved in a simple way through acquiring single mutations, but there may actually be more mechanisms involved that are not as obvious.

The potential for alternative unknown resistance mechanisms being present also appeared in chapter 4 when an increased resistance to Aviator^{235} Xpro was identified in the current UK *Bgt* population compared to older UK isolate JIW11. Increased resistance to succinate dehydrogenase inhibitors (SDHIs) has been shown in other organisms, e.g. *Zymoseptoria tritici*[47], to be conferred by mutations within the genes encoding SDHB, SDHC, and SDHD subunits of the SDH complex. While the 2014 and 2015 isolates lacked mutations within these genes, and had greater resistance to prothioconazole than older isolates, a rigorous test of whether partial resistance to Aviator^{235} Xpro involves the SDHI, the triazole or both would require experiments to done with bixafen alone if it were available. If increased resistance to the SDHI has indeed occurred in these isolates, this suggests alternative mechanisms of resistance other than mutations within the genes have evolved. This has wider implications for crop pathogen management because if this happens in *Blumeria*, then it most likely happens, or will happen, in other organisms too.

Additionally, chapter 4 highlighted the potentially high fitness penalty resulting from the accumulation of resistances in *Bgt* isolates to several different groups of fungicides. It was clear from the SSR analysis in particular that when selection pressure was removed by ceasing to apply cyflufenamid, the cyflufenamid-resistant *Bgt* isolates could not compete with the sensitive

isolates and were rapidly replaced. This implied that there is either a large fitness penalty associated with cyflufenamid-resistance alone, or that this accumulation of resistances has affected normal mildew growth in so many different ways that they were no longer able to reproduce as rapidly as cyflufenamid-sensitive isolates could.

6.1.3 Practical implications

The research carried out in this thesis highlights the important issue that pathogens are most certainly able to acquire resistance to multiple pesticides without survival or reproductive fitness being impaired too significantly. Although it is not always possible for resistance to evolve in the simple form of a single mutation due to high fitness penalties incurred by such mutations, if put under enough selection pressure, pathogens will ultimately undoubtedly evolve alternative mechanisms of resistance. The evolution of resistance to cyflufenamid is a prime example of the selection for resistance being exacerbated by the inappropriate application of fungicides. Cyflufenamid was applied eleven times in one glasshouse within the space of 15 months and nine times in a second glasshouse in only three months. As this fungicide should only be applied twice within one growing season, this number of applications was excessive and eventually ceased to control wheat powdery mildew.

Chapter 4 also showed that three cyflufenamid-sensitive isolates from the glasshouse in 2015 and from the UK field population were able to form a small number of colonies at the recommended field application rate. This brings into question whether this rate is suitable and if it could (or should) be raised to a higher rate. In order to raise the recommended rate, the cost of doing so and the safety of the operators must also be taken into consideration, as well as the effect a higher dose would have on the environment. On the other hand, the ability of three isolates to form a small number of colonies at the field application rate could be a limitation of the spray test method used in this thesis. The effects of increasing pesticide application doses on the risk of pathogens developing resistance have been discussed in a review which concluded that while a high dose may be required to effectively control a pathogen, it may also increase the rate at which resistance develops, particularly in diploid organisms[169]. This is because, with diploids, using a high dose of a pesticide is more likely

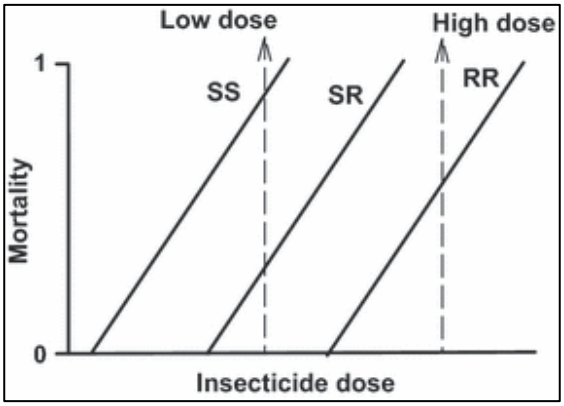

Figure 6.1.3.1: The impact of using a higher dose rate on the prevalence of resistant and sensitive alleles within a diploid population. Figure taken from Bosch et al. *(2011).*

to eradicate individuals within a population which contain sensitive alleles in a homozygous or heterozygous state (figure 6.1.4.1). This leaves for the most part only resistant alleles in the population so resistant individuals can mostly only mate with other resistant individuals resulting in the establishment of a highly-resistant population. The review suggested that if a lower dose of pesticide is applied then maintaining sensitive alleles within the population will keep the number of resistance alleles present down thus keeping the level of resistance low[169]. As *Bgt* isolates are haploid organisms, this theory is not strictly applicable here, but many fungicides used to control powdery mildew fungi also control other pathogens therefore the effect of increasing application doses needs to be carefully considered. Before raising the application dose rate of cyflufenamid, it would be useful to test its effectiveness against other common plant pathogens in the UK.

6.1.4 Value of understanding molecular biology of fungicide action and resistance

It is important to understand not only the mode of action of a fungicide and how resistance evolves to it in pathogenic organisms, but also to understand how to deliver the fungicide into the pathogen and how to alter the fungicide molecule and formulation to make it as effective as possible against a broad range of pathogens. A key example shown in this thesis is with cyflufenamid which potentially targets MAD1, a protein which is conserved across many organisms, but despite this, this fungicide is only able to control a limited number of organisms. If MAD1 truly is the target of cyflufenamid then here I have identified a new target for fungicides that could be exploited in the development of future chemicals for multi-pathogen control if a compound which inhibits MAD1 in a wider range of fungi but not plants or animals can be discovered.

As fenpropimorph has remained effective for the last 35 years, it begs the question of whether there should be future investment in further developing morpholine fungicides for use in agriculture or not. As shown in chapter 3, *Bgt* isolates had a higher baseline tolerance to fenpropimorph than *B. graminis* f. sp. *hordei* (*Bgh*) isolates did as *Bgh* was originally one of the principal targets of this fungicide. By obtaining a crystal structure of the *Bgt* ERG24 protein and studying its interaction with fenpropimorph, could it be possible to re-design the molecule and create new products that better target and control wheat powdery mildew as well as a broader spectrum of other fungi? A better understanding of the ERG24 protein in other plant pathogens would be useful for further development of this group of fungicides. The Agricultural and Horticultural Development Board (AHDB) has shown that fenpropimorph also provides acceptable control of yellow rust and brown rust[88] therefore it would be greatly beneficial for growing crops in the UK if morpholines could be improved.

It would also be beneficial to study the ERG24 protein in these pathogens and see if they too have gained this V295L mutation, or a similar mutation as with D291N in *Bgh*, so that a re-designed morpholine molecule can better target all three pathogens. The AHDB also showed that fenpropimorph is not particularly effective at controlling septoria of wheat[88]. Could this be due to differences in the ERG24 protein between rusts, mildew, and septoria? A BLAST search comparing the *Bgt* ERG24 protein with the protein database from *Z. tritici* IPO323 (GenBank taxid 336722) had 56% identity between the proteins and showed that ERG24 in septoria should have the wild-type V at position 313 (V295 in *Bgh*/*Bgt*) and D at position 309 (D291 in *Bgh*/*Bgt*) therefore this enzyme should be inhibited by fenpropimorph. Likewise, when the ERG24 protein in *Puccinia striiformis* f. sp. *tritici* PST-78 (GenBank taxid 1165861) was compared with that of *Bgt* there was 41% identity and had wild-type amino acids at V281 and D277, respectively. As mentioned, there are other factors that also affect the efficacy of a fungicide, for example how well it is delivered into the pathogen itself or how well it is taken up and transported around the plant. The information gained from the research in this chapter shows that there is scope for further development of morpholine fungicides and their potential for broad-spectrum activity against many wheat fungal pathogens. Perhaps further investigation into the molecule design and delivery method of morpholines would be beneficial for making them useful at controlling many plant pathogens which have developed resistance to triazoles, SDHIs, and QoIs.

Additionally, with knowing what mutations confer increased resistance to fungicides, such as with ERG24 described above, would it be possible to use this information to design new fungicide molecules which have a higher affinity for the mutated form of the target protein? For example, would it be possible to design a new morpholine that has a higher affinity for ERG24 with the V295L mutation than fenpropimorph does? This is a prospect that shows the value of understanding mechanisms that have evolved to increase resistance to fungicides as well as the value of modern technology and modelling tools for predicting the effect mutations may have on protein function including potential fitness costs. This in turn may help predict the durability of fungicides if the mechanisms of resistance and effects of amino acid mutations are known and well understood.

6.2 Conclusions

The work presented in this thesis has contributed to advancing knowledge of how resistance has evolved to morpholines and cyflufenamid. It has also contributed to a better understanding of mechanisms involved in increasing resistance to the triazoles, which are much better understood, including novel features of the genome organisation. This knowledge can be exploited in the design of new fungicide molecules that can target both wild-type and mutated

versions of the proteins in a range of pathogens, as well as the development and use of new fungicide formulations.

Abbreviations

ABC	ATP-binding cassette
AHDB	Agriculture and Horticulture Development Board
ANOVA	Analysis of variance
ATP	Adenosine triphosphate
Bgh	*Blumeria graminis* f. sp. *hordei*
Bgt	*Blumeria graminis* f. sp. *tritici*
BLAST	Basic Local Alignment Search Tool
BUSCO	Benchmarking universal single-copy orthologs
CRISPR	Clustered Regularly Interspaced Short Palindromic Repeats
dATP	Deoxyadenosine triphosphate
ddPCR	Droplet digital PCR
DMI	De-methylation inhibitor
DNA	Deoxyribonucleic acid
dNTPs	Deoxynucleotide triphosphates
ED_{50}	Median effective dose
ETC	Electron transport chain
F	Isolates containing Y136F mutation
FRAC	Fungicide Resistance Action Committee
f. sp.	*forma specialis*
ff. spp.	*formae speciales*
H	Isolates containing both wild-type and Y136F/S509T alleles
ITS	Internal transcribed spacer
JIC	John Innes Centre
MAT1	Mating type 1
MAT2	Mating type 2
MIC	Minimum inhibitory concentration
mRNA	messenger RNA
NADPH	Nicotinamide adenine dinucleotide phosphate (reduced)
NB-LRR	Nucleotide-binding leucine-rich repeat proteins
ORF	Open reading frame

PCR	Polymerase chain reaction
QoI	Quinone outside inhibitor
qRT-PCR	Quantitative reverse transcription PCR
R gene	*Resistance* gene
RNA	Ribonucleic acid
SDH	Succinate dehydrogenase
SDHI	Succinate dehydrogenase inhibitor
SEM	Scanning electron microscopy
SNP	Single nucleotide polymorphism
SOC	Super optimal broth with catabolite repression
SSR	Simple sequence repeat
TEM	Transmission electron microscopy
USDA-ARS	United States Department of Agriculture – Agricultural Research Service
UV	Ultraviolet
Y	Isolates containing the wild-type *Cyp51* allele

Units

bp	Base pairs
cm	Centimetres
Cq	Quantitation cycle
FPKM	Fragments per kilobase of transcript per million mapped reads
g	Grams
g/L	Grams per litre
L	Litre
mL/ha	Millilitres per hectare
mg/L	Milligrams per litre
mL/L	Millilitres per litre
ng	Nanograms
ng/µL	Nanograms per microlitre
pg	Picograms
pg/mL	Picograms per millilitre
ppm	Parts per million
rpm	Revolutions per minute

U	Units (of enzyme)
µg	Micrograms
µg/mL	Micrograms per millilitre
µL	Microlitres
µM	Micromolar
V	Volts

References

1 Finckh, M. *et al.* Cereal variety and species mixtures in practice, with emphasis on disease resistance. *Agronomie* **20**, 813-837 (2000).

2 Dean, R. *et al.* The Top 10 fungal pathogens in molecular plant pathology. *Molecular Plant Pathology* **13**, 414-430 (2012).

3 Brading, P. A., Verstappen, E. C. P., Kema, G. H. J. & Brown, J. K. M. A gene-for-gene relationship between wheat and *Mycosphaerella graminicola*, the septoria tritici blotch pathogen. *Phytopathology* **92**, 439-445 (2002).

4 Fones, H. & Gurr, S. The impact of Septoria tritici Blotch disease on wheat: An EU perspective. *Fungal Genetics and Biology* **79**, 3-7 (2015).

5 Pretorius, Z. A., Singh, R. P., Wagoire, W. W. & Payne, T. S. Detection of virulence to wheat stem rust resistance gene *Sr31* in *Puccinia graminis.* f. sp. *tritici* in Uganda. *Plant Disease* **84**, 203-203 (2000).

6 Hovmøller, M. S. *et al.* Replacement of the European wheat yellow rust population by new races from the centre of diversity in the near-Himalayan region. *Plant Pathology* **65**, 402-411 (2016).

7 Lewis, C. M. *et al.* Potential for re-emergence of wheat stem rust in the United Kingdom. *Communications Biology* **1**, 13 (2018).

8 Brown, J. K. M. Durable resistance of crops to disease: a Darwinian perspective. *Annual Review of Phytopathology* **53**, 513-539 (2015).

9 AHDB Cereals and Oilseeds. *Powdery Mildew*, <https://cereals.ahdb.org.uk/cereal-disease-encyclopedia/diseases/powdery-mildew.aspx> (30/08/2018).

10 AHDB Cereals and Oilseeds. *Fusarium (Foot Rot, Seedling Blight, Ear (Head) Blight)*, <https://cereals.ahdb.org.uk/cereal-disease-encyclopedia/diseases/fusarium-(foot-rot,-seedling-blight,-ear-(head)-blight).aspx> (30/08/2018).

11 Lofgren, L. A. *et al. Fusarium graminearum*: pathogen or endophyte of North American grasses? *New Phytologist* **217**, 1203-1212 (2018).

12 Beres, B. L. *et al.* Exploring Genotype × Environment × Management synergies to manage fusarium head blight in wheat. *Canadian Journal of Plant Pathology* **40**, 179-188 (2018).

13 Marques, L. N. *et al.* Occurrence of mycotoxins in wheat grains exposed to fungicides on fusarium head blight control in southern Brazil. *Journal of Environmental Science and Health, Part B* **52**, 244-250 (2017).

14 Miedaner, T. *et al.* A multiple disease test for field-based phenotyping of resistances to *Fusarium* head blight, yellow rust and stem rust in wheat. *European Journal of Plant Pathology* **151**, 451-461 (2018).

15 Laraba, I. *et al.* Population genetic structure and mycotoxin potential of the wheat crown rot and head blight pathogen *Fusarium culmorum* in Algeria. *Fungal Genetics and Biology* **103**, 34-41 (2017).

16 Jia, H. *et al.* A journey to understand wheat *Fusarium* head blight resistance in the Chinese wheat landrace Wangshuibai. *The Crop Journal* **6**, 48-59 (2017).

17 Kelly, L. A., Tan, Y. P., Ryley, M. J. & Aitken, E. A. B. *Fusarium* species associated with stalk rot and head blight of grain sorghum in Queensland and New South Wales, Australia. *Plant Pathology* **66**, 1413-1423 (2017).

18 Flood, J. The importance of plant health to food security. *Food Security* **2**, 215-231 (2010).

19 Shaw, M. W. & Royle, D. J. Airborne inoculum as a major source of Septoria tritici (*Mycosphaerella graminicola*) infections in winter wheat crops in the UK. *Plant Pathology* **38**, 35-43 (1989).

20 Prew, R. D. *et al.* Effects of eight factors on the growth and nutrient uptake of winter wheat and on the incidence of pests and diseases. *The Journal of Agricultural Science* **100**, 363-382 (1983).

21 Mendgen, K. & Hahn, M. Plant infection and the establishment of fungal biotrophy. *Trends in Plant Science* **7**, 352-356 (2002).

22 Spanu, P. D. *et al.* Genome expansion and gene loss in powdery mildew fungi reveal tradeoffs in extreme parasitism. *Science* **330**, 1543-1546 (2010).

23 Oliver, R., Tan, K.-C. & Moffat, C. Necrotrophic pathogens of wheat. *Encyclopedia of Food Grains* Vol. 4 273-278 (2016).

24 Yang, F., Li, W. & Jørgensen, H. J. L. Transcriptional reprogramming of wheat and the hemibiotrophic pathogen *Septoria tritici* during two phases of the compatible interaction. *PLoS One* **8**, e81606 (2013).

25 Carver, T. L. W., Kunoh, H., Thomas, B. J. & Nicholson, R. L. Release and visualization of the extracellular matrix of conidia of *Blumeria graminis*. *Mycological Research* **103**, 547-560 (1999).

26 Edwards, H. H. Development of primary germ tubes by conidia of *Blumeria graminis* f. sp. *hordei* on leaf epidermal cells of *Hordeum vulgare*. *Canadian Journal of Botany* **80**, 1121-1125 (2002).

27 Glawe, D. A. The powdery mildews: a review of the world's most familiar (yet poorly known) plant pathogens. *Annual Review of Phytopathology* **46**, 27 (2008).

28 Hall, A. A. & Gurr, S. J. Initiation of appressorial germ tube differentiation and appressorial hooking: distinct morphological events regulated by cAMP signalling in *Blumeria graminis* f. sp. *hordei*. *Physiological and Molecular Plant Pathology* **56**, 39-46 (2000).

29 Zhang, Z. *et al.* Of genes and genomes, needles and haystacks: *Blumeria graminis* and functionality. *Molecular Plant Pathology* **6**, 561-575 (2005).

30 Aist, J. R. Papillae and related wound plugs of plant cells. *Annual Review of Phytopathology* **14**, 145-163 (1976).

31 Both, M., Csukai, M., Stumpf, M. P. H. & Spanu, P. D. Gene expression profiles of *Blumeria graminis* indicate dynamic changes to primary metabolism during development of an obligate biotrophic pathogen. *Plant Cell* **17**, 2107-2122 (2005).

32 Kiss, L. *et al.* Microcyclic conidiogenesis in powdery mildews and its association with intracellular parasitism by *Ampelomyces*. *European Journal of Plant Pathology* **126**, 445-451 (2010).

33 Robinson, H. L., Ridout, C. J., Sierotzki, H., Gisi, U. & Brown, J. K. M. Isogamous, hermaphroditic inheritance of mitochondrion-encoded resistance to Qo inhibitor fungicides in *Blumeria graminis* f. sp. *tritici*. *Fungal Genetics and Biology* **36**, 98-106 (2002).

34 Koltin, Y. & Kenneth, R. The role of the sexual stage in the over-summering of *Erysiphe graminis* DC. f. sp. *hordei* Marchal under semi-arid conditions. *Annals of Applied Biology* **65**, 263-268 (1970).

35 Jankovics, T. *et al.* New insights into the life cycle of the wheat powdery mildew: direct observation of ascosporic infection in *Blumeria graminis* f. sp. *tritici*. *Phytopathology* **105**, 797-804 (2015).

36 Moseman, J. G. & Powers, H. R. Function and longevity of cleistothecia of *Erysiphe graminis* f. sp. *hordei*. *Phytopathology* **47**, 53-56 (1957).

37 Turner, D. M. Studies on cereal mildew in Britain. *Transactions of the British Mycological Society* **39**, 495-IN497 (1956).

38 Eshed, N. & Wahl, I. Host ranges and interrelations of *Erysiphe graminis hordei, E. graminis tritici*, and *E. graminis avenae*. *Phytopathology* **60**, 628-634 (1970).

39 Lyngkjær, M. F. & Carver, T. L. W. Induced accessibility and inaccessibility to *Blumeria graminis* f. sp. *hordei* in barley epidermal cells attacked by a compatible isolate. *Physiological and Molecular Plant Pathology* **55**, 151-162 (1999).

40 Marchal, E. De la spécialisation du parasitisme chez l'*Erysiphe graminis* D. C. *Comptes Rendus Hebdomadaires des Séances de l'Académie des Sciences* **135**, 210-212 (1902).

41 Oku, T., Yamashita, S., Doi, Y. & Nishihara, N. Host range and *forma specialis* of cocksfoot powdery mildew fungus (*Erysiphe graminis* DC.) found in Japan. *Japanese Journal of Phytopathology* **51**, 613-615 (1985).

42 Troch, V. *et al. Formae speciales* of cereal powdery mildew: close or distant relatives? *Molecular Plant Pathology* **15**, 304-314 (2014).

43 Inuma, T., Khodaparast, S. A. & Takamatsu, S. Multilocus phylogenetic analyses within *Blumeria graminis*, a powdery mildew fungus of cereals. *Molecular Phylogenetics and Evolution* **44**, 741-751 (2007).

44 Large, E. C. & Doling, D. A. The measurement of cereal mildew and its effect on yield. *Plant Pathology* **11**, 47-57 (1962).

45 Piffanelli, P. *et al.* A barley cultivation-associated polymorphism conveys resistance to powdery mildew. *Nature* **430**, 887-891 (2004).

46 Herrera-Foessel, S. A. *et al.* Lr67/Yr46 confers adult plant resistance to stem rust and powdery mildew in wheat. *Theoretical and Applied Genetics* **127**, 781-789 (2014).

47 Sierotzki, H. & Scalliet, G. A review of current knowledge of resistance aspects for the next-generation succinate dehydrogenase inhibitor fungicides. *Phytopathology* **103**, 880-887 (2013).

48 Fraaije, B. A. *et al.* Risk assessment studies on succinate dehydrogenase inhibitors, the new weapons in the battle to control Septoria leaf blotch in wheat. *Molecular Plant Pathology* **13**, 263-275 (2012).

49 Ma, Z. & Michailides, T. J. Advances in understanding molecular mechanisms of fungicide resistance and molecular detection of resistant genotypes in phytopathogenic fungi. *Crop Protection* **24**, 853-863 (2005).

50 AHDB Cereals and Oilseeds. Fungicide activity and performance in wheat. (2018).

51 Lewis, K. A., Tzilivakis, J., Warner, D. J. & Green, A. An international database for pesticide risk assessments and management. *Human and Ecological Risk Assessment: An International Journal* **22**, 1050-1064 (2016).

52 Uesugi, Y. Fungicides, multisite inhibitors—broad spectrum surface protectants. *Encyclopedia of Agrochemicals* (2003).

53 Russell, P. E. A century of fungicide evolution. *The Journal of Agricultural Science* **143**, 11-25 (2005).

54 Sierotzki, H., Wullschleger, J. & Gisi, U. Point mutation in cytochrome *b* gene conferring resistance to strobilurin fungicides in *Erysiphe graminis* f. sp. *tritici* field isolates. *Pesticide Biochemistry and Physiology* **68**, 107-112 (2000).

55 Hull, C. M. *et al.* Facultative sterol uptake in an ergosterol-deficient clinical isolate of *Candida glabrata* harboring a missense mutation in ERG11 and exhibiting cross-resistance to azoles and amphotericin B. *Antimicrobial Agents and Chemotherapy* **56**, 4223-4232 (2012).

56 Benveniste, P. Sterol biosynthesis. *Annual Review of Plant Physiology* **37**, 275-308 (1986).

57 Mori, Y., Sato, Y. & Takamatsu, S. Molecular phylogeny and radiation time of *Erysiphales* inferred from the nuclear ribosomal DNA sequences. *Mycoscience* **41**, 437-447 (2000).

58 Takamatsu, S. Molecular phylogeny reveals phenotypic evolution of powdery mildews (*Erysiphales*, Ascomycota). *General Plant Pathology* **79**, 218-226 (2013).

59 Cook, R. T. A., Inman, A. J. & Billings, C. Identification and classification of powdery mildew anamorphs using light and scanning electron microscopy and host range data. *Mycological Research* **101**, 975-1002 (1997).

60 Wyand, R. A. & Brown, J. K. M. Genetic and *forma specialis* diversity in *Blumeria graminis* of cereals and its implications for host-pathogen co-evolution. *Molecular Plant Pathology* **4**, 187-198 (2003).

61 Oberhaensli, S. *et al.* Comparative sequence analysis of wheat and barley powdery mildew fungi reveals gene colinearity, dates divergence and indicates host-pathogen co-evolution. *Fungal Genetics and Biology* **48**, 327-334 (2011).

62 Menardo, F., Wicker, T. & Keller, B. Reconstructing the evolutionary history of powdery mildew lineages (*Blumeria graminis*) at different evolutionary time scales with NGS data. *Genome Biology and Evolution* **9**, 446-456 (2017).

63 Braun, U. & Cook, R. T. A. *Taxonomic manual of the Erysiphales (powdery mildews)*. (CBS-KNAW Fungal Biodiversity Centre Utrecht, The Netherlands, 2012).

64 Eshed, N. & Wahl, I. Role of wild grasses in epidemics of powdery mildew on small grains in Israel. *Phytopathology* (1975).

65 Matsuda, S. & Takamatsu, S. Evolution of host–parasite relationships of *Golovinomyces* (Ascomycete: *Erysiphaceae*) inferred from nuclear rDNA sequences. *Molecular Phylogenetics and Evolution* **27**, 314-327 (2003).

66 Wicker, T. *et al.* The wheat powdery mildew genome shows the unique evolution of an obligate biotroph. *Nature Genetics* **45**, 1092-1096 (2013).

67 Menardo, F. *et al.* Hybridization of powdery mildew strains gives rise to pathogens on novel agricultural crop species. *Nature Genetics* **48**, 201 (2016).

68 Troch, V. *et al.* Phylogeography and virulence structure of the powdery mildew population on its 'new' host triticale. *BMC Evolutionary Biology* **12**, 76 (2012).

69 Takamatsu, S. & Matsuda, S. Estimation of molecular clocks for ITS and 28S rDNA in *Erysiphales*. *Mycoscience* **45**, 340-344 (2004).

70 Bremer, K. & Gustafsson, M. H. G. East Gondwana ancestry of the sunflower alliance of families. *Proceedings of the National Academy of Sciences* **94**, 9188-9190 (1997).

71 The Editors of Encyclopaedia Britannica. *Miocene Epoch*, <https://www.britannica.com/science/Miocene-Epoch> (2018).

72 Prieto, M. & Wedin, M. Dating the diversification of the major lineages of Ascomycota (Fungi). *PLoS One* **8**, e65576 (2013).

73 Beimforde, C. *et al.* Estimating the Phanerozoic history of the Ascomycota lineages: combining fossil and molecular data. *Molecular Phylogenetics and Evolution* **78**, 386-398 (2014).

74 Chaw, S.-M., Chang, C.-C., Chen, H.-L. & Li, W.-H. Dating the monocot–dicot divergence and the origin of core eudicots using whole chloroplast genomes. *Molecular Evolution* **58**, 424-441 (2004).

75 Bouchenak-Khelladi, Y., Verboom, G. A., Savolainen, V. & Hodkinson, T. R. Biogeography of the grasses (Poaceae): a phylogenetic approach to reveal evolutionary history in geographical space and geological time. *Botanical Journal of the Linnean Society* **162**, 543-557 (2010).

76 Johnson, W. H. *Pleistocene Epoch*, <https://www.britannica.com/science/Pleistocene-Epoch> (2018).

77 Agenbroad, L. D. & Fairbridge, R. W. *Holocene Epoch*, <https://www.britannica.com/science/Holocene-Epoch> (2014).

78 Brown, J. K. M., Jessop, A. C., Thomas, S. & Rezanoor, H. N. Genetic control of the response of *Erysiphe graminis* f. sp. *hordei* to ethirimol and triadimenol. *Plant Pathology* **41**, 126-135 (1992).

79 AHDB Cereals and Oilseeds. *Fungicide Activity and Performance in Wheat: Information sheet 26*, 2013).

80 Hollomon, D. W. Genetic control of ethirimol resistance in a natural population of *Erysiphe graminis* f. sp. *hordei* [Barley powdery mildew]. *Phytopathology* **71**, 536-540 (1981).

81 Brown, J. K. M., Slater, S. E. & See, K. A. Sensitivity of *Erysiphe graminis* f. sp. *hordei* to morpholine and piperidine fungicides. *Crop Protection* **10**, 445-454 (1991).

82 Brown, J. K. M. & Evans, N. Selection on responses of barley powdery mildew to morpholine and piperidine fungicides. *Crop Protection* **11**, 449-457 (1992).

83 Bueno-Sancho, V. *et al.* Pathogenomic analysis of wheat yellow rust lineages detects seasonal variation and host specificity. *Genome Biology and Evolution* **9**, 3282-3296 (2017).

84 Trapnell, C. *et al.* Differential gene and transcript expression analysis of RNA-seq experiments with TopHat and Cufflinks. *Nature Protocols* **7**, 562 (2012).

85 Langmead, B., Trapnell, C., Pop, M. & Salzberg, S. L. Ultrafast and memory-efficient alignment of short DNA sequences to the human genome. *Genome Biology* **10**, R25 (2009).

86 Li, H. *et al.* The sequence alignment/map format and SAMtools. *Bioinformatics* **25**, 2078-2079 (2009).

87 Hubbard, A. *et al.* Field pathogenomics reveals the emergence of a diverse wheat yellow rust population. *Genome Biology* **16**, 23 (2015).

88 AHDB Cereals and Oilseeds. *Fungicide Activity and Performance in Wheat: Information Sheet 56*, 2017).

89 Marcireau, C., Guilloton, M. F. & Karst, F. In vivo effects of fenpropimorph on the yeast *Saccharomyces cerevisiae* and determination of the molecular basis of the antifungal property. *Antimicrobial Agents and Chemotherapy* **34**, 989-993 (1990).

90 Kerkenaar, A., Van Rossum, J. M., Versluis, G. G. & Marsman, J. W. Effect of fenpropimorph and imazalil on sterol biosynthesis in *Penicillium italicum*. *Pest Management Science* **15**, 177-187 (1984).

91 Baloch, R. I., Mercer, E. I., Wiggins, T. E. & Baldwin, B. C. Inhibition of ergosterol biosynthesis in *Saccharomyces cerevisiae* and *Ustilago maydis* by tridemorph, fenpropimorph and fenpropidin. *Phytochemistry* **23**, 2219-2226 (1984).

92 Baloch, R. I. & Mercer, E. I. Inhibition of sterol $\Delta^8 \rightarrow \Delta^7$-isomerase and Δ^{14}-reductase by fenpropimorph tridemorph and fenpropidin in cell-free enzyme systems from *Saccharomyces cerevisiae*. *Phytochemistry* **26**, 663-668 (1987).

93 Lai, M. H. *et al.* The identification of a gene family in the *Saccharomyces cerevisiae* ergosterol biosynthesis pathway. *Gene* **140**, 41-49 (1994).

94 Lorenz, R. T. & Parks, L. W. Cloning, sequencing, and disruption of the gene encoding sterol C-14 reductase in *Saccharomyces cerevisiae*. *DNA and Cell Biology* **11**, 685-692 (1992).

95 Shah Alam Bhuiyan, M., Eckstein, J., Barbuch, R. & Bard, M. Synthetically lethal interactions involving loss of the yeast *ERG24*: The sterol C-14 reductase gene. *Lipids* **42**, 69-76 (2007).

96 Crowley, J. H., Tove, S. & Parks, L. W. A calcium-dependent ergosterol mutant of *Saccharomyces cerevisiae*. *Current Genetics* **34**, 93-99 (1998).

97 Brown, J. K. M., Le Boulaire, S. & Evans, N. Genetics of responses to morpholine-type fungicides and of avirulences in *Erysiphe graminis* f. sp. *hordei*. *European Journal of Plant Pathology* **102**, 479-490 (1996).

98 Engels, A. J. G., Holub, E. F., Swart, K. & De Waard, M. A. Genetic analysis of resistance to fenpropimorph in *Aspergillus niger*. *Current Genetics* **33**, 145-150 (1998).

99 Markoglou, A. N. & Ziogas, B. N. Genetic control of resistance to fenpropimorph in *Ustilago maydis*. *Plant Pathology* **48**, 521-530 (1999).

100 Marcireau, C., Joets, J., Pousset, D., Guilloton, M. & Karst, F. *FEN2*: A gene implicated in the catabolite repression-mediated regulation of ergosterol biosynthesis in yeast. *Yeast* **12**, 531-539 (1996).

101 Stolz, J. & Sauer, N. The fenpropimorph resistance gene *FEN2* from *Saccharomyces cerevisiae* encodes a plasma membrane H^+-pantothenate symporter. *Biological Chemistry* **274**, 18747-18752 (1999).

102 Meyer, V. *et al.* Survival in the presence of antifungals: Genome-wide expression profiling of *Aspergillus niger* in response to sublethal concentrations of caspofungin and fenpropimorph. *Biological Chemistry* **282**, 32935-32948 (2007).

103 Wyand, R. A. & Brown, J. K. M. Sequence variation in the *CYP51* gene of *Blumeria graminis* associated with resistance to sterol demethylase inhibiting fungicides. *Fungal Genetics and Biology* **42**, 726-735 (2005).

104 Kelley, L. A., Mezulis, S., Yates, C. M., Wass, M. N. & Sternberg, M. J. E. The Phyre2 web portal for protein modeling, prediction and analysis. *Nature Protocols* **10**, 845 (2015).

105 Wass, M. N., Kelley, L. A. & Sternberg, M. J. E. 3DLigandSite: predicting ligand-binding sites using similar structures. *Nucleic Acids Research* **38**, W469-W473 (2010).

106 Sonnhammer, E. L. L., Von Heijne, G. & Krogh, A. A hidden Markov model for predicting transmembrane helices in protein sequences. *Intelligent Systems for Molecular Biology.* 175-182 (1998).

107 Zhang, Y. I-TASSER server for protein 3D structure prediction. *BMC Bioinformatics* **9**, 40 (2008).

108 Li, X., Roberti, R. & Blobel, G. Structure of an integral membrane sterol reductase from *Methylomicrobium alcaliphilum*. *Nature* **517**, 104 (2014).

109 Emsley, P., Lohkamp, B., Scott, W. G. & Cowtan, K. Features and development of Coot. *Acta Crystallographica Section D: Biological Crystallography* **66**, 486-501 (2010).

110 McNicholas, S., Potterton, E., Wilson, K. S. & Noble, M. E. M. Presenting your structures: the CCP4mg molecular-graphics software. *Acta Crystallographica Section D: Biological Crystallography* **67**, 386-394 (2011).

111 Ryan, O. W., Poddar, S. & Cate, J. H. D. CRISPR–Cas9 genome engineering in *Saccharomyces cerevisiae* cells. *Cold Spring Harbor Protocols* **2016**, 525-533 (2016).

112 Pirondi, A., Nanni, I. M., Brunelli, A. & Collina, M. First Report of Resistance to Cyflufenamid in *Podosphaera xanthii*, Causal Agent of Powdery Mildew, from Melon and Zucchini Fields in Italy. *Plant Disease* **98**, 1581-1581 (2014).

113 Hosokawa, H. *et al.* Occurrence and biological properties of cyflufenamid resistant *Sphaerotheca cucurbitae*. *Japanese Journal of Phytopathology* **72**, 260-261 (2006).

114 Haramoto, M., Yamanaka, H., Sano, H., Sano, S. & Otani, H. Fungicidal activities of cyflufenamid against various plant-pathogenic fungi. *Pesticide Science* **31**, 95-101 (2006).

115 Cecchini, G. Function and structure of complex II of the respiratory chain. *Annual Review of Biochemistry* **72**, 77-109 (2003).

116 Avenot, H. F., Sellam, A., Karaoglanidis, G. & Michailides, T. J. Characterization of mutations in the iron-sulphur subunit of succinate dehydrogenase correlating with boscalid resistance in *Alternaria alternata* from California pistachio. *Phytopathology* **98**, 736-742 (2008).

117 Avenot, H., Sellam, A. & Michailides, T. Characterization of mutations in the membrane-anchored subunits AaSDHC and AaSDHD of succinate dehydrogenase from *Alternaria alternata* isolates conferring field resistance to the fungicide boscalid. *Plant Pathology* **58**, 1134-1143 (2009).

118 Scalliet, G. *et al.* Mutagenesis and functional studies with succinate dehydrogenase inhibitors in the wheat pathogen *Mycosphaerella graminicola*. *PLoS One* **7**, e35429 (2012).

119 Dooley, H., Shaw, M. W., Mehenni-Ciz, J., Spink, J. & Kildea, S. Detection of *Zymoseptoria tritici* SDHI-insensitive field isolates carrying the *SdhC*-H152R and *SdhD*-R47W substitutions. *Pest Management Science* **72**, 2203-2207 (2016).

120 Rehfus, A., Strobel, D., Bryson, R. & Stammler, G. Mutations in *sdh* genes in field isolates of *Zymoseptoria tritici* and impact on the sensitivity to various succinate dehydrogenase inhibitors. *Plant Pathology* **67**, 175-180 (2018).

121 Miyamoto, T., Ishii, H. & Tomita, Y. Occurrence of boscalid resistance in cucumber powdery mildew in Japan and molecular characterization of the iron–sulfur protein of succinate dehydrogenase of the causal fungus. *General Plant Pathology* **76**, 261-267 (2010).

122 Parks, W., Booth, W. & Cowger, C. Characterization of polymorphic microsatellite loci for *Blumeria graminis* f. sp. *tritici*, cause of powdery mildew of wheat. *Molecular Ecology Resources* **11**, 586-589 (2011).

123 Ishii, H. *et al.* Occurrence and molecular characterization of strobilurin resistance in cucumber powdery mildew and downy mildew. *Phytopathology* **91**, 1166-1171 (2001).

124 Ma, Z., Felts, D. & Michailides, T. J. Resistance to azoxystrobin in *Alternaria* isolates from pistachio in California. *Pesticide Biochemistry and Physiology* **77**, 66-74 (2003).

125 Moseman, J. G., Macer, R. C. F. & Greeley, L. W. Genetic studies with cultures of *Erysiphe graminis* f. sp. *hordei* virulent on *Hordeum spontaneum*. *Transactions of the British Mycological Society* **48**, 479-489 (1965).

126 Dooley, H., Shaw, M. W., Spink, J. & Kildea, S. The effect of succinate dehydrogenase inhibitor/azole mixtures on selection of *Zymoseptoria tritici* isolates with reduced sensitivity. *Pest Management Science* **72**, 1150-1159 (2016).

127 Avenot, H. F. & Michailides, T. J. Progress in understanding molecular mechanisms and evolution of resistance to succinate dehydrogenase inhibiting (SDHI) fungicides in phytopathogenic fungi. *Crop Protection* **29**, 643-651 (2010).

128 Gudmestad, N. C., Arabiat, S., Miller, J. S. & Pasche, J. S. Prevalence and impact of SDHI fungicide resistance in *Alternaria solani*. *Plant Disease* **97**, 952-960 (2013).

129 Oliver, R. P. A reassessment of the risk of rust fungi developing resistance to fungicides. *Pest Management Science* **70**, 1641-1645 (2014).

130 Blatter, R. H. E., Brown, J. K. M. & Wolfe, M. S. Genetic control of the resistance of *Erysiphe graminis* f.sp. *hordei* to five triazole fungicides. *Plant Pathology* **47**, 570-579 (1998).

131 Stammler, G., Cordero, J., Koch, A., Semar, M. & Schlehuber, S. Role of the Y134F mutation in *cyp51* and overexpression of *cyp51* in the sensitivity response of *Puccinia triticina* to epoxiconazole. *Crop Protection* **28**, 891-897 (2009).

132 Cools, H. J. *et al.* Impact of recently emerged sterol 14{alpha}-demethylase (CYP51) variants of *Mycosphaerella graminicola* on azole fungicide sensitivity. *Applied and Environmental Microbiology* **77**, 3830-3837 (2011).

133 Rallos, L. E. E. & Baudoin, A. B. Co-occurrence of two allelic variants of CYP51 in *Erysiphe necator* and their correlation with over-expression for DMI resistance. *PLoS One* **11**, e0148025 (2016).

134 Sanglard, D. *et al.* Mechanisms of resistance to azole antifungal agents in *Candida albicans* isolates from AIDS patients involve specific multidrug transporters. *Antimicrobial Agents and Chemotherapy* **39**, 2378-2386 (1995).

135 Venkateswarlu, K., Denning, D. W., Manning, N. J. & Kelly, S. L. Resistance to fluconazole in *Candida albicans* from AIDS patients correlated with reduced intracellular accumulation of drug. *FEMS Microbiology Letters* **131**, 337-341 (1995).

136 Sanglard, D., Ischer, F., Koymans, L. & Bille, J. Amino acid substitutions in the cytochrome P-450 lanosterol 14α-demethylase (CYP51A1) from azole-resistant *Candida albicans* clinical isolates contribute to resistance to azole antifungal agents. *Antimicrobial Agents and Chemotherapy* **42**, 241-253 (1998).

137 Délye, C., Laigret, F. & Corio-Costet, M.-F. A mutation in the 14 alpha-demethylase gene of *Uncinula necator* that correlates with resistance to a sterol biosynthesis inhibitor. *Applied and Environmental Microbiology* **63**, 2966-2970 (1997).

138 Délye, C., Bousset, L. & Corio-Costet, M.-F. PCR cloning and detection of point mutations in the eburicol 14a-demethylase (*CYP51*) gene from *Erysiphe graminis* f. sp. *hordei*, a "recalcitrant" fungus. *Current Genetics* **34**, 399-403 (1998).

139 Cools, H. J. & Fraaije, B. A. Are azole fungicides losing ground against Septoria wheat disease? Resistance mechanisms in *Mycosphaerella graminicola*. *Pest Management Science* **64**, 681-684 (2008).

140 Cools, H. J. *et al.* Heterologous expression of mutated eburicol 14α-demethylase (CYP51) proteins of *Mycosphaerella graminicola* to assess effects on azole fungicide sensitivity and intrinsic protein function. *Applied and Environmental Microbiology* **76**, 2866-2872 (2010).

141 Fraaije, B. A. *et al.* A novel substitution I381V in the sterol 14α-demethylase (*CYP51*) of *Mycosphaerella graminicola* is differentially selected by azole fungicides. *Molecular Plant Pathology* **8**, 245-254 (2007).

142 Brunner, P. C., Stefanato, F. L. & McDonald, B. A. Evolution of the *CYP51* gene in *Mycosphaerella graminicola*: evidence for intragenic recombination and selective replacement. *Molecular Plant Pathology* **9**, 305-316 (2008).

143 Leroux, P., Albertini, C., Gautier, A., Gredt, M. & Walker, A.-S. Mutations in the *CYP51* gene correlated with changes in sensitivity to sterol 14α-demethylation inhibitors in field isolates of *Mycosphaerella graminicola*. *Pest Management Science* **63**, 688-698 (2007).

144 Hamamoto, H. *et al.* Tandem repeat of a transcriptional enhancer upstream of the sterol 14α-demethylase gene (*CYP51*) in *Penicillium digitatum*. *Applied and Environmental Microbiology* **66**, 3421-3426 (2000).

145 Ma, Z., Proffer, T. J., Jacobs, J. L. & Sundin, G. W. Overexpression of the 14α-demethylase target gene (*CYP51*) mediates fungicide resistance in *Blumeriella jaapii*. *Applied and Environmental Microbiology* **72**, 2581-2585 (2006).

146 Schnabel, G. & Jones, A. L. The 14α-demethylasse (*CYP51A1*) gene is overexpressed in *Venturia inaequalis* strains resistant to myclobutanil. *Phytopathology* **91**, 102-110 (2001).

147 Marichal, P. *et al.* Molecular biological characterization of an azole-resistant *Candida glabrata* isolate. *Antimicrobial Agents and Chemotherapy* **41**, 2229-2237 (1997).

148 Jones, L. *et al.* Adaptive genomic structural variation in the grape powdery mildew pathogen, *Erysiphe necator*. *BMC Genomics* **15**, 1081 (2014).

149 Hayashi, K., Schoonbeek, H.-j. & De Waard, M. A. Expression of the ABC transporter BcatrD from *Botrytis cinerea* reduces sensitivity to sterol demethylation inhibitor fungicides. *Pesticide Biochemistry and Physiology* **73**, 110-121 (2002).

150 Zwiers, L.-H. & De Waard, M. A. Characterization of the ABC transporter genes *MgAtr1* and *MgAtr2* from the wheat pathogen *Mycosphaerella graminicola*. *Fungal Genetics and Biology* **30**, 115-125 (2000).

151 Bissinger, P. H. & Kuchler, K. Molecular cloning and expression of the *Saccharomyces cerevisiae STS1* gene product. A yeast ABC transporter conferring mycotoxin resistance. *Biological Chemistry* **269**, 4180-4186 (1994).

152 Chen, F. P. *et al.* Baseline sensitivity of *Monilinia fructicola* from China to the DMI fungicide SYP-Z048 and analysis of DMI-resistant mutants. *Plant Disease* **96**, 416-422 (2012).

153 Lamb, D. C. *et al.* The mutation T315A in *Candida albicans* sterol 14α-demethylase causes reduced enzyme activity and fluconazole resistance through reduced affinity. *Biological Chemistry* **272**, 5682-5688 (1997).

154 Li, H. & Durbin, R. Fast and accurate short read alignment with Burrows–Wheeler transform. *Bioinformatics* **25**, 1754-1760 (2009).

155 Hindson, B. J. *et al.* High-throughput droplet digital PCR system for absolute quantitation of DNA copy number. *Analytical Chemistry* **83**, 8604-8610 (2011).

156 Sherwood, J. E. & Somerville, S. C. Sequence of the *Erysiphe graminis* f. sp. *hordei* gene encoding beta-tubulin. *Nucleic Acids Research* **18**, 1052-1052 (1990).

157 Pfaffl, M. W. A new mathematical model for relative quantification in real-time RT–PCR. *Nucleic Acids Research* **29**, e45-e45 (2001).

158 Bolger, A. M., Lohse, M. & Usadel, B. Trimmomatic: a flexible trimmer for Illumina sequence data. *Bioinformatics* **30**, 2114-2120 (2014).

159 Pertea, M., Kim, D., Pertea, G. M., Leek, J. T. & Salzberg, S. L. Transcript-level expression analysis of RNA-seq experiments with HISAT, StringTie and Ballgown. *Nature Protocols* **11**, 1650 (2016).

160 How to Feed the World in 2050. *Food and Agriculture Organisation of the United Nations*, 1-35 (2009).

161 Appels, R. *et al.* Shifting the limits in wheat research and breeding using a fully annotated reference genome. *Science* **361**, eaar7191 (2018).

162 McHale, L., Tan, X., Koehl, P. & Michelmore, R. W. Plant NBS-LRR proteins: adaptable guards. *Genome Biology* **7**, 212 (2006).

163 Jupe, F. *et al.* Resistance gene enrichment sequencing (R en S eq) enables reannotation of the NB-LRR gene family from sequenced plant genomes and rapid mapping of resistance loci in segregating populations. *The Plant Journal* **76**, 530-544 (2013).

164 Soreng, R. J. *et al.* A worldwide phylogenetic classification of the Poaceae (Gramineae). *Journal of Systematics and Evolution* **53**, 117-137 (2015).

165 Wyand, R. A. *Molecular evolution of Blumeria graminis*, University of East Anglia, (2001).

166 Baer, C. F., Miyamoto, M. M. & Denver, D. R. Mutation rate variation in multicellular eukaryotes: causes and consequences. *Nature Reviews Genetics* **8**, 619 (2007).

167 Lynch, M. *et al.* Perspective: spontaneous deleterious mutation. *Evolution* **53**, 645-663 (1999).

168 Simão, F. A., Waterhouse, R. M., Ioannidis, P., Kriventseva, E. V. & Zdobnov, E. M. BUSCO: assessing genome assembly and annotation completeness with single-copy orthologs. *Bioinformatics* **31**, 3210-3212 (2015).

169 Van Den Bosch, F., Paveley, N., Shaw, M., Hobbelen, P. & Oliver, R. The dose rate debate: does the risk of fungicide resistance increase or decrease with dose? *Plant Pathology* **60**, 597-606 (2011).

170 Hubbard, A., Wilderspin, S. & Holdgate, S. United Kingdom Cereal Pathogen Virulence Survey 2017 Annual Report. (AHDB Cereals and Oilseeds, 2017).

Appendix I

In this appendix, I document the standard errors for all of the ED_{50} estimations calculated in this thesis. As the standard errors were calculated in Genstat using log-transformed dose values, transforming back resulted in unequal errors either side of the ED_{50} value. Here is documented the values after adding or subtracting the standard error to or from the estimated ED_{50} then converting back from the logged form.

Standard errors of ED_{50} values after converting back from log-transformation

Chapter 3 section 3.3.1

Table I.1: Corbel ED_{50} estimations and standard error (SE) calculations.

Group	Log(ED_{50})	Estimated SE	ED_{50} (mL/ha)	ED_{50} – SE (mL/ha)	ED_{50} + SE (mL/ha)
Sensitive	1.053039	0.000697	11.3	11.28	11.32
Field resistant	1.914504	0.042835	82.13	74.42	90.64
Glasshouse resistant	2.108971	0.019035	128.5	134.3	123

Chapter 3 section 3.5 epilogue

Table I.2: Fenpropimorph ED_{50} estimations and standard error (SE) calculations. The dose values entered into Genstat were the original dose values. These should have been halved as the dose is halved when it is added to the 96-well plate with yeast therefore the unlogged ED_{50} value has been halved here to accommodate this.

Group	Log(ED_{50})	Estimated SE	ED_{50} (µM)	Half ED_{50} (µM)	Half ED_{50} – SE (µM)	Half ED_{50} + SE (µM)
Wild-type	-2.22632546	0.12183397	5.94	2.97	2.24	3.93
Guide 1	-1.18632635	0.02191703	65.11	32.56	30.95	34.24
Guide 2	-1.08757726	0.02193308	81.74	40.87	38.86	42.99
Guide 3	-1.07712399	0.02507036	83.73	41.86	39.52	44.35

Chapter 4 section 4.3.2

Table I.3: Cyflamid ED_{50} estimations and standard error (SE) calculations.

Group	Log(ED_{50})	Estimated SE	ED_{50} (mL/ha)	ED_{50} – SE (mL/ha)	ED_{50} + SE (mL/ha)
Sensitive	1.9608	0.0174	91.36	87.77	95.11

Table I.4: Aviator[235] Xpro ED_{50} estimations and standard error (SE) calculations.

Group	Log(ED_{50})	Estimated SE	ED_{50} (mL/ha)	ED_{50} – SE (mL/ha)	ED_{50} + SE (mL/ha)
Old UK	1.688312	0.273828	48.79	25.97	91.65
UK field	2.24854	0.0243	177.23	167.59	187.43
2014 Glasshouse	2.393743	0.016854	247.6	238.17	257.39

Chapter 5 section 5.3.1

Table I.5: Proline ED_{50} estimations and standard error (SE) calculations.

Group	Log(ED_{50})	Estimated SE	ED_{50} (mL/ha)	ED_{50} – SE (mL/ha)	ED_{50} + SE (mL/ha)
Y136	2.015695	0.474237	103.68	34.79	308.98
F136	2.64638	0.305837	442.98	219.05	895.81
Y136/F136	2.865511	N/A	733.69	N/A	N/A

Table I.6: Folicur ED_{50} estimations and standard error (SE) calculations.

Group	Log(ED_{50})	Estimated SE	ED_{50} (mL/ha)	ED_{50} – SE (mL/ha)	ED_{50} + SE (mL/ha)
Y136	1.356568	0.043414	22.73	20.57	25.12
F136	2.011322	0.074515	102.64	86.46	121.85
Y136/F136	2.254398	0.039801	179.64	163.91	196.88

Appendix II

In this appendix, I describe the rationale for estimating the mutation rate of *Blumeria graminis*, summarise the current literature surrounding divergence time estimations of the *B. graminis formae speciales*, and detail the experiments I performed in an attempt to calculate a more appropriate mutation rate for *B. graminis*.

Mutation rate estimation

Fungicide resistance appears very quickly in powdery mildew fungi as was demonstrated by the emergence of resistance to quinone outside inhibitors (discussed in chapter 1) and with cyflufenamid (chapter 4). This could largely be due to their epiphytic lifestyle as all of their reproductive cells are exposed to both fungicides as a selective agent and to environmental mutagens. This exposure could mean that they have an unusually high mutation rate compared to other organisms. This hypothesis was raised previously by Troch *et al.* (2014) in the context of evolution and specialisation of the *B. graminis formae speciales* (ff. spp.) on crops.

Table II.1: A summary of B. graminis formae speciales *divergence time estimated or proposed to date.* Bgh = *f. sp.* hordei*;* Bgt = *f. sp.* tritici*.*

Study	***B. graminis* included**	**Divergence time**
Wyand and Brown (2003)	*Bgh*, *Bgt*, *B.g. secalis*, and *B.g. avenae*	14,000 years ago
Matsuda and Takamatsu (2003)	*Bgh* and *Bgt*	12 MYA approx.
Inuma *et al*. (2007)	All ff. spp.	4.6 MYA between *Hordeum* and *Triticum* clades
Oberhaensli *et al*. (2011)	*Bgh* and *Bgt*	10 MYA approx.
Wicker *et al*. (2013)	*Bgh* and *Bgt*	6.3 MYA approx.
Menardo *et al*. (2016)	*Bgt*, *B. g. secalis*, and *B. g. triticale*	168,245 – 240,169 years ago between *Bgt* and *B. g. secalis*
Menardo *et al*. (2017)	All ff. spp.	170,000 – 280,000 years ago between *Bgt*, *B. g. secalis*, *B. g. dactylidis* 7.1 – 8 MYA between *Bgh* and *Bgt* 14.3 – 12.8 MYA between *B. g. avenae* and *Lolium* 22.4 – 25.1 MYA between *B.g.* on *Poae* and all other ff. spp.

A very wide range of divergence times of the ff. spp. have been proposed, ranging from the early Miocene to the Holocene (table II.1[43,60-62,65-67]) and the dating depends crucially on the mutation rate of the fungus. The methods that have been used so far to estimate this rate are

questionable. For example, many of these calculations rely on using nucleotide substitution rates estimated for plant evolution[61,65,69] but given that plants and fungi do not have the same life cycle lengths (i.e. generation times) and that *B. graminis* is so greatly exposed to environmental mutagens[42], it seems inappropriate to apply those substitution rates to date the divergence time of the *B. graminis* ff. spp.

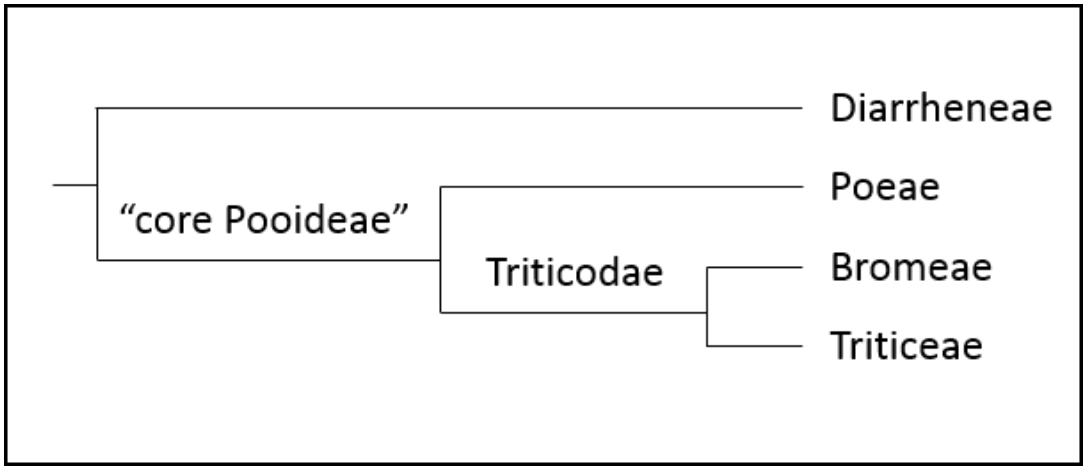

Figure II.1: A simplified portion of the Pooideae sub-family phylogenetic tree showing the relationships between the B. graminis *wild grass and cultivated crop host tribes. Figure is adapted from figure 1, Soreng* et al*. (2015).*

Additionally, the relationship of *B. graminis forma specialis* (f. sp.) *avenae* on cultivated oats (*Avena sativa*) with other ff. spp. has been somewhat overlooked in most of these studies. Troch *et al*. (2014) showed that this f. sp. grouped with ff. spp. from other crops, wheat, barley, and rye, and that crop-infecting *B. graminis* formed a disctinct clade within a very diverse phylogeny of isolates from wild grasses. Other studies have hypothesised that *B. graminis* ff. spp. co-evolved with their host plants but did not necessarily compare crop-infecting isolates with those from wild grasses. If this latter hypothesis is true, then there has been an enormous coincidence that f. sp. *avenae* evolved as the sister group of ff. spp. on other crops, even though oats are in the Poeae tribe of Poaceae while wheat, barley, and rye are in the Triticodae clade (figure II.1[164]). There are many wild grasses which are hosts of *B. graminis* in both these clades. The Diarrheneae tribe contains the *Diarrhena* genus. The Poeae tribe includes the *Avena* genus in chloroplast group 1 and the *Poa*, *Lolium*, and *Dactylis* genera in chloroplast group 2[164]. The Bromeae tribe contains the *Bromus* genus and finally, the Triticeae tribe includes the *Triticum*, *Hordeum*, *Secale*, *Agropyron*, and *Elymus* genera[164]. This is an incomplete list of some of the known hosts of *B. graminis*. Based on this phylogeny, if the *B. graminis* ff. spp. did truly co-evolve with their hosts then one would expect isolates from *Avena*, regardless of whether they are from cultivated or wild oats, to be more closely related to isolates that infect *Poa*, *Lolium*, and *Dactylis* than to those that infect hosts from the Triticodae clade. F. sp. *avenae* has also been shown to be

polyphyletic with isolates from cultivated oats falling within the crop-infecting clade and isolates from wild oats being more closely-related to isolates from *Dactylis* and/or *Lolium*[43,165].

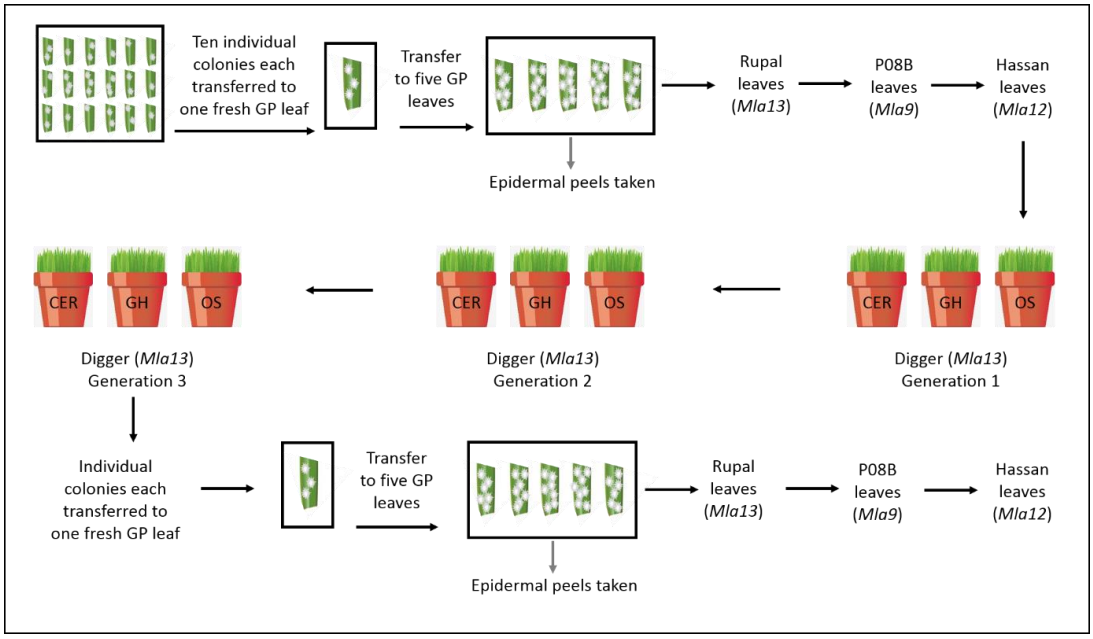

Figure II.2: Diagrammatic representation of isolate collection and the process of exposing CC52 isolates to three different levels of natural mutagens.

The conclusion of this research on the evolution of the *formae speciales* is that either the mutation rate of *B. graminis* lies within the range that would be calculated by calibration against other species and there has been an enormous coincidence in the evolution of f. sp. *avenae* on *A. sativa* (but not on wild *Avena*) within the crop-infecting clade, or that one clade of *B. graminis* specialised on different crop species in the early Holocene as proposed previously[42,60] and that this fungus has a very high mutation rate.

The mutation rate is therefore of interest not only in relation to evolution of fungicide resistance but also in the evolution of *B. graminis* as a species. In an attempt to estimate the mutation rate directly, I used the mutation accumulation method[166,167] to expose *Bgh* isolates to natural mutagens and used an RNA-seq approach to identify mutations in core eukaryotic genes that occurred between isolates pre- and post-exposure in order to estimate a rate of nucleotide substitution per nucleotide site per generation. The hypotheses tested here were that *Bgh* has an exceptionally high mutation rate in comparison to other eukaryotes and that this high rate is driven by exposure to environmental mutagens.

The method used is summarised in figure II.2 which illustrates how older UK *Bgh* isolate CC52 was inoculated onto a large box of barley cv. Golden Promise leaves so individual single-spore colonies could be isolated. Ten of these colonies were transferred successively onto three near-isogenic lines: Rupal (*Mla13*), P08B (*Mla9*) and Hassan (*Mla12*) as CC52 is virulent on all three of

these lines. Virulence to both *Mla9* and *Mla13* is rare in the UK[170], therefore the combination of all three virulences is also rare and any isolates with this combination are most likely to be descendants of CC52 and contamination in the laboratory is unlikely. After transferring conidia onto Rupal leaves, epidermal peels of the Golden Promise leaves covered with CC52 mycelia were collected from all ten sub-cultures as described in chapter 2 section 2.4.

One isolate was picked to inoculate three 2 L pots of ten-day old Digger (*Mla13*) seedlings. After inoculation, all three Digger pots were kept in the laboratory overnight to allow the spores to germinate. One pot was then placed outside with full exposure to the natural environment, one pot was placed in a glasshouse where there was partial exposure to UV and cosmic rays, and the third pot was placed in a controlled environment cabinet (CER) with artificial lighting and very little exposure to natural mutagens. These pots were watered and maintained for nine days until colonies were clearly visible and beginning to sporulate. All three pots were brought into the laboratory to allow the colonies to re-sporulate for two days. This was particularly important for the outside pot as all the spores were continuously being blown away. After two days, spores were transferred onto three fresh pots of Digger seedlings which were kept in the laboratory overnight before being placed back in the three locations for nine days.

This was repeated twice so the CC52 isolates were exposed to different levels of mutagens for three generations. With the third generation, the pots were kept in their locations for seven days until colonies were visible. Individual colonies were then cut from the three pots, allowed to sporulate for three days, transferred to one Golden Promise leaf each, then transferred to five Golden Promise leaves in order to increase the amount of mycelia and spores available. Isolates were then sequentially transferred onto Rupal, P08B, and Hassan leaves to remove any contaminating isolates. After the first transfer onto Rupal, epidermal peels were taken from the Golden Promise leaves covered with mycelia. Peels were taken from isolates from all three locations giving four sets of isolates in total – one from the start of the experiment ("pre-exposure") and three from the end ("post-exposure"). This experiment was repeated twice – once in 2016 and once in 2017. The number of isolates collected post-exposure are outline in table II.2.

Table II.2: A summary of the number of post-exposure isolates collected from each of the three Digger pots in each experimental replicate.

	2016	**2017**
Outside pot	7	2
Glasshouse pot	8	7
CER pot	7	5

One pre-exposure isolate and three post-exposure isolates (one from each environment) were sent for RNA sequencing so SNPs could be identified in 1315 core eukaryotic genes using the BUSCO pipeline[168] in order to calculate a nucleotide substitution rate. This experiment was performed in both 2016 and 2017 so eight samples were sequenced in total.

Table II.3 summarises the total number of SNPs identified between all possible combinations of isolates in both 2016 and 2017. Due to the large difference between the two replications, the *Cyp51* and *Erg24* gene sequences for all isolates were checked for contamination as CC52 has wild-type *Cyp51* and *Erg24* genes. For the CER and outside isolates collected from 2016, there was not enough sequencing coverage of these two genes to check for contamination. Likewise, the 2017 CER and glasshouse isolates did not have enough coverage for *Cyp51*, and the 2017 outside isolate for *Erg24*. Sequencing of the *Cyp51* gene in the 2017 outside isolate showed that it contained the mutated F136 allele therefore it is likely that this was a contaminating isolate despite the precautions taken.

Table II.3: Two matrices comparing mRNA sequences from 1315 single-copy orthologous genes in CC52 isolates before and after exposure to natural mutagens. Matrix A shows four isolates from 2016 (one isolate from each condition) and matrix B shows four isolates from 2017 (one isolate from each condition). CER = controlled environment cabinet; GH = glasshouse; OS = outside.

A	**2016 CC52**	**2016 CER**	**2016 GH**	**2016 OS**	**B**	**2017 CC52**	**2017 CER**	**2017 GH**	**2017 OS**
2016 CC52		0	0	1	**2017 CC52**		0	0	209
2016 CER	0		0	1	**2017 CER**	0		0	209
2016 GH	0	0		1	**2017 GH**	0	0		209
2016 OS	1	1	1		**2017 OS**	209	209	209	

Calculating an accurate mutation rate for *Blumeria graminis* remains a difficult task as has been shown here. Due to the biotrophic lifestyle of this pathogen, performing a mutation accumulation experiment relies on repeatedly establishing a strong infection on the host plant from one generation to the next. Here, only three generations were possible as the quantity of spores available on the outside pots at the end of each generation was low. This is particularly reflected in the 2017 experiment as only two colonies were found on the outside pot at the end of the third generation. In order to maintain the fungus for more generations, the experiment

could be performed on a larger scale by using more pots in each condition. This would give a greater chance of more colonies surviving from one generation to the next and would allow the experiment to be continued for more generations thus potentially accumulating more mutations in the fully-exposed isolates.

Additionally, only one isolate from each location per year was included in the RNA-seq analysis which means there are several more isolates that were collected which could be included in the final analysis. As a contaminating isolate was present in the isolates already sequenced, it would be greatly beneficial to include an extra screening process before isolates are sent for RNA sequencing. This could include collecting extra material from isolates for a separate DNA extraction and sequencing the relevant sections of the *Cyp51* and *Erg24* genes to identify if they possess the sensitive or resistant alleles.

By altering the experimental design in the two ways outlined here, it should be possible to estimate a more accurate mutation rate for *B. graminis*. Doing this would not only test the hypothesis that *B. graminis* has an exceptionally high mutation rate due to its unusual exposure to natural mutagens, which in turn would explain how it evolves resistance to fungicides so rapidly, but would also supply a more appropriate mutation rate for dating the divergence of the ff. spp.